

# **BornAgain**

Software for simulating and fitting  
X-ray and neutron small-angle scattering  
at grazing incidence

User Manual  
0.2.6  
October 27, 2014

C. Durniak, M. Ganeva, G. Pospelov, W. Van Herck, J. Wuttke

Scientific Computing Group  
Jülich Centre for Neutron Science  
outstation at Heinz Maier-Leibnitz Zentrum Garching  
Forschungszentrum Jülich GmbH

## Disclaimer

This manual is under development and does not yet constitute a comprehensive listing of all BornAgain features and functionality. The included information and instructions are subject to substantial changes and are provided only as a preview.

# Contents

<b>Introduction</b>	<b>6</b>
<b>1 Quick start</b>	<b>8</b>
1.1 Quick start on Unix Platforms . . . . .	8
1.2 Quick start on Windows Platforms . . . . .	9
1.3 Getting help . . . . .	9
<b>2 Installation</b>	<b>10</b>
2.1 Building and installing on Unix Platforms . . . . .	10
2.1.1 Third-party software . . . . .	11
2.1.2 Getting <b>BornAgain</b> source code . . . . .	12
2.1.3 Building and installing the code . . . . .	13
2.1.4 Running the first simulation . . . . .	14
2.2 Installing on Windows Platforms . . . . .	14
<b>3 Simulation</b>	<b>16</b>
3.1 General methodology . . . . .	16
3.2 Geometry of the sample . . . . .	16
3.3 Example 1: two types of islands on top of substrate without interference . . . . .	18
3.4 Example 2: working with sample parameters . . . . .	23
<b>4 Graphical User Interface</b>	<b>26</b>
<b>5 Scattering cross-section</b>	<b>27</b>
5.1 Position of the problem . . . . .	27
5.2 Collection of particles . . . . .	27
5.2.1 Size-distribution models . . . . .	28
5.2.2 Layout of particles . . . . .	30
5.2.3 Implementation in BornAgain . . . . .	32
5.2.4 Summary . . . . .	44
5.3 Particles - Form factors . . . . .	46
5.3.1 Born approximation . . . . .	46
5.3.2 Distorted Wave Born Approximation . . . . .	48
5.4 More complicated particles' shapes . . . . .	55

5.4.1	Core-shell particles . . . . .	55
5.4.2	Rotation of particles . . . . .	56
5.4.3	Polydispersity . . . . .	57
5.5	Material layers . . . . .	57
5.5.1	Roughness . . . . .	57
5.6	Polarisation . . . . .	57
<b>6</b>	<b>Fitting</b>	<b>58</b>
6.1	Implementation in BornAgain . . . . .	58
6.1.1	Preparing the sample and the simulation description . . . . .	60
6.1.2	Choice of parameters to be fitted . . . . .	60
6.1.3	Associating reference and simulated data . . . . .	61
6.1.4	Minimizer settings . . . . .	61
6.1.5	Running the fitting and retrieving the results . . . . .	63
6.2	Basic Python fitting example . . . . .	63
6.3	Advanced fitting . . . . .	67
6.3.1	Affecting $\chi^2$ calculations . . . . .	67
6.3.2	Simultaneous fits of several data sets . . . . .	67
6.3.3	Using fitting strategies . . . . .	67
6.3.4	Masking the real data . . . . .	67
6.3.5	Tuning fitting algorithms . . . . .	67
6.3.6	Fitting with correlated sample parameters . . . . .	67
6.4	How to get the right answer from fitting . . . . .	67
<b>7</b>	<b>Software architecture</b>	<b>69</b>
<b>A</b>	<b>Listings</b>	<b>71</b>
A.1	Python simulation example . . . . .	71
A.2	Python fitting example . . . . .	73
<b>B</b>	<b>Theory</b>	<b>75</b>
B.1	Scattering on nanoparticles - Formal treatment . . . . .	75
B.2	Small angle approximation . . . . .	77
B.3	Born approximation . . . . .	78
B.4	Distorted Wave Born Approximation . . . . .	82
<b>C</b>	<b>Form factors</b>	<b>85</b>
C.1	Box . . . . .	86
C.2	Prism3 . . . . .	88
C.3	Tetrahedron . . . . .	90
C.4	Prism6 . . . . .	92
C.5	Cone6 . . . . .	94
C.6	Pyramid . . . . .	96
C.7	Anisotropic pyramid . . . . .	98
C.8	Cuboctahedron . . . . .	100

C.9 Cylinder . . . . .	102
C.10 Ellipsoidal cylinder . . . . .	104
C.11 Cone . . . . .	106
C.12 Full Sphere . . . . .	108
C.13 Truncated Sphere . . . . .	110
C.14 Full Spheroid . . . . .	112
C.15 Truncated Spheroid . . . . .	114
C.16 Hemi ellipsoid . . . . .	116
C.17 Ripple1 . . . . .	118
C.18 Ripple2 . . . . .	120
<b>D User API</b>	<b>122</b>
D.1 IntensityData . . . . .	122
<b>E Python examples</b>	<b>125</b>
E.1 General conventions . . . . .	125
E.2 Example 1: Cylinders and prisms . . . . .	127
E.3 Example 2: Cylinders with size distribution . . . . .	128
E.4 Example 3: "Cylinder" form factor . . . . .	129
E.5 Example 4: Cylinders - Paracrystal . . . . .	131
E.6 Example 5: Lattice with disorder . . . . .	133
E.7 Example 6: Rotated pyramids . . . . .	136
E.8 Example 7: Core-shell nanoparticles . . . . .	137
E.9 Example 8: Correlated roughness . . . . .	138
E.10 Example 9: Ripple . . . . .	140
E.11 Example 10: Beam divergence . . . . .	143

# Introduction

BornAgain is a free software package to simulate and fit small-angle scattering at grazing incidence (GISAS). It supports analysis of both X-ray (GISAXS) and neutron (GISANS) data. Its name, BornAgain, indicates the central role of the distorted-wave Born approximation (DWBA) in the physical description of the scattering process. The software provides a generic framework for modeling multilayer samples with smooth or rough interfaces and with various types of embedded nanoparticles.

BornAgain almost completely reproduces the functionality of the widely used program IsGISAXS by R. Lazzari [1].

BornAgain goes beyond IsGISAXS by supporting an unrestricted number of layers and particles, diffuse reflection from rough layer interfaces, particles with inner structures, neutron polarization and magnetic scattering. Adhering to a strict object-oriented design, BornAgain provides a solid base for future extensions in response to specific user needs.

BornAgain is a platform-independent software, with active support for Linux, MacOS and Microsoft Windows. It is a free and open source software provided under the terms of the GNU General Public License (GPL). This documentation is released under the Creative Commons license CC-BY-SA.

The authors will be grateful for all kind of feedback: criticism, praise, bug reports, feature requests or contributed modules. When BornAgain is used in preparing scientific papers, please cite this manual as follows:

C. Durniak, M. Ganeva, G. Pospelov, W. Van Herck, J. Wuttke (2013),  
BornAgain - Software for simulating and fitting X-ray and neutron small-angle  
scattering at grazing incidence, version 0.2.6,  
<http://apps.jcns.fz-juelich.de/BornAgain>

This user guide starts with a brief description of the steps necessary for installing the software and running a simulation on Unix and Windows platforms in Section 1. A more detailed description of the installation procedure is given in Section 2. The general methodology of a simulation with BornAgain and detailed simulation usage examples are given in Section 3. The fitting toolkit, provided by the framework, is presented in Section 6, while

Section 7 provides a brief overview of the software architecture.

Icons used in this manual:

 : this sign highlights further remarks.

 : this sign highlights essential points.

# Chapter 1

## Quick start

### 1.1 Quick start on Unix Platforms

This section shortly describes how to build and install BornAgain from source and run the first simulation on Unix Platforms. Further details about the installation procedure are given in Section 2.

#### Step I: installing the third party software

- compilers: clang versions  $\geq$  3.1 or GCC versions  $\geq$  4.2
- cmake ( $\geq$  2.8)
- boost library ( $\geq$  1.48)
- GNU scientific library ( $\geq$  1.15)
- fftw3 library ( $\geq$  3.3.1)
- Python-2.7, python-devel, python-numpy-devel

#### Step II: getting the source

Download BornAgain source tarball from <http://apps.jcns.fz-juelich.de/BornAgain> or use the following git repository

```
git clone git://apps.jcns.fz-juelich.de/BornAgain.git
```

#### Step III: building the libraries and executable

```
mkdir <build_dir>; cd <build_dir>;
cmake -DCMAKE_INSTALL_PREFIX=<install_dir> <source_dir>
make -j4
make check
make install
```

**Step IV: running an example**

```
python <install_dir>/share/BornAgain/Examples/python/simulation/  
    ex001_CylindersAndPrisms/CylindersAndPrisms.py
```

## 1.2 Quick start on Windows Platforms

**Step I: installing the third party software**

The current version of BornAgain requires Python, numpy, matplotlib to be installed on the system. If you don't have them already installed, you can use PythonXY installer available at <https://code.google.com/p/pythonxy> which, with default installation options, contains at least these three packages.

**Step II: using BornAgain installation package**

Windows installation package can be downloaded from <http://apps.jcns.fz-juelich.de/BornAgain>. Double-click on it to start the installation process. Then follow the instructions.

**Step III: running the example**

Run an example located in BornAgain installation directory:

```
python C:/BornAgain-<Version>/Examples/python/simulation/  
    ex001_CylindersAndPrisms/CylindersAndPrisms.py
```

## 1.3 Getting help

Users of the software who encounter problems during the installation of the framework or during the run of a simulation can use the web-based issue tracking system at <http://apps.jcns.fz-juelich.de/redmine/projects/bornagain/issues> to report a bug. The same system can be used to request new features. This system is open for all users in read mode, while submitting bug reports and feature requests are possible only after a simple registration procedure.

# Chapter 2

# Installation

BornAgain is supported under x86/x86\_64 Linux, Mac OS X and Windows operating systems. It has been successfully compiled and tested on

- Microsoft Windows 7 64-bit, Windows 8 64-bit
- Mac OS X 10.8 (Mountain Lion), 10.9 (Maverick)
- OpenSuse 12.3 64-bit
- Ubuntu 12.10, 13.04 64-bit
- Debian 7.1.0, 32-bit, 64-bit

At the moment we support build and installation from source on Unix Platforms (Linux, Mac OS) and installation using binary installer packages on MS Windows 7, 8 (see Section 2.1 and Section 2.2, respectively). In the next releases we are planning to provide binary installers for Mac OS X and Debian.

We welcome feedback and bug reports related to installation and use of BornAgain via <http://apps.jcns.fz-juelich.de/redmine/projects/bornagain/issues>

## 2.1 Building and installing on Unix Platforms

BornAgain uses CMake to configure a build system for compiling and installing the framework. There are three major steps to build BornAgain :

1. Acquiring the required third-party libraries.
2. Getting BornAgain source code.
3. Using CMake to build and install the software.

The remainder of this section explains each step in detail.

### 2.1.1 Third-party software

To successfully build BornAgain a number of prerequisite packages must be installed.

- compilers: clang versions  $\geq 3.1$  or GCC versions  $\geq 4.1.2$
- cmake ( $\geq 2.8.3$ )
- boost library ( $\geq 1.48$ )
- GNU scientific library ( $\geq 1.15$ )
- fftw3 library ( $\geq 3.3$ )
- Python ( $\geq 2.7, < 3.0$ ), python-devel, python-numpy-devel, python-matplotlib

Other packages are optional

- ROOT framework (adds several additional fitting algorithms to BornAgain)

All required packages can be easily installed on most Linux distributions using the system's package manager. Below we give examples for a few selected operation systems. Please note, that other distributions (Fedora, Mint, etc) may have different commands for invoking the package manager as well as slightly different names of packages (like "boost" instead of "libboost" etc). Besides the installation should be very similar.

#### Ubuntu (12.10, 13.04), Debian (7.1)

Installing the required packages

```
sudo apt-get install git cmake libgsl0-dev libboost-all-dev  
libfftw3-dev python-dev python-numpy python-matplotlib python  
-matplotlib-tk
```

Installing the optional packages

```
sudo apt-get install root-system
```

#### OpenSuse 12.3

Installing the required packages

```
sudo zypper install git-core cmake gsl-devel boost-devel fftw3-  
devel python-devel python-numpy-devel python-matplotlib  
python-matplotlib-tk
```

Installing the optional packages. First add the "scientific" repository for your version of OpenSuse

```
sudo zypper ar http://download.opensuse.org/repositories/science/  
openSUSE_12.3 science
```

Then install optional ROOT framework

```
sudo zypper root -system
```

### Mac OS X 10.8, 10.9

To simplify the installation of third party open-source software on a Mac OS X system we recommend the use of MacPorts package manager. The easiest way to install MacPorts is by downloading the dmg from [www.macports.org/install.php](http://www.macports.org/install.php) and running the system's installer. After the installation new command "port" will be available in a terminal window of your Mac.

Installing the required packages

```
sudo port -v selfupdate
sudo port install git-core cmake
sudo port install fftw-3 gsl
sudo port install boost -no_single -no_static+python27
sudo port install py27-matplotlib py27-numpy py27-scipy
sudo port select --set python python27
```

Installing the optional packages

```
sudo port install root +fftw3+python27
```

#### 2.1.2 Getting BornAgain source code

BornAgain source can be downloaded at <http://apps.jcns.fz-juelich.de/BornAgain> and unpacked with

```
tar xfz BornAgain-<version>.tar.gz
```

Alternatively one can obtain BornAgain source from our public Git repository.

```
git clone git://apps.jcns.fz-juelich.de/BornAgain.git
```

#### More about Git

Our Git repository holds two main branches called "master" and "develop". We consider "master" branch to be the main branch where the source code of HEAD always reflects the latest stable release. `git clone` command shown above

1. gives you a source code snapshot corresponding to the latest stable release,
2. automatically sets up your local master branch to track our remote master branch, so you will be able to fetch changes from the remote branch at any time using `git pull` command.

"Master" branch is updated approximately once per month. The second branch, "develop" branch, is a snapshot of the current development. This is where any automatic nightly builds are built from. The develop branch is always expected to work. So in order to get the most recent features of the source code, one can switch to it by

```
cd BornAgain
git checkout develop
git pull
```

### 2.1.3 Building and installing the code

BornAgain should be built using CMake cross platform build system. Having the third-party libraries installed on your system and BornAgain source code acquired as explained in the previous sections, type the build commands

```
mkdir <build_dir>
cd <build_dir>
cmake -DCMAKE_INSTALL_PREFIX=<install_dir> <source_dir>
make -j4
```

Here <source\_dir> is the name of the directory, where BornAgain source code has been copied, <install\_dir> is the directory, where you want the package to be installed, and <build\_dir> is the directory where the building will occur.

#### About CMake

 Having a dedicated directory <build\_dir> for the build process is recommended by CMake. This allows several builds with different compilers/options from the same source and keeps the source directory clean from build remnants.

The compilation process invoked by the command “make” lasts about 10 minutes on an average laptop of 2012 edition. On multi-core machines the compilation time can be decreased by invoking command “make” with the parameter “make -j[N]”, where N is the number of cores.

Running functional tests is an optional but recommended step. Command “make check” will compile several additional tests and run them one by one. Each test contains the simulation of a typical GISAS geometry and the comparison on numerical level of simulation results with reference files. Having 100% tests passed ensures that your local installation is correct.

```
make check
...
100% tests passed, 0 tests failed out of 26
Total Test time (real) = 89.19 sec
[100%] Build target check
```

The last command “make install” copies the compiled libraries and some usage examples into the installation directory.

```
make install
```

### After installation

After the installation is completed, the location of BornAgain libraries needs to be included into your LD\_LIBRARY\_PATH and PYTHONPATH environment variables. This can be done by running BornAgain setup script in the terminal session

```
source <install_dir>/bin/thisbornagain.sh
```

Conveniently, a given call can be placed in your .bashrc file.

### Troubleshooting

In the case of a complex system setup, with libraries of different versions scattered across multiple places (/opt/local, /usr/local etc.), you may want to help CMake in finding the correct library paths by running cmake with additional parameter

```
cmake -DCMAKE_PREFIX_PATH=/usr/local -DCMAKE_INSTALL_PREFIX=<  
install_dir> <source_dir>
```

#### 2.1.4 Running the first simulation

In your installation directory you will find

```
./include/BornAgain - header files for compilation of your C++  
program  
.lib - libraries to import into python or link with your C++  
program  
.share/BornAgain/Examples - directory with examples
```

Run your first example and enjoy the first BornAgain simulation plot.

```
python <install_dir>/share/BornAgain/Examples/python/simulation/  
ex001_CylindersAndPrisms/CylindersAndPrisms.py
```

## 2.2 Installing on Windows Platforms

### Step I: install the third party software

The current version of BornAgain requires Python, numpy, matplotlib to be installed on the system.

### If you do not have have Python installed

You can use PythonXY installer at <https://code.google.com/p/pythonxy> which, with the default installation options, contains at least these three packages. The user has to download and install this package before proceeding to the installation of BornAgain.

**If you have Python already installed**

You might want to keep using this installation and to install the missing modules. The required libraries can be found at

```
matlab:  
http://matplotlib.org/downloads.html  
  
numpy, dateutil, pyparsing:  
http://www.lfd.uci.edu/~gohlke/pythonlibs
```

**Step II: use the installation package**

BornAgain installation package for Windows can be downloaded from <http://apps.jcns.fz-juelich.de/BornAgain>. Double-click on it to start the installation process. And then follow the instructions.

**Step IV: run an example**

Run an example located in BornAgain installation directory:

```
python C:/BornAgain-<Version>/Examples/python/simulation/  
ex001_CylindersAndPrisms/CylindersAndPrisms.py
```

# Chapter 3

## Simulation

### 3.1 General methodology

A simulation of GISAXS using BornAgain consists of following steps:

- define materials by specifying name and refractive index,
- define embedded particles by specifying shape, size, constituting material, interference function,
- define layers by specifying thickness, roughness, material,
- include particles in layers, specifying density, position, orientation,
- assemble a multilayered sample,
- specify input beam and detector characteristics,
- run the simulation,
- save the simulated detector image.

We are planning to organize all these steps in a graphical user interface (GUI). For the time being, however, BornAgain must be used via a C++ program or Python scripts. In the following, we describe how to write a Python script which runs a BornAgain simulation. For tutorials about this programming language, the users are referred to [2].

More information about the general software architecture and BornAgain internal design are given in Section 7.

### 3.2 Geometry of the sample

The geometry used to describe the sample is shown in figure 3.1. The  $z$ -axis is perpendicular to the sample's surface and pointing upwards. The  $x$ -axis is perpendicular to the detector plane. The input and the scattered output beams are each characterized by two

angles  $\alpha_i, \phi_i$  and  $\alpha_f, \phi_f$ , respectively. Our choice of orientation for the angles  $\alpha_i$  and  $\alpha_f$  is so that they are positive as shown in figure 3.1.

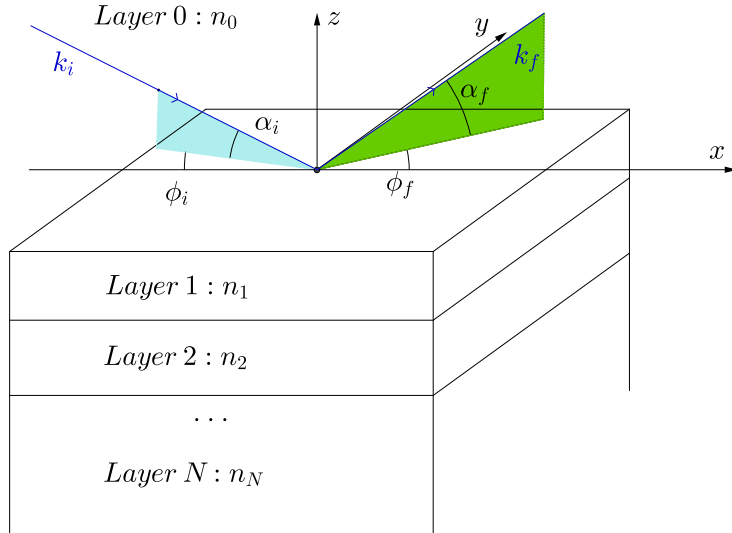


Figure 3.1: Representation of the scattering geometry.  $n_j$  is the refractive index of layer  $j$  and  $\alpha_i$  and  $\phi_i$  are the incident angles of the wave propagating.  $\alpha_f$  is the exit angle with respect to the sample's surface and  $\phi_f$  is the scattering angle with respect to the scattering plane.

The layers are defined by their thicknesses (parallel to the  $z$ -direction), their possible roughnesses (equal to 0 by default) and the materials they are made of. They have an infinite extension in the  $x$  and  $y$  directions. And, except for roughness, their interfaces are plane and perpendicular to the  $z$ -axis. There is also no limitation to the number of layers that could be defined in BornAgain. Note that the thickness of the top and bottom layer are not defined.

The nanoparticles are characterized by their form factors (*i.e.* the Fourier transform of the shape function - see Appendix C for a list of form factors implemented in BornAgain) and the composing material. The number of input parameters for the form factor depends on the particle symmetry; it ranges from one parameter for a sphere (its radius) to three for an ellipsoid (its three main axis lengths).

By placing the particles inside or on top of a layer, we impose their vertical positions, whose values correspond to the bottoms of the particles. The in-plane distribution of particles is linked with the way the particles interfere with each other. It is therefore implemented when dealing with the interference function.

The complex refractive index associated with a layer or a particle is written as  $n = 1 - \delta + i\beta$ , with  $\delta, \beta \in \mathbb{R}$ . In our program, we input  $\delta$  and  $\beta$  directly.

The input beam is assumed to be monochromatic without any spatial divergence.

**Units:** By default the angles are expressed in radians and the lengths are given in nanometers. But it is possible to use other units by specifying them right after the value of the corresponding parameter like, for example, 20.0\*micrometer.

### 3.3 Example 1: two types of islands on top of substrate without interference

In this example, we simulate the scattering from a mixture of cylindrical and prismatic nanoparticles without any interference between them. These particles are placed in air, on top of a substrate.

We are going to go through each step of the simulation. The Python script specific to each stage will be given at the beginning of the description. But for the sake of completeness the full code is given in Appendix A.1.

#### Importing Python modules

```

1 import numpy
2 import matplotlib
3 import pylab
4 from libBornAgainCore import *
```

We start by importing different functions from external modules, for example NumPy (lines 1-3), which is a fundamental package for scientific computing with Python [3]. In particular, line 4 imports the features of BornAgain software.

#### Defining the materials

```

5 def get_sample():
6     """
7         Build and return the sample representing cylinders and
8             pyramids on top of substrate without interference.
9     """
10    # defining materials
11    m_air = HomogeneousMaterial("Air", 0.0, 0.0)
12    m_substrate = HomogeneousMaterial("Substrate", 6e-6, 2e-8)
13    m_particle = HomogeneousMaterial("Particle", 6e-4, 2e-8)
```

Line 5 marks the beginning of the function to define our sample. Lines 10, 11 and 12 define different materials using class HomogeneousMaterial. The general syntax is the following

```
<material_name> = HomogeneousMaterial("name", delta, beta)
```

where `name` is the name of the material associated with its complex refractive index  $n=1-\delta+i\beta$ . `<material_name>` is later used when referring to this particular material. The three materials defined in this example are `Air` with a refractive index of 1 ( $\delta = \beta = 0$ ), a `Substrate` associated with a complex refractive index equal to  $1 - 6 \times 10^{-6} + i2 \times 10^{-8}$ , and the material of the particles, whose refractive index is  $n = 1 - 6 \times 10^{-4} + i2 \times 10^{-8}$ .

### Defining the particles

```

14 # collection of particles
15 cylinder_ff = FormFactorCylinder(5*nanometer, 5*nanometer)
16 cylinder = Particle(m_particle, cylinder_ff)
17 prism_ff = FormFactorPrism3(10*nanometer, 5*nanometer)
18 prism = Particle(m_particle, prism_ff)

```

We implement two different shapes of particles: cylinders and prisms (*i.e.* elongated particles with a constant equilateral triangular cross section).

All particles implemented in BornAgain are defined by their form factors (see Appendix C), their sizes and the material they are made of. Here, for the cylindrical particle, we input its radius and height. For the prism, the possible inputs are the length of one side of its equilateral triangular base and its height.

In order to define a particle, we proceed in two steps. For example for the cylindrical particle, we first specify the form factor of a cylinder with its radius and height, both equal to 5 nanometers in this particular case (see line 15). Then we associate this shape with the constituting material as in line 16. The same procedure has been applied for the prism in lines 17 and 18, respectively.

### Characterizing particles assembly

```

19 particle_layout = ParticleLayout()
20 particle_layout.addParticle(cylinder, 0.0, 0.5)
21 particle_layout.addParticle(prism, 0.0, 0.5)
22 interference = InterferenceFunctionNone()
23 particle_layout.addInterferenceFunction(interference)

```

The object which holds the information about the positions and densities of particles in our sample is called `ParticleLayout` (line 19). We use the associated function `addParticle` for each particle shape (lines 20, 21). Its general syntax is

```
addParticle(<particle_name>, depth, abundance)
```

where `<particle_name>` is the name used to define the particles (lines 16 and 18), `depth` (default value = 0) is the vertical position, expressed in nanometers, of the particles in a given layer (the association with a particular layer will be done during the next step) and `abundance` is the proportion of this type of particles, normalized to the total number of particles. Here we have 50% of cylinders and 50% of prisms.

**Remark: Depth of particles**

 The vertical positions of the particles in a layer are given in relative coordinates. For the top layer, the bottom of the layer corresponds to depth=0 and negative values would correspond to particles floating above layer 1 since the vertical axis, shown in figure 3.1 is pointing upwards. But for all the other layers, it is the top of the layer which corresponds to depth=0.

Finally, lines 22 and 23 specify that there is **no coherent interference** between the waves scattered by these particles. In this case, the intensity is calculated by the incoherent sum of the scattered waves:  $\langle |F_j|^2 \rangle$ , where  $F_j$  is the form factor associated with the particle of type  $j$ . The way these waves interfere imposes the horizontal distribution of the particles as the interference reflects the long or short-range order of the particles distribution (see Section 5.2). On the contrary, the vertical position is imposed when we add the particles in a given layer by parameter depth, as shown in lines 20 and 21.

**Multilayer**

```

24 # air layer with particles and substrate form multi layer
25     air_layer = Layer(m_air)
26     air_layer.addLayout(particle_layout)
27     substrate_layer = Layer(m_substrate, 0)
28     multi_layer = MultiLayer()
29     multi_layer.addLayer(air_layer)
30     multi_layer.addLayer(substrate_layer)
31     return multi_layer

```

We now have to configure our sample. For this first example, the particles, *i.e.* cylinders and prisms, are on top of a substrate in an air layer. **The order in which we define these layers is important: we start from the top layer down to the bottom one.**

Let us start with the air layer. It contains the particles. In line 25, we use the previously defined `mAmbience` ("air" material) (line 10). The command in line 26 shows that this layer contains particles which are defined using particle layout object. The substrate layer only contains the substrate material (line 27).

There are different possible syntaxes to define a layer. As shown in lines 25 and 27, we can use `Layer(<material_name>, thickness)` or `Layer(<material_name>)`. The second case corresponds to the default value of the thickness, equal to 0. The thickness is expressed in nanometers.

Our two layers are now fully characterized. The sample is assembled using `MultiLayer()` constructor (line 28): we start with the air layer decorated with the particles (line 29), which is the layer at the top and end with the bottom layer, which is the substrate (line 30).

**Characterizing the input beam and output detector**

```

32 def get_simulation():
33     """

```

```

34     Create and return GISAXS simulation with beam and detector
35         defined
36     """
37     simulation = Simulation()
38     simulation.setDetectorParameters(100, -1.0*degree, 1.0*degree
39                                     , 100, 0.0*degree, 2.0*degree)
40     simulation.setBeamParameters(1.0*angstrom, 0.2*degree, 0.0*
41                                   degree)
42     return simulation

```

The first stage is to create the `Simulation()` object (line 36). Then we define the detector (line 37) and beam parameters (line 38). Those functions are part of the `Simulation` class. The different incident and exit angles are shown in figure 3.1.

The detector parameters are set using ranges of angles via the function:

```
setDetectorParameters(n_phi, phi_f_min, phi_f_max, n_alpha,
                      alpha_f_min, alpha_f_max),
```

where number of bins `n_phi`, low edge of first bin `phi_f_min` and upper edge of last bin `phi_f_max` all together define  $\phi_f$  detector axis, while `n_alpha`, `alpha_f_min` and `alpha_f_max` are related to  $\alpha_f$  detector axis.

Remark: Axis binning

**!** By default axes are binned to provide constant bin size in k-space, which means slightly non-equidistant binning in angle space. Other possible options, including user defined axes with custom variable bin size are explained elsewhere.

To characterize the beam we use function

```
setBeamParameters(lambda, alpha_i, phi_i),
```

where `lambda` is the incident beam wavelength, `alpha_i` is the incident grazing angle on the surface of the sample, `phi_i` is the in-plane direction of the incident beam (measured with respect to the *x*-axis).

Remark: Scattering vector

**!** In BornAgain the wave vector **q** is defined as  $\mathbf{k}_i - \mathbf{k}_f$ , where  $\mathbf{k}_i$  is the incident wave vector and  $\mathbf{k}_f$  the scattered one.

### Running the simulation and plotting the results

```

40 def run_simulation():
41     """
42     Run simulation and plot results
43     """
44     sample = get_sample()
45     simulation = get_simulation()
46     simulation.setSample(sample)
47     simulation.runSimulation()
48     result = simulation.getIntensityData().getArray() + 1 # for
49         log scale

```

```

49     pylab.imshow(numpy.rot90(result, 1), norm=matplotlib.colors.
50                  LogNorm(), extent=[-1.0, 1.0, 0, 2.0])
      pylab.show()

```

The function, whose definition starts from line 40, gathers all items. We create the sample and the simulation objects at the lines 44 and 45, using calls to the previously defined functions. We assign the sample to the simulation at line 46 and finally launch the simulation at line 47.

In line 48 we obtain the simulated intensity as a function of outgoing angles  $\alpha_f$  and  $\phi_f$  for further uses (plots, fits,...) as a NumPy array containing  $n_{\text{phi}} \times n_{\text{alpha}}$  datapoints. Lines 49-50 produces the two-dimensional contourplot of the intensity as a function of  $\alpha_f$  and  $\phi_f$  shown in figure 3.2.

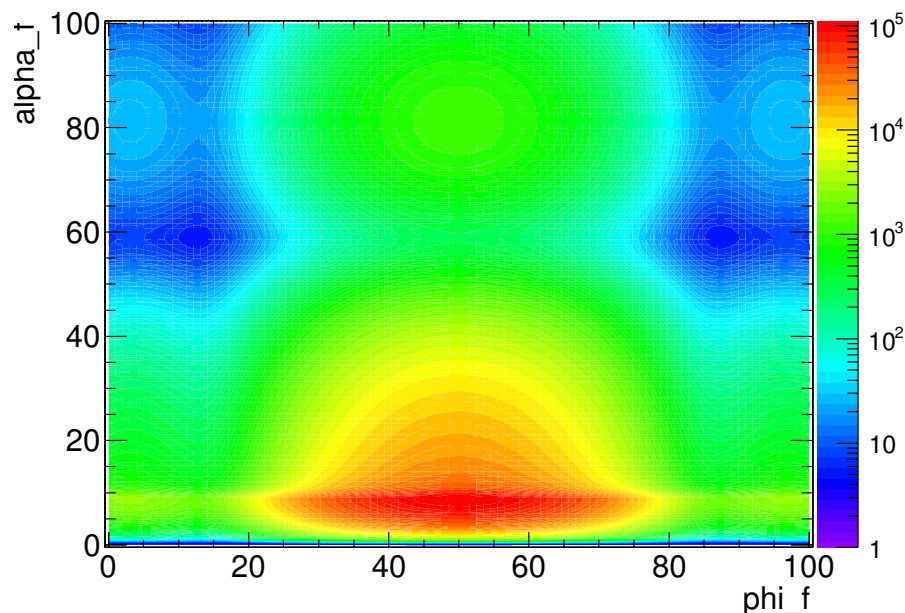


Figure 3.2: Simulated grazing-incidence small-angle X-ray scattering from a mixture of cylindrical and prismatic nanoparticles without any interference, deposited on top of a substrate. The input beam is characterized by a wavelength  $\lambda$  of 1 Å and incident angles  $\alpha_i = 0.2^\circ$ ,  $\phi_i = 0^\circ$ . The cylinders have a radius and a height both equal to 5 nm, the prisms are characterized by a side length equal to 10 nm and they are 5 nm high. The material of the particles has a refractive index of  $1 - 6 \times 10^{-4} + i2 \times 10^{-8}$ . For the substrate it is equal to  $1 - 6 \times 10^{-6} + i2 \times 10^{-8}$ . The colorscale is associated with the output intensity in arbitrary units.

### 3.4 Example 2: working with sample parameters

This section gives additional details about the manipulation of sample parameters during run time; that is after the sample has already been constructed. For a single simulation this is normally not necessary. However it might be useful during interactive work when the user tries to find optimal sample parameters by running a series of simulations. A similar task also arises when the theoretical model, composed of the description of the sample and of the simulation, is used for fitting real data. In this case, the fitting kernel requires a list of the existing sample parameters and a mechanism for changing the values of these parameters in order to find their optima.

In BornAgain this is done using the so-called sample parameter pool mechanism. We are going to briefly explain this approach using the example of Section 3.3.

In BornAgain a sample is described by a hierarchical tree of objects. For the multilayer created in the previous section this tree can be graphically represented as shown in Fig. 3.3. Similar trees can be printed in a Python session by running `multi_layer.printSampleTree()`

The top `MultiLayer` object is composed of three children, namely `Layer #0`, `Layer Interface #0` and `Layer #1`. The children objects might themselves also be decomposed into tree-like structures. For example, `Layer #0` contains a `ParticleLayout` object, which holds information related to the two types of particles populating the layer. All numerical values used during the sample construction (thickness of layers, size of particles, roughness parameters) are part of the same tree structure. They are marked in the figure with shaded gray boxes.

These values are registered in the sample parameter pool using the name composed of the corresponding nodes' names. And they can be accessed/changed during run time. For example, the height of the cylinders populating the first layer can be changed from the current value of 5 nm to 1 nm by running the command

```
multi_layer.setParameterValue('/MultiLayer/Layer0/ParticleLayout/
    ParticleInfo0/Particle/FormFactorCylinder/height', 1.0)
```

A list of the names and values of all registered sample's parameters can be displayed using the command

```
> multi_layer.printParameters()
The sample contains following parameters ('name':value)
'/MultiLayer/Layer0/ParticleLayout/ParticleInfo0/Particle/
    FormFactorCylinder/height':5
'/MultiLayer/Layer0/ParticleLayout/ParticleInfo0/Particle/
    FormFactorCylinder/radius':5
'/MultiLayer/Layer0/ParticleLayout/ParticleInfo0/abundance':0.5
'/MultiLayer/Layer0/ParticleLayout/ParticleInfo0/depth':0
'/MultiLayer/Layer0/ParticleLayout/ParticleInfo1/Particle/
    FormFactorPrism3/length':5
'/MultiLayer/Layer0/ParticleLayout/ParticleInfo1/Particle/
    FormFactorPrism3/height':5
'/MultiLayer/Layer0/ParticleLayout/ParticleInfo1/abundance':0.5
'/MultiLayer/Layer0/ParticleLayout/ParticleInfo1/depth':0
```

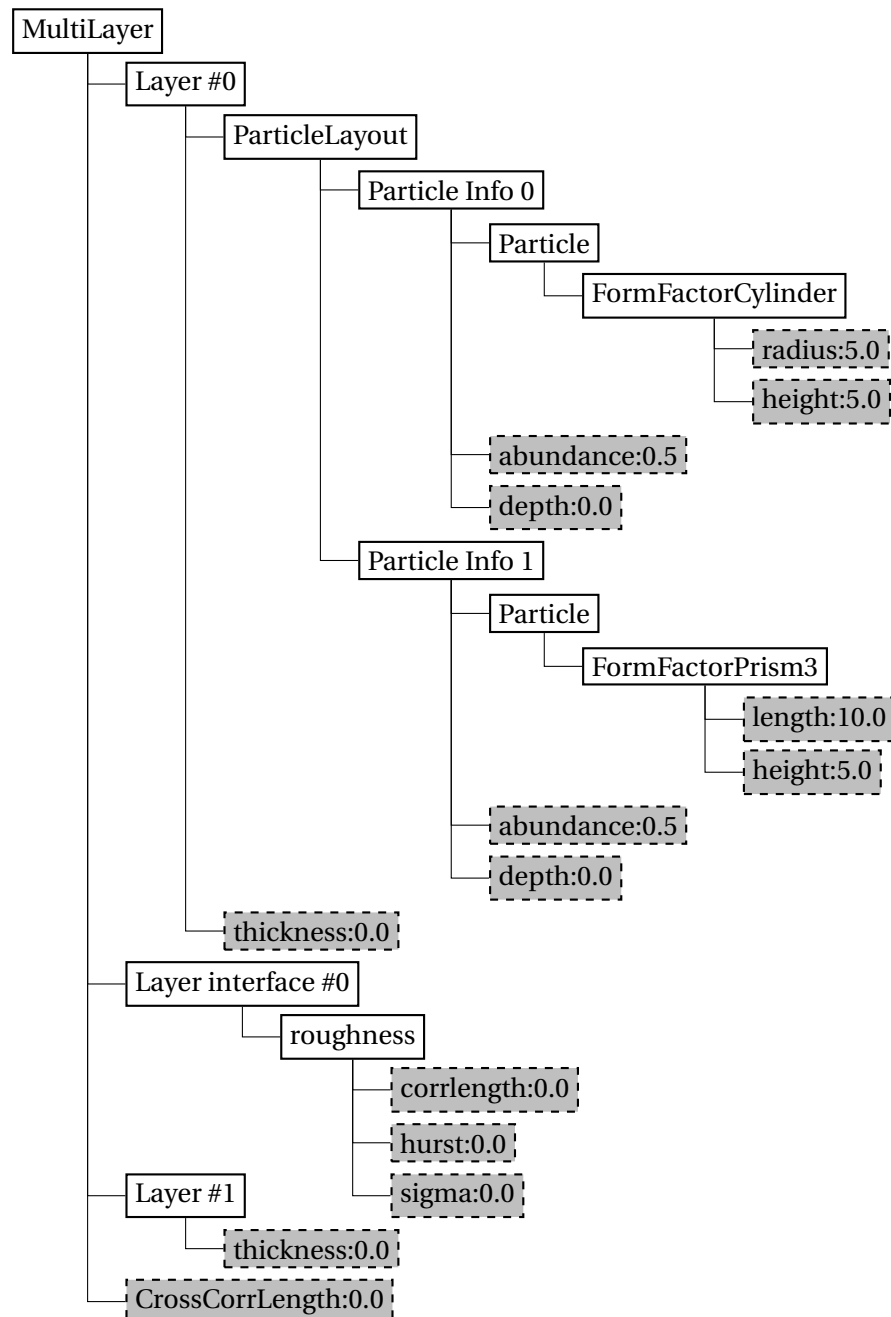


Figure 3.3: Tree representation of the sample structure.

```
'/MultiLayer/Layer0/thickness':0  
'/MultiLayer/Layer1/thickness':0  
'/MultiLayer/LayerInterface/roughness/corrlength':0  
'/MultiLayer/LayerInterface/roughness/hurst':0  
'/MultiLayer/LayerInterface/roughness/sigma':0  
'/MultiLayer/crossCorrLength':0
```

Wildcards '\*' can be used to reduce typing or to work on a group of parameters. In the example below, the first command will change the height of all cylinders in the same way, as in the previous example. The second line will change simultaneously the height of *both* cylinders and prisms.

```
multi_layer.setParameterValue('*FormFactorCylinder/height', 1.0)  
multi_layer.setParameterValue('*height', 1.0)
```

The complete example described in this section can be found at

```
./Examples/python/fitting/ex001_SampleParametersIntro/  
SampleParametersIntro.py
```

## **Chapter 4**

# **Graphical User Interface**

To be completed.

## Chapter 5

# Scattering cross-section

### 5.1 Position of the problem

This section describes how assemblies of particles and layers of materials contribute to the scattering cross-section *i.e.* the way their spatial distributions, the distribution of shapes and their correlations or layers' roughness can influence the output intensity.

The samples generated with BornAgain are made of different layers of materials characterized by their thicknesses, refractive indices, and possible surface roughnesses. Except for the thickness, the other dimensions of the layers are infinite.

Particles can be embedded in or deposited on the top of any layers. Those particles are characterized by their shapes, refractive indices, their spatial distribution and concentration in the sample. The influence of the particles' shapes is described by the form factors. When the particles are densely packed, the distance relative to each other becomes of the same order as the particles' sizes. The radiation scattered from these various particles are going to interfere together.

We are first going to give a short overview of the theory involved, mostly in order to define the terminology. For a more complete theoretical description, the user is referred to, for example, reference [4] and appendix B of this manual. Then we are going to describe how the interference features, the form factors and the characteristics of the material layers have been implemented in BornAgain and give some examples.

### 5.2 Collection of particles

Let us consider the general geometry of a scattering experiment. An incident neutron with a wave vector  $\mathbf{k}_i$  is scattered in a new direction  $\mathbf{k}_f$  after interacting with a particle. This scattering occurs in a cone of solid angle  $d\Omega$  around the direction of the scattered wave vector  $\mathbf{k}_f$ . Considering a set of  $N$  particles labeled with index  $i$ , located at  $\mathbf{R}_i$  and having shapes  $S_i(\mathbf{r})$  ( $S_i = 0$  outside the particle and 1 inside), occupying a total volume  $V$ , the differential

cross-section per particle is given by:

$$\frac{d\sigma}{d\Omega}(\mathbf{q}) = \frac{1}{N} \left\{ \sum_i |F_i(\mathbf{q})|^2 + \sum_{i \neq j} F_i(\mathbf{q}) F_j^*(\mathbf{q}) \exp[i\mathbf{q} \cdot (\mathbf{R}_i - \mathbf{R}_j)] \right\}.$$

where  $\mathbf{q} = \mathbf{k}_i - \mathbf{k}_f$  is the wave vector transfer and  $F_i$  is the form factor of particle  $i$  (see Section 5.3 for a description).

Since in most experimental conditions only the statistical properties of the particles are known, one can consider the probabilistic value of this cross-section *i.e.* its expectation value. Assuming that the particles' shapes are determined by their class  $\alpha$ , with the abundance ratio  $p_\alpha \equiv N_\alpha/N$ , and defining the particle density as  $\rho_V \equiv N/V$ , the expectation value becomes:

$$\begin{aligned} \left\langle \frac{d\sigma}{d\Omega}(\mathbf{q}) \right\rangle &= \sum_\alpha p_\alpha |F_\alpha(\mathbf{q})|^2 + \frac{\rho_V}{V} \sum_{\alpha, \beta} p_\alpha p_\beta F_\alpha(\mathbf{q}) F_\beta^*(\mathbf{q}) \\ &\quad \times \iint_V d^3\mathbf{R}_\alpha d^3\mathbf{R}_\beta \mathcal{G}_{\alpha, \beta}(\mathbf{R}_\alpha, \mathbf{R}_\beta) \exp[i\mathbf{q} \cdot (\mathbf{R}_\alpha - \mathbf{R}_\beta)], \end{aligned}$$

where  $\mathcal{G}_{\alpha, \beta}(\mathbf{R}_\alpha, \mathbf{R}_\beta)$  is called the *partial pair correlation function*. It represents the normalized probability of finding particles of type  $\alpha$  and  $\beta$  in positions  $\mathbf{R}_\alpha$  and  $\mathbf{R}_\beta$  respectively.

### 5.2.1 Size-distribution models

To proceed further, when the morphology and topology are not exactly known, some hypotheses need to be made since the correlation between the kinds of scatterers and their relative positions included in the pair correlation functions are difficult to estimate. Several options are available:

**Decoupling approximation (DA)** neglects all correlations. It supposes that the particles are positioned in a way that is completely independent on their kinds (shapes, sizes). An example is given in figure 5.1. Thus the kind of scattering objects and their positions are not correlated and the partial pair correlation function is independent of the particle class  $\alpha$ . We can therefore replace  $\mathcal{G}_{\alpha, \beta}(\mathbf{R}_\alpha, \mathbf{R}_\beta)$  by  $g(\mathbf{R}_\alpha, \mathbf{R}_\beta)$ .

This leads to the following expression of the scattering cross-section:

$$\left\langle \frac{d\sigma}{d\Omega}(\mathbf{q}) \right\rangle = I_d(\mathbf{q}) + |\langle F_\alpha(\mathbf{q}) \rangle_\alpha|^2 \times S(\mathbf{q}),$$

where  $I_d$  is the diffuse part of the scattering. It is the signature of the fluctuations of shapes, sizes or orientations of the particles; its maximum is located in  $q_{\parallel} = 0$ . In the second term of the expression of the scattering cross-section,  $S(\mathbf{q})$  is the interference function and is given by

$$S(\mathbf{q}) = 1 + \rho_V \int_V d^3\mathbf{R} g(\mathbf{R}) \exp[i\mathbf{q} \cdot \mathbf{R}].$$

In concentrated systems, DA breaks down because of correlations. One solution is to reintroduce some correlations between particles sizes and distributions using, for example, the size spacing correlation approximation described below.

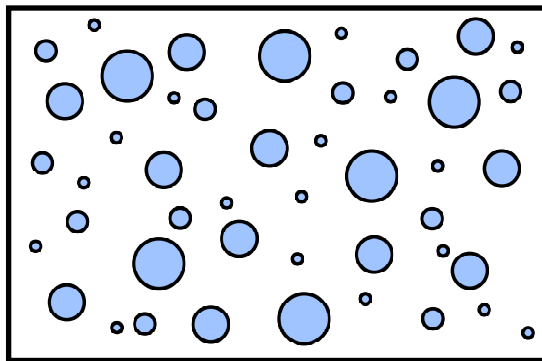


Figure 5.1: Sketch of a collection of particles deposited on a substrate whose scattering could be described by the decoupled approximation.

**Local monodisperse approximation (LMA)** partially accounts for some coupling between the positions and the kinds of the particles [5]. It requires a subdivision of the layers of particles into monodisperse domains. The contributions of these subdomains are then incoherently summed up and weighted by the size-shape probabilities.

In this approximation, a particle is supposed to be surrounded by particles of the same size and shape, within the coherence length of the input beam (see fig. 5.2). The scattering cross-section is expressed as

$$\left\langle \frac{d\sigma}{d\Omega}(\mathbf{q}) \right\rangle \simeq \left\langle |F_\alpha(\mathbf{q})|^2 S_\alpha(\mathbf{q}) \right\rangle_\alpha.$$

Contrary to the Decoupling Approximation, the Local Monodisperse Approximation can account for particle class/size/shape-dependent pair correlation functions by having distinct interference functions  $S_\alpha(\mathbf{q})$ .

One has to remember that in most cases, this approximation corresponds to an unphysical description of the investigated systems.

DA and LMA separate the contributions of the form factors and of the interference function. For disordered systems DA and LMA give the same result as the scattering vector gets larger *i.e.* the scattered intensity is dominated by the contribution of the form factor.

**Size spacing correlation approximation (SSCA)** introduces correlations between polydisperse particles, more precisely between the shape/size of the particles and their mutual spacing. A classical example would consist of particles whose closest-neighbour spacing depends linearly on the sum of their respective sizes [6].

For a sample where only the statistical properties of particle positions and shape/size are known, the scattered intensity per scattering particle is expressed as the average over an ensemble of the Fourier transform of the Patterson function, which is the autocorrelation

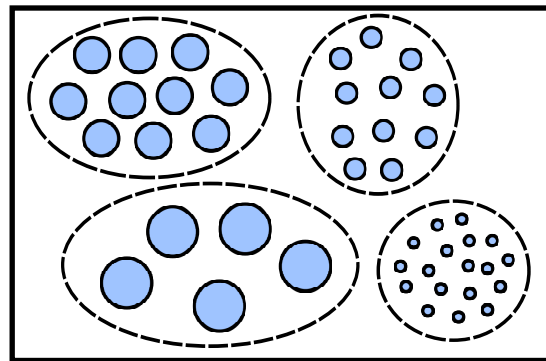


Figure 5.2: Sketch of a collection of particles deposited on a substrate whose scattering could be described by the local monodisperse correlation approximation. The dashed areas mark the coherent domains. In this case, the total scattering intensity is the incoherent sum from all these domains.

of the scattering length density  $\mathcal{P}(\mathbf{r}) \equiv \sum_{ij} S_i(-\mathbf{r}) \otimes S_j(\mathbf{r}) \otimes \delta(\mathbf{r} + \mathbf{r}_i - \mathbf{r}_j)$ :

$$I(\mathbf{q}) = \frac{1}{N} \langle \mathcal{F}(\mathcal{P}(\mathbf{r})) \rangle ,$$

where  $\mathcal{F}$  denotes the Fourier transform and  $\mathcal{P}$  the Patterson function

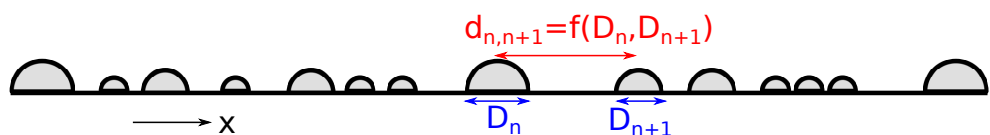


Figure 5.3: Sketch of a 1D distributed collection of particles, whose scattering could be described by the size-spacing correlation approximation: the distance between two particles depends on their sizes.

#### Terminology

 For collections of particles, the scattered intensity contains contributions from neighboring particles. This additional pattern can be called the structure factor, the interference function or even in crystallography, the lattice factor. In this manual, we use the term "interference function" or interferences.

### 5.2.2 Layout of particles

#### The uncorrelated or disordered lattice

For very diluted distributions of particles, the particles are too far apart from each other to lead to any interference between the waves scattered by each of them. In this case the

interference function is equal to 1. The scattered intensity is then entirely determined by the form factors of the particles distributed in the sample.

### The regular lattice

The particles are positioned at regular intervals generating a layout characterised by its base vectors **a** and **b** (in direct space) and the angle between these two vectors. This lattice can be two or one-dimensional depending on the characteristics of the particles. For example when they are infinitely long, the implementation can be simplified and reduced to a "pseudo" 1D system.

### The ideal paracrystal

A paracrystal, whose notion was developed by Hosemann[7], allows fluctuations of the lengths and orientations of lattice vectors. Paracrystals can be defined as distorted crystals in which the crystalline order has not disappeared and for which the behavior of the interference functions at small angles is coherent. It is a transition between the regular lattice and the disordered state.

For example, in one dimension, a paracrystal is generated using the following method. First we place a particle at the origin. The second particle is put at a distance  $x$  with a density probability  $p(x)$  that is peaked at a mean value  $D$ :  $\int_{-\infty}^{\infty} p(x)dx = 1$  and  $\int_{-\infty}^{\infty} xp(x)dx = D$ . The third one is added at a distance  $y$  from the second site using the same rule with a density probability  $p_2(y) = \int_{-\infty}^{\infty} p(x)p(y-x)dx = p \otimes p(y)$ .

With such a method, the pair correlation function  $g(x)$  is built step by step. Its expression and the one of its Fourier transform, which is the interference function are

$$g(x) = \delta(x) + p(x) + p(x) \otimes p(x) + \dots + p(-x) + \dots \text{ and } S(q) = \text{Re} \left( \frac{1 + P(q)}{1 - P(q)} \right),$$

where  $P(q)$  is the Fourier transform of the density probability  $p(x)$ .

In two dimensions, the paracrystal is constructed on a pseudo-regular lattice with base vectors **a** and **b** using the following conditions for the densities of probabilities:

$$\int p_a(\mathbf{r})d^2\mathbf{r} = \int p_b(\mathbf{r})d^2\mathbf{r} = 1, \int \mathbf{r}p_a(\mathbf{r})d^2\mathbf{r} = \mathbf{a}, \int \mathbf{r}p_b(\mathbf{r})d^2\mathbf{r} = \mathbf{b}.$$

In the ideal case the deformations along the two axes are decoupled and each unit cell should retain a parallelogram shape. The interference function is given by

$$S(q_{||}) = \prod_{k=a,b} \text{Re} \left( \frac{1 + P_k(q_{||})}{1 - P_k(q_{||})} \right) \text{ with } P_k \text{ the Fourier transform of } p_k, k = a, b.$$

### Probability distributions

The scattering by an ordered lattice gives rise to a series of Bragg peaks situated at the nodes of the reciprocal lattice. Any divergence from the ideal crystalline case modifies the output spectrum by, for example, widening or attenuating the Bragg peaks. The influence of these "defects" can be accounted for in direct space using correlation functions or by truncating

the lattice or, in reciprocal space with structure factors or interference functions by convoluting the scattered pics with a function which could reproduce the experimental shapes.

### 5.2.3 Implementation in BornAgain

This section describes the implementation of the interference functions in BornAgain. For an implementation of all the components of a simulation, the use is referred, for example, to Section 3.3.



**Remark:** In BornAgain the particles are positioned in the same vertical layer.

#### Size-distribution models

The decoupled approximation, local monodisperse approximation and size spacing correlation approximation can be used in BornAgain. The selection is made using

`ILayout.setApproximation(EInterferenceFunction approximation)` when defining the characteristics of the way particles and interference functions are embedded in a layer. For example,

```
particle_layout = ParticleLayout()
...
# interference approx chosen between: DA (default) and SSCA
particle_layout.setApproximation(ILayout.DA)
```

#### Probability distribution functions

The probability distribution functions have been implemented in the reciprocal space in BornAgain. Their expressions are given in Table 5.1.

Function	One dimension	Two dimensions
Cauchy	$(1 + q^2 \omega^2)^{-3/2}$	$(1 + q_x^2 c l_x^2 + q_y^2 c l_y^2)^{-3/2}$
Gauss	$\frac{1}{2} \exp(-\frac{q^2 \omega^2}{4})$	$\frac{1}{2} \exp\left(-\frac{q_x^2 c l_x^2 + q_y^2 c l_y^2}{4}\right)$
Voigt	$\frac{\eta}{2} \exp\left(-\frac{q^2 \omega^2}{4}\right) + \frac{1-\eta}{(1+q^2 \omega^2)^{3/2}}$	$\frac{\eta}{2} \exp\left(-\frac{q_x^2 c l_x^2 + q_y^2 c l_y^2}{4}\right) + \frac{1-\eta}{(1+q_x^2 c l_x^2 + q_y^2 c l_y^2)^{3/2}}$

Table 5.1: List of probability distribution functions in reciprocal space.  $\omega$ ,  $cl$  stand for coherence lengths (the index refers to the axis) and  $\eta$  is a weighting coefficient.

The Cauchy distribution corresponds to  $\exp(-r)$  in real space and the Voigt one is a linear combination of the Gaussian and Cauchy probability distribution functions.

#### One dimension

- `FTDistribution1DCauchy( $\omega$ )`,

- `FTDistribution1DGauss( $\omega$ ),`
- `FTDistribution1DVoigt( $\omega, \eta$ ).`

where  $\omega$  is the coherence length and  $\eta$  is a weighting factor.

### Two dimensions

- `FTDistribution2DCauchy( $cl_x, cl_y$ ),`
- `FTDistribution2DGauss( $cl_x, cl_y$ ),`
- `FTDistribution2DVoigt( $cl_x, cl_y$ )`

where  $cl_{x,y}$  are the coherence lengths in the  $x$  or  $y$  direction, respectively.

These functions can be used with all interference functions except the case without any interference and the one dimensional paracrystal, for which only the Gaussian case has already been implemented.

### **Interferences**

The interference function is specified when building the sample. It is linked with the particles (shape, material). Examples of implementation are given at the end of each description.

**Syntax:** `particle_layout.addInterferenceFunction(interference_function)`, where `particle_layout` holds the information about the different shapes and their proportions for a given layer of particles, and `interference_function` is one of the following expressions:

- `InterferenceFunctionNone()`
- `InterferenceFunction1DLattice(lattice_parameters)`
- `InterferenceFunction1DParaCrystal(peak_distance, width, corr_length)`
- `InterferenceFunction2DLattice(lattice_parameters)`
- `InterferenceFunction2DParaCrystal(length_1, length_2,  $\alpha_lattice$ ,  $\xi$ , damping_length)`



**Remark:** `InterferenceFunction1DLattice` can only be used for particles which are infinitely long in one direction of the sample's surface like for example a rectangular grating.

**» InterferenceFunctionNone()**

The particles are placed randomly in the dilute limit and are considered as individual, non-interacting scatterers. The scattered intensity is function of the form factors only.

**Example** The sample is made of a substrate on which are deposited half-spheres. Script 5.1 details the commands necessary to generate such a sample. Figure 5.4 shows an example of output intensity: Script 5.1 + detector's + input beam's characterizations. The full script UMInterferencesNone.py can be found in /Examples/python/UserManual.

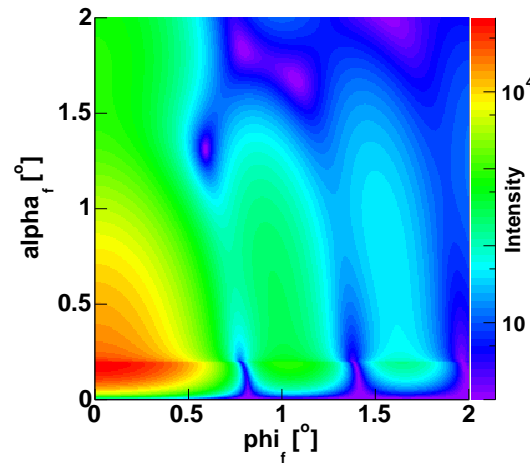


Figure 5.4: Output intensity scattered from a sample made of half-spheres with no interference between them.

Listing 5.1: Python script to simulate a sample made of half-spheres deposited on a substrate layer without any interference. The part specific to the interferences is marked in red italic font.

```
def get_sample():
    """
        Build and return the sample representing particles with no
        interference
    """
    # defining materials
    m_ambience = HomogeneousMaterial("Air", 0.0, 0.0)
    m_substrate = HomogeneousMaterial("Substrate", 6e-6, 2e-8)
    m_particle = HomogeneousMaterial("Particle", 6e-4, 2e-8)
    # collection of particles
    sphere_ff = FormFactorTruncatedSphere(5*nanometer, 5*
        nanometer)
    sphere = Particle(m_particle, sphere_ff)
    particle_layout = ParticleLayout()
    particle_layout.addParticle(sphere, 0.0, 1.0)
    interference = InterferenceFunctionNone()
    particle_layout.addInterferenceFunction(interference)
    # assembling the sample
    air_layer = Layer(m_ambience)
    air_layer.addLayout(particle_layout)
    substrate_layer = Layer(m_substrate, 0)

    multi_layer = MultiLayer()
    multi_layer.addLayer(air_layer)
    multi_layer.addLayer(substrate_layer)
    return multi_layer
```

► `InterferenceFunction1DLattice(lattice_length, xi)`

where `lattice_length` is the lattice constant and  $\xi$  the angle in radian between the lattice unit vector and the **x**-axis of the "GISAS experiment" referential as shown in fig. 5.5.

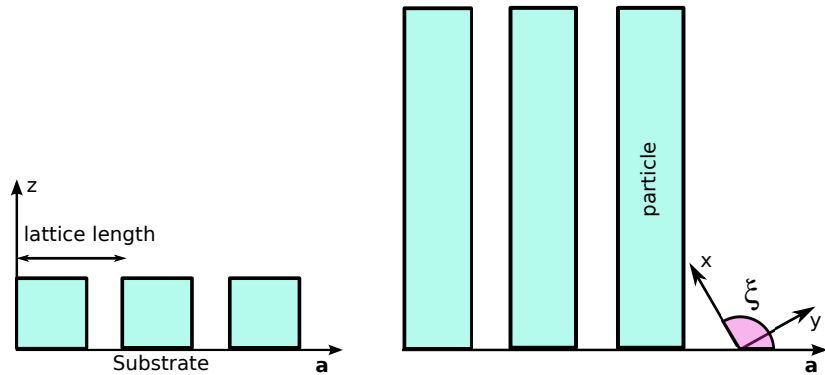


Figure 5.5: Schematic representation of a 1D lattice (side and top views). Such a lattice is characterized by a lattice length and the angle  $\xi$ .



**Remark:** By default the long axis of the particles in this 1D lattice is along the beam axis:  $\xi = 90^\circ$ .

A probability distribution function `pdf` has to be chosen from the list in section 5.2.3 in order to apply some modifications to the scattering peaks. This function is implemented using `setProbabilityDistribution(pdf)`.

**Example:** Script 5.2 details how to build in BornAgain a sample using `InterferenceFunction1DLattice` as the interference function. As mentioned previously, this interference function can only be used with infinitely wide or long particles. Here the sample is made of infinitely long boxes deposited on a substrate (these particles are characterized by their widths and heights). They are also rotated by  $90^\circ$  in the sample surface in order to have their long axis perpendicular to the input beam, which is along the  $x$ -axis.

The lattice parameters (the lattice length and angle between the lattice main axis and the  $x$ -axis) are passed into the constructor of the interference function.

Listing 5.2: Python script to generate a sample made of infinitely long boxes deposited on a substrate layer with the `1DLatticeInterference` function. The part specific to the interferences is marked in red italic font.

```
def get_sample():
    """
        Build and return the sample with 1DLatticeInterference
        function
    """

    # defining materials
    m_air = HomogeneousMaterial("Air", 0.0, 0.0)
    m_substrate = HomogeneousMaterial("Substrate", 6e-6, 2e-8)
    m_particle = HomogeneousMaterial("Particle", 6e-4, 2e-8)

    # collection of particles
    ff = FormFactorInfLongBox(10.*nanometer, 15.0*nanometer)
    box = Particle(m_particle, ff)
    particle_layout = ParticleLayout()
    transform = Transform3D.createRotateZ(90.0*degree)
    particle_layout.addParticle(box, transform)

    # interference function
    interference = InterferenceFunction1DLattice(30.0*nanometer,
    0.0*degree)
    pdf = FTDistribution1DCauchy(200./2./M_PI*nanometer)
    interference.setProbabilityDistribution(pdf)
    particle_layout.addInterferenceFunction(interference)

    # air layer with particles and substrate form multi layer
    air_layer = Layer(m_air)
    air_layer.setLayout(particle_layout)
    substrate_layer = Layer(m_substrate, 0)

    multi_layer = MultiLayer()
    multi_layer.addLayer(air_layer)
    multi_layer.addLayer(substrate_layer)
    return multi_layer
```

► `InterferenceFunction1DParaCrystal(peak_distance, width, corr_length)`

where `peak_distance` is the average distance to the first neighbor peak,

`width` is the width parameter of the probability distribution,

`corr_length` is the correlation length (equal to 0 by default).

For this particular interference function, the implemented probability distribution function is Gaussian:

$$p(x) = \frac{1}{\omega\sqrt{2\pi}} \exp\left(-\frac{(x-D)^2}{\omega^2}\right), \quad P(q_{\parallel}) = \exp\left(-\frac{q_{\parallel}^2\omega^2}{2}\right) \exp(iq_{\parallel}D)$$

where  $\omega \equiv \text{width}$ ,  $D \equiv \text{peak\_distance}$ , and  $q_{\parallel} = \sqrt{\text{Re}^2(q_x) + \text{Re}^2(q_y)}$  (see fig. 5.6).

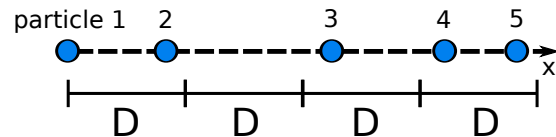


Figure 5.6: Schematic representation of a 1D paracrystal in real space (side view).  $D$  is the average spacing between the particles.

Using the procedure described in Section 5.2.2, the interference function of a one-dimensional paracrystal is given by

$$S(q_{\parallel}) = \text{Re}\left(\frac{1 + \Phi(q_{\parallel})}{1 - \Phi(q_{\parallel})}\right),$$

where  $\Phi(q_{\parallel}) = \begin{cases} P(q_{\parallel}) & \text{if } \text{corr\_length} = 0 \\ P(q_{\parallel}) \exp\left(-\frac{D}{\text{corr\_length}}\right) & \text{otherwise} \end{cases}$

Figure 5.7 shows the evolution of  $S(q)$  for different values of  $\omega/D$ .

**Remark** In BornAgain the one-dimensional disorder linked with this interference function is radial.

**Example** To illustrate the 1D paracrystal interference function, we use the same sample as in the case without interference: half-spheres deposited on a substrate.

Listing 5.3: Python script to define the 1D paracrystal interference function between half-spheres, where `trsphere` is of type `Particle`.

```
particle_layout = ParticleLayout()
particle_layout.addParticle(trsphere, 0.0, 1.0)
```

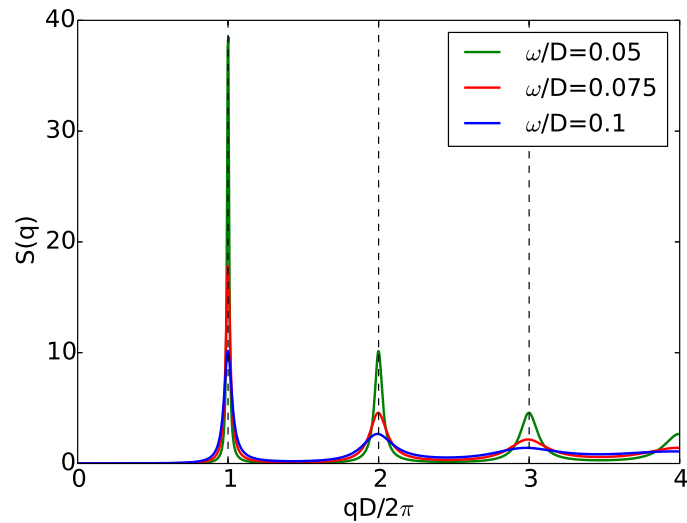


Figure 5.7: Interference function of a 1D Gaussian paracrystal plotted for different values of  $\omega/D$ . The peaks broaden with a decreasing amplitude as  $\omega/D$  increases. This shows the transition between an ordered and a disordered states.

```
interference = InterferenceFunction1DParaCrystal(25.0*
    nanometer, 7*nanometer, 1e3*nanometer)
particle_layout.addInterferenceFunction(interference)
```

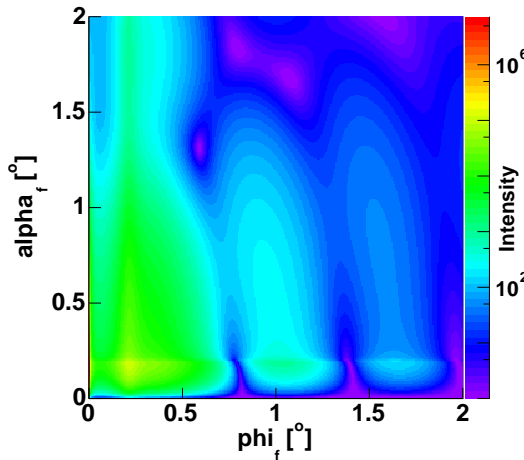


Figure 5.8: Output intensity scattered from a sample made of half-spheres with 1Dparacrystal interference between them. This figure has been generated using Script 5.3 for the interference function. The full script UMInterferences1DParaCrystal.py can be found in /Examples/python/UserManual.

► `InterferenceFunction2DLattice(L_1, L_2, alpha, xi)`

where  $(L_1, L_2, \alpha, \xi)$  are shown in figure 5.9) with

$L_1, L_2$  the lengths of the lattice cell,

$\alpha$  the angle between the lattice basis vectors  $\mathbf{a}, \mathbf{b}$  in direct space,

$\xi$  is the angle defining the lattice orientation (set to 0 by default); it is taken as the angle between the  $\mathbf{a}$  vector of the lattice basis and the  $\mathbf{x}$  axis of the "GISAS experiment" referential (as shown in figure 3.1).

Like for the one-dimensional case, a probability distribution function `pdf` has to be defined. One can choose between those listed in Section 5.2.3 and implements it using `setProbabilityDistribution(pdf)`.

**Example** The sample used to run the simulation is made of half-spheres deposited on a substrate. The interference function is "2Dlattice" and the particles are located at the nodes of a square lattice with  $L_1 = L_2 = 20$  nm,  $\mathbf{a} \equiv \mathbf{b}$  and the probability distribution function is Gaussian. We also use the Decoupling Approximation.

Listing 5.4: Python script to define a 2DLattice interference function between hemispherical particles as well as the Decoupling Approximation in `getSimulation()`. The part specific to the interferences is marked in red italic font.

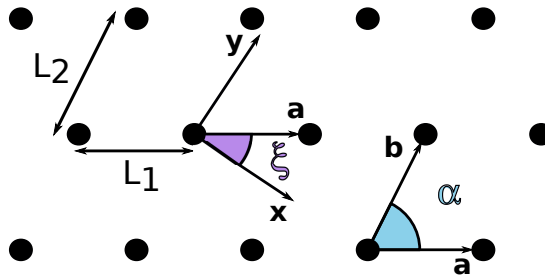


Figure 5.9: Schematic representation of a 2D lattice (top view). Such a lattice is characterized by lattice lengths  $L_1$ ,  $L_2$  and angles  $\alpha$  and  $\xi$ .

```
#collection of particles
sphere_ff = FormFactorTruncatedSphere(5*nanometer, 5*
    nanometer)
sphere = Particle(m_particle, sphere_ff)
interference = InterferenceFunction2DLattice(20.0*nanometer,
    20.0*nanometer, 90.0*degree, 0.0*degree)
pdf = FTDistribution2DGauss(200.0*nanometer/2.0/M_PI, 75.0*
    nanometer/2.0/M_PI)
interference.setProbabilityDistribution(pdf)
particle_layout = ParticleLayout()
particle_layout.addParticle(sphere, 0.0, 1.0)
particle_layout.addInterferenceFunction(interference)

# interference approx chosen between: DA (default) and SSCA
particle_layout.setApproximation(ILayout.DA)
```

```
def get_simulation():
    """
    Create and return GISAXS simulation with beam and detector
    """
    simulation = Simulation()
    simulation.setDetectorParameters(100, 0.0*degree, 2.0*degree,
        100, 0.0*degree, 2.0*degree, True)
    simulation.setBeamParameters(1.0*angstrom, 0.2*degree, 0.0*
        degree)
    return simulation
```

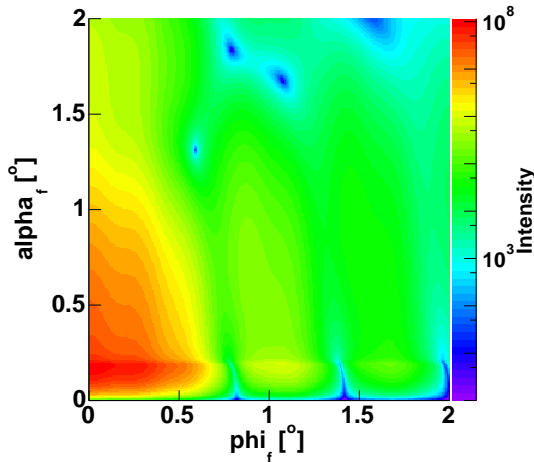


Figure 5.10: Output intensity scattered from a sample made of half-spheres with 2DLattice interference function. Python script available in /Examples/python/UserManual/UMInterferences2DLattice.py.

**»** `InterferenceFunction2DParaCrystal(L_1, L_2, lattice_angle, ξ, damping_length)`  
where  $L_1, L_2$  are the lengths of the lattice cell,

`lattice_angle` the angle between the lattice basis vectors **a**,**b** in direct space,

`ξ` is the angle defining the lattice orientation (set to 0 by default).

`damping_length` is a "damping" length. It is used to introduce finite size effects by applying a multiplicative coefficient equal to  $\exp(\text{peak\_distance}/\text{damping\_length})$  to the Fourier transform of the probability densities. `damping_length` is equal to 0 by default and, in this case, no correction is applied.

Two predefined interference functions can also be used:

- `createSquare(peak_distance, damping_length, domain_size_1, domain_size_2)`  
where the angle between the base vectors of the lattice is set to  $\pi/2$ , it creates a squared lattice,
- `createHexagonal(peak_distance, damping_length, domain_size_1, domain_size_2)`  
where the angle between the base vectors of the lattice is set to  $2\pi/3$ ,

where `domain_size1, 2` are the dimensions of coherent domains of the paracrystal along the main axes,

`peak_distance` is the same in both directions and  $\mathbf{a} \equiv \mathbf{x}$ .

Probability distribution functions have to be defined. As the two-dimensional paracrystal is defined from two independent 1D paracrystals, we need two of these functions, using `setProbabilityDistributions(pdf_1, pdf_2)`, with `pdf_1,2` are related to each main axis of the paracrystal (see figure 5.11).

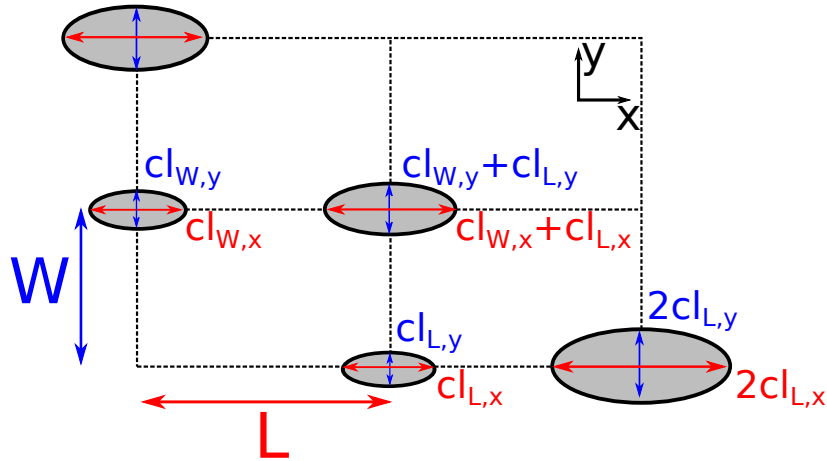


Figure 5.11: Schematics of the ideal 2D paracrystal. The grey-shaded areas mark the regions where the probability to find a node is larger than the width at half-maximum of the distribution.  $L$  and  $W$  are the mean inter-node distances along the two crystallographic axes.  $cl_{(L,W),(x,y)}$  are the widths of the distribution of distance. The disorder is propagated as we add more nodes. Such a structure would be generated using `InterferenceFunction2DParacrystal(L,W,90.*degrees,0,damp_length)`, with `pdf1 = FTDistribution2DGauss(cl_{L,x},cl_{L,y})` and `pdf2 = FTDistribution2DGauss(cl_{W,x},cl_{W,y})`.

**Example** The particles deposited on a substrate are half-spheres. The scattered beams interference via the 2DParacrystal distribution function. The paracrystal is based on a 2D hexagonal lattice with a Gaussian probability distribution function in reciprocal space. Script 5.5 shows the implementation of the interference function and fig. 5.12 an example of output intensity using hemi-spherical particles. The full script, `UMInterferences2DParacrystal.py` is available in `/Examples/python/UserManual`.

Listing 5.5: Python script to define a "2DParacrystal" interference function between particles forming an hexagonal monolayer.

```
interference = InterferenceFunction2DParaCrystal.
    createHexagonal(30.0*nanometer, 0.0, 40.0*micrometer,
        40.0*micrometer)
pdf = FTDistribution2DCauchy(1.0*nanometer, 1.0*nanometer)
interference.setProbabilityDistributions(pdf, pdf)
particle_layout.addInterferenceFunction(interference)
```

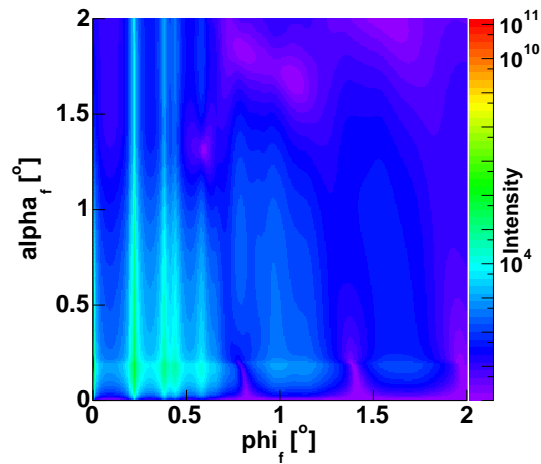


Figure 5.12: Output intensity scattered from a sample made of half-spheres with 2DParacrystal interference function.

#### 5.2.4 Summary

Function	Parameters	Comments
InterferenceFunctionNone	None	disordered distribution
InterferenceFunction1DLattice	lattice_length $\xi = \widehat{(\mathbf{x}, \mathbf{a})}$	use only with infinitely long/wide particles pdf=(Cauchy, Gauss or Voigt) to be defined
InterferenceFunction1DParaCrystal	peak_distance of pdf width of pdf corr_length (optional)	only Gaussian pdf implemented (no option)
InterferenceFunction2DLattice	L_1, L_2: lattice lengths lattice_angle= $\widehat{(\mathbf{a}, \mathbf{b})}$ $\xi = \widehat{(\mathbf{x}, \mathbf{a})}$	pdf=(Cauchy, Gauss or Voigt) to be defined
InterferenceFunction2DParaCrystal	L_1, L_2: lattice lengths lattice_angle= $\widehat{(\mathbf{a}, \mathbf{b})}$ $\xi = \widehat{(\mathbf{x}, \mathbf{a})}$ damping_length (optional)	2D pdf=(Cauchy, Gauss or Voigt) to be defined (1 pdf per axis) same for both axes

Table 5.2: List of interference functions implemented in BornAgain. pdf : probability distribution function,  $\mathbf{a}, \mathbf{b}$  are the lattice base vector, and  $\mathbf{x}$  is the axis vector perpendicular to the detector plane.

## 5.3 Particles - Form factors

### 5.3.1 Born approximation

In BornAgain the form factor is defined using Born approximation as

$$F(\mathbf{q}) = \int_V \exp(i\mathbf{q} \cdot \mathbf{r}) d^3\mathbf{r}, \quad (5.1)$$

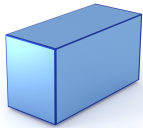
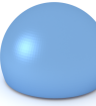
where  $V$  is the volume of the particle,  $\mathbf{q} = \mathbf{k}_i - \mathbf{k}_f$  is the scattering vector with  $\mathbf{k}_f$  and  $\mathbf{k}_i$  the scattered and incident wave vector, respectively.

The particle's shape is parametrized in a cartesian frame, with its  $z$ -axis pointing upwards and its origin at the center of the bottom of the particle:  $\mathbf{r} = (x, y, z)$ .

All form factors have been implemented with complex scattering vectors in order to take any material absorption into account.

Table 5.3 lists the shapes whose form factors have been implemented in BornAgain and a detailed description is given in Appendix C.

Table 5.3: Table of form factors implemented in BornAgain.

Box, Section C.1	Prism3, Section C.2	Tetrahedron, Section C.3	Prism6, Section C.4
			
Cone6, Section C.5	Pyramid, Section C.6	Anisotropic pyramid, Section C.7	Cuboctahe- dron, Section C.8
			
Cylinder, Section C.9	Ellipsoidal cylinder, Section C.10	Cone, Section C.11	Full Sphere, Section C.12
			
Truncated Sphere, Section C.13	Full Spheroid, Section C.14	Truncated Spheroid, Section C.15	Hemi Ellipsoid, Section C.16
			
Ripple1, Section C.17	Ripple2, Section C.18		
			

### 5.3.2 Distorted Wave Born Approximation

Born approximation fails when multiple reflections and refractions have to be taken into account at interfaces because of the presence of underlying layers of materials and the closeness of the incident angle  $\alpha_i$  to the critical angle of total external reflection  $\alpha_c$ . The first order correction to the scattering theory is the Distorted Wave Born Approximation (DWBA), whereas the Born approximation is the zeroth order.

The collective effects between the particles are not considered in this section. They have been described in Section 5.2. We also do not take any polarization effects into account. They will be described in...

In the DWBA, the form factor of a particle in a multilayer system is given by

$$F_{\text{DWBA}}(\mathbf{k}_i, \mathbf{k}_f, r_z) = T_i T_f F_{\text{BA}}(\mathbf{k}_i - \mathbf{k}_f) e^{i(k_{i,z} - k_{f,z})r_z} + R_i T_f F_{\text{BA}}(\tilde{\mathbf{k}}_i - \mathbf{k}_f) e^{i(-k_{i,z} - k_{f,z})r_z} \\ + T_i R_f F_{\text{BA}}(\mathbf{k}_i - \tilde{\mathbf{k}}_f) e^{i(k_{i,z} + k_{f,z})r_z} + R_i R_f F_{\text{BA}}(\tilde{\mathbf{k}}_i - \tilde{\mathbf{k}}_f) e^{i(-k_{i,z} + k_{f,z})r_z}, \quad (5.2)$$

where  $F_{\text{BA}}$  is the expression of the form factor in the Born approximation,  $r_z$  is the  $z$ -coordinate of the particle's position (measured from the bottom of the particle),  $\mathbf{k}_i = (k_{i,x}, k_{i,y}, k_{i,z})$ ,  $\mathbf{k}_f = (k_{f,x}, k_{f,y}, k_{f,z})$  are the incident and scattered wave vectors in air, respectively [8]. With a tilde ( $\tilde{\cdot}$ ), these wavevectors components are evaluated in the multilayer system (the refractive indices of the different constituting materials have to be taken into account).  $T_i$ ,  $T_f$ ,  $R_i$ ,  $R_f$  are the transmission and reflection coefficients for the incident wave (index  $i$ ) or the scattered one (index  $f$ ). These coefficients can be calculated using the Parratt formalism [9] or the matrix method [10].  $\mathbf{k}_i - \mathbf{k}_f$  is equal to the scattering vector  $\mathbf{q}$  and the  $z$ -axis is pointing upwards.



**Remark:** The particles cannot sit in between layers. At most they can be sitting on any inner interfaces.

In the followings, the DWBA will be illustrated for two different layouts of particles:

- particles deposited on a substrate,
- particles buried in a layer on a substrate.



**Remark:** In BornAgain there is no limitation to the number of layers composing the sample.

#### Particles deposited on a substrate

In this configuration, the particles are sitting on top of a substrate layer, in the air as shown in fig. 5.13. In the DWBA the expression of a form factor becomes

$$F_{\text{DWBA}}(q_{\parallel}, k_{i,z}, k_{f,z}) = F_{\text{BA}}(q_{\parallel}, k_{i,z} - k_{f,z}) + R_i F_{\text{BA}}(q_{\parallel}, -k_{i,z} - k_{f,z}) \\ + R_f F_{\text{BA}}(q_{\parallel}, k_{i,z} + k_{f,z}) + R_i R_f F_{\text{BA}}(q_{\parallel}, -k_{i,z} + k_{f,z}), \quad (5.3)$$

where  $q_{\parallel}$  is the component of the scattering beam in the plane of the interface ( $\mathbf{q} = \mathbf{k}_i - \mathbf{k}_f$ ),  $k_{i,z}$  and  $k_{f,z}$  are the z-component of the incident and scattered beam, respectively.  $R_i$ ,  $R_f$  are the reflection coefficients in incidence and reflection. They are defined as

$$R = \frac{k_z + \sqrt{n_s^2 k_0^2 - |k_{\parallel}|^2}}{k_z - \sqrt{n_s^2 k_0^2 - |k_{\parallel}|^2}}, \text{ where } n_s = 1 - \delta_s + i\beta_s \text{ is the refractive index of the substrate, } k_0 \text{ is the wavelength in vacuum } (2\pi/\lambda), k_z \text{ and } k_{\parallel} \text{ are the } z\text{-component and the in-plane component of } \mathbf{k}_i \text{ or } \mathbf{k}_f.$$

**Remark:** If the particles are sitting on a multilayered system, the expression of the form factor in the DWBA is obtained by replacing the Fresnel coefficient by the corresponding coefficients of the underlying layers [9, 10].

Figure 5.13 illustrates the four scattering processes for a supported particle, taken into account in the DWBA. The first term of eq. 5.3 corresponds to the Born approximation. Each term of  $F_{\text{DWBA}}$  is weighted by a Fresnel coefficient.

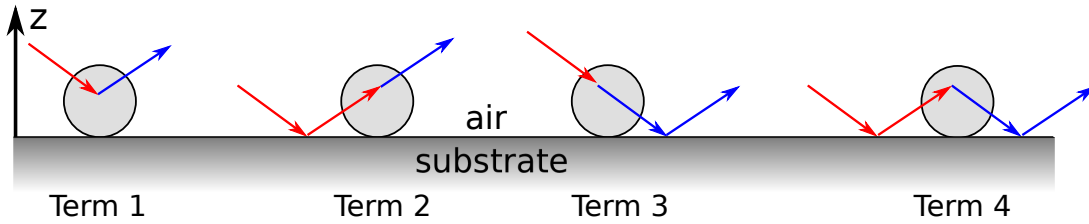


Figure 5.13: Schematic views of the different terms appearing in the expression of the form factor under DWBA for particles sitting on a substrate layer.

Script 5.6 illustrates the difference between BA and DWBA in BornAgain when generating the sample. We consider the simple case of:

- one kind of particles' shape,
- no interference between the particles,
- in the DWBA, a sample made of a layer of substrate on which are deposited the particles,
- in the BA, a sample composed of the particles in air.

Figure 5.14 shows the intensity contourplot generated using this script with truncated spheroids as particles. Note that the full Python script UMFormFactorBA\_DWBA.py is available in /Examples/Python/UserManual/.

Listing 5.6: Python script to generate a sample using Born or Distorted Wave Born Approximation. The difference between BA and DWBA in this simple case is the absence or presence of a substrate layer in the sample.

```
def get_sample():
    """
        Build and return the sample to calculate form factor of
        truncated spheroid in Born or Distorted Wave Born
        Approximation.
    """
    # defining materials
    m_ambience = HomogeneousMaterial("Air", 0.0, 0.0)
    m_substrate = HomogeneousMaterial("Substrate", 6e-6, 2e-8)
    m_particle = HomogeneousMaterial("Particle", 6e-4, 2e-8)

    # collection of particles
    ff= FormFactorTruncatedSpheroid(7.5*nanometer, 9.0*nanometer,
                                    1.2)
    particleshape = Particle(m_particle, ff)
    particle_layout = ParticleLayout()
    particle_layout.addParticle(particleshape, 0.0, 1.0)

    # interferences
    interference = InterferenceFunctionNone()
    particle_layout.addInterferenceFunction(interference)

    # assembling the sample
    air_layer = Layer(m_ambience)
    air_layer.addLayout(particle_layout)
    substrate_layer = Layer(m_substrate, 0)

    multi_layer = MultiLayer()
    multi_layer.addLayer(air_layer)
    # Comment the following line out for Born Approximation
    multi_layer.addLayer(substrate_layer)
    return multi_layer
```

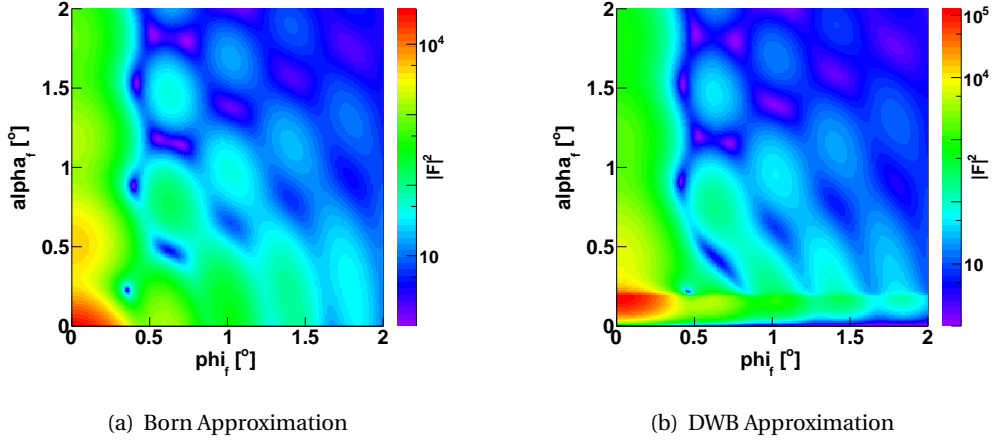


Figure 5.14: Intensity map of TruncatedSpheroid form factor in BA and DWBA computing using script 5.6 for the sample.

**⚠ Remark:** In BornAgain, the DWBA is implemented automatically when assembling the sample with more than the air layer.

### Buried particles

The system considered in this section consists of particles encapsulated in a layer, which is sitting on a substrate (see fig. 5.15). In this case the form factor in the DWBA is given by

$$\begin{aligned} F_{\text{DWBA}}(q_{\parallel}, k_{i,z}, k_{f,z}) = & T_i T_f F_{\text{BA}}(q_{\parallel}, k_{i,z} - k_{f,z}) e^{i(k_{i,z} - k_{f,z})d} + R_i T_f F_{\text{BA}}(q_{\parallel}, -k_{i,z} - k_{f,z}) e^{i(-k_{i,z} - k_{f,z})d} \\ & + R_f T_i F_{\text{BA}}(q_{\parallel}, k_{i,z} + k_{f,z}) e^{i(k_{i,z} + k_{f,z})d} + R_f R_i F_{\text{BA}}(q_{\parallel}, -k_{i,z} + k_{f,z}) e^{i(-k_{i,z} + k_{f,z})d}, \end{aligned} \quad (5.4)$$

$$R_j = \frac{t_{0,1}^j r_{1,2}^j \exp(2ik_{j,z}t)}{1 + r_{0,1}^j r_{1,2}^j \exp(2ik_{j,z}t)}, \quad T_j = \frac{t_{0,1}^j}{1 + r_{0,1}^j r_{1,2}^j \exp(2ik_{j,z}t)}, \quad j = i, f$$

where  $q_{\parallel}$  is the component of the scattering beam in the plane of the interface,  $k_{i,z}$  and  $k_{f,z}$  are the z-component of the incident and scattered beams, respectively.  $d$  is the depth at which the particles are sitting in the layer. Note that this value is given relative to the top of this layer and it is not the coordinate in the absolute referential (linked with the full sample) and it is measured up to the bottom of the particle.  $R_{i,f}$  and  $T_{i,f}$  are the reflection and transmission coefficients in incidence and reflection (they can be calculated using Parratt or matrix formalism).  $r_{0,1}^j$ ,  $r_{1,2}^j$ ,  $t_{0,1}^j$  are the reflection and transmission coefficients between layers; the indices are related to different boundaries with 0: air, 1: intermediate layer and 2: substrate layer and the

superscript  $j$  is associated with the incident or scattered beams:

$$r_{n,n+1}^j = \frac{k_{j,z,n} - k_{j,z,n+1}}{k_{j,z,n} + k_{j,z,n+1}}, \quad t_{n,n+1}^j = \frac{2k_{j,z,n}}{k_{j,z,n} + k_{j,z,n+1}}, \quad n = 0, 1, \quad j = i, f,$$

where index  $n$  is related to the layers,  $z$  to the vertical component, and  $j$  to the beams (incident and outgoing).

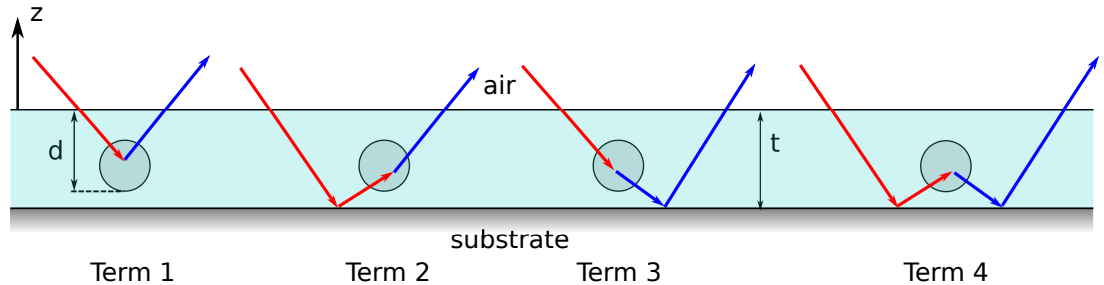


Figure 5.15: Schematic views of the different terms appearing in the expression of the form factor under the DWBA for buried particles.

Figure 5.16 shows a typical example of the output intensity scattered from a sample made of 3 layers: air, substrate, and in between, spherical particles embedded in the middle of a 30 nm-thick layer. This figure had been generated using listing 5.7 (The full script UMFormFactor\_Buried\_DWBA.py can be found in /Examples/Python/UserManual).

Listing 5.7: Python script to generate a sample where spherical particles are embedded in the middle of a layer on a substrate.

```
def get_sample():
    """
        Build and return the sample with buried spheres in DWBA.
    """

    # defining materials
    m_ambience = HomogeneousMaterial("Air", 0.0, 0.0)
    m_interm_layer = HomogeneousMaterial("InterLayer", 3.45e-6,
                                          5.24e-9)
    m_substrate = HomogeneousMaterial("Substrate", 7.43e-6, 1.72e-7)
    m_particle = HomogeneousMaterial("Particle", 0.0, 0.0)

    # collection of particles
    ff = FormFactorFullSphere(10.2*nanometer)
    particleshape = Particle(m_particle, ff)
    particle_layout = ParticleLayout()
    particle_layout.addParticle(particleshape, 20.1, 1.0)

    # interferences
    interference = InterferenceFunctionNone()
```

```
particle_layout.addInterferenceFunction(interference)

# assembling the sample
air_layer = Layer(m_ambience)
intermediate_layer = Layer(m_interm_layer, 30.*nanometer)
intermediate_layer.addLayout(particle_layout)
substrate_layer = Layer(m_substrate, 0)

multi_layer = MultiLayer()
multi_layer.addLayer(air_layer)
multi_layer.addLayer(intermediate_layer)
multi_layer.addLayer(substrate_layer)
return multi_layer
```

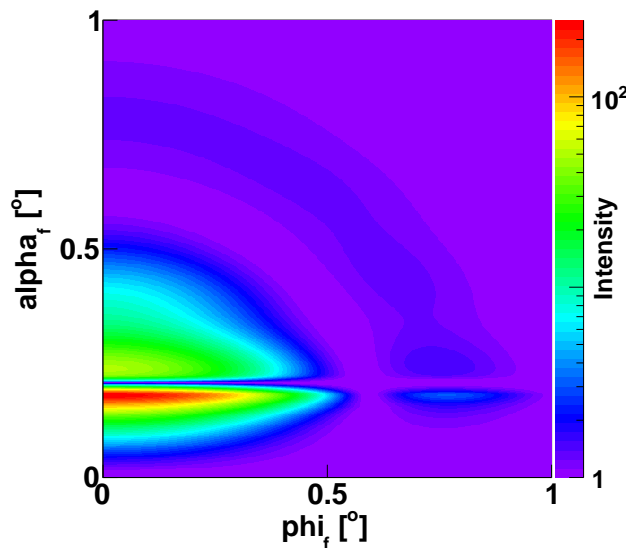


Figure 5.16: Map of intensity scattered from a sample made of spherical particles embedded in the middle of a 30 nm-thick layer on a substrate (see Script 5.7 for details about the sample).

**⚠** **Remark:** For layers different from the air layer, the top interface is considered as the reference level to position the encapsulated particles. For example, spheres positioned at depth  $d$  (positive) are located at a distance  $d$  from the top of the layer up to the bottom of these particles. This convention is different for the top air layer, where particles sitting at the interface with an underlying layer (*i.e.* the bottom of the air layer) are located at depth 0 (see fig. 5.17).

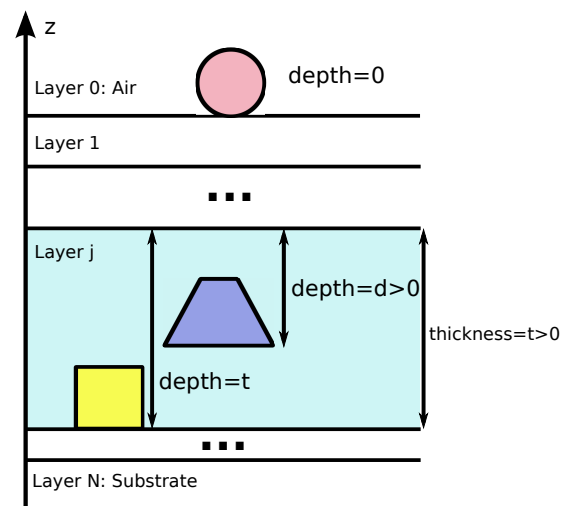


Figure 5.17: Illustration of the convention about depth used in BornAgain to encapsulate particles in layers.

## 5.4 More complicated particles' shapes

BornAgain also offers the possibility to simulate more complicated shapes of particles by combining those listed in Table 5.3.

### 5.4.1 Core-shell particles

To generate a core-shell particle, the combination is performed using the following command:

`ParticleCoreShell(shell_particle, core_particle, relative_core_position)`, where `shell_particle` and `core_particle` are the outer and inner parts of the core-shell particle, respectively. They refer to one of the form factors defined previously and to an associated material. For example, for the outer part,

`shell_particle=Particle(material_shell, outer_form_factor)`, where `material_shell` is the material of the shell and `outer_form_factor` is the shape of the outer part (cf. listing 5.8).

`relative_core_position` defines the position of the inner shape with respect to the outer one; it is defined with respect to the centre of the base of the particular form factor. An example in fig. 5.18 shows a core shell particle made of a box for the outer part and of a shifted pyramidal shape for the inner one.

Figure 5.19 displays the output intensity scattered in the Born Approximation using the code listed in 5.8 to generate the core-shell particle. The full script can be found at /Examples/python/UserManual/UMFormFactor\_CoreShell.py.

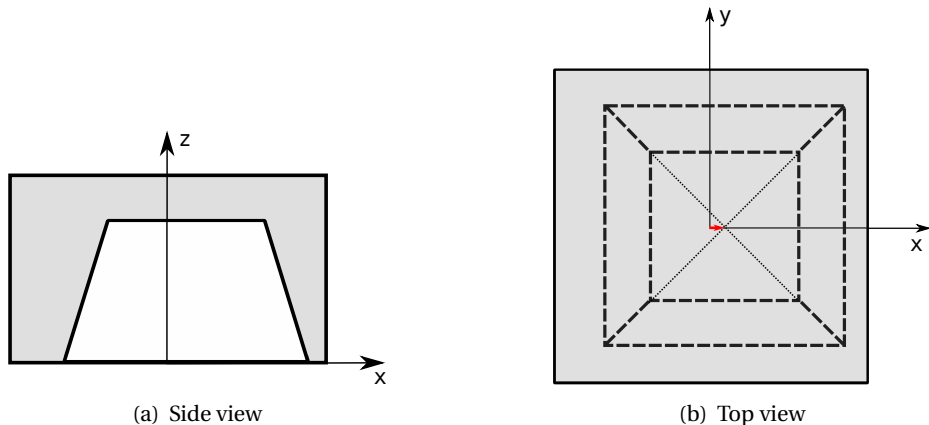


Figure 5.18: Example of a core-shell particle composed of a box with a pyramidal inset. The relative core shell position is marked by the positions of the centres of the bases.

Listing 5.8: Python script to create a core-shell particle made of a box with a pyramidal shifted inset.

```

outer_ff = FormFactorBox(16.0*nanometer, 16.0*nanometer, 8.0*
    nanometer)
inner_ff = FormFactorPyramid(12.0*nanometer, 7.0*nanometer,
    60.0*degree)
shell_particle = Particle(m_shell, outer_ff)
core_particle = Particle(m_core, inner_ff)
core_position = kvector_t(1.5, 0.0, 0.0)

particle = ParticleCoreShell(shell_particle, core_particle,
    core_position)

```

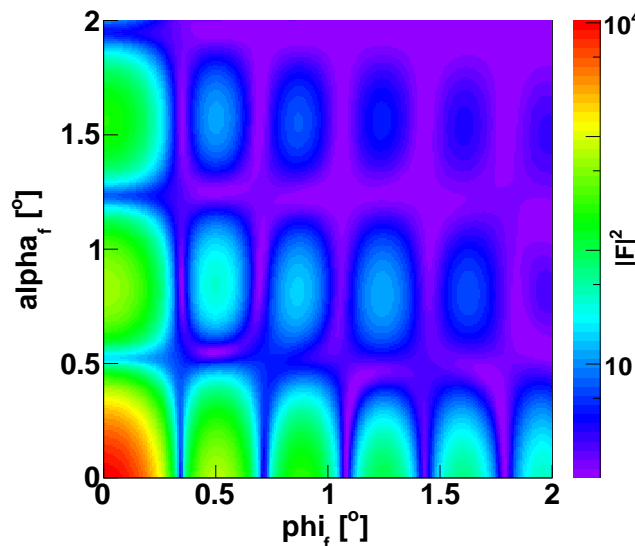


Figure 5.19: Intensity map of a core-shell form factor in Born Approximation using `FormFactorBox(16*nanometer, 16*nanometer, 8*nanometer)` and `FormFactorPyramid(12*nanometer, 7*nanometer, 60*degree)` for the outer and inner shells, respectively. The core particle is shifted by 1.5 nm in the  $x$ -direction with respect to the centre of the outer shell. The sample used to generate the particle is listed in 5.8. There is no substrate and no interference between the particles.

#### 5.4.2 Rotation of particles

The particles can be rotated in a different direction by using one of the following transformations: `CreateRotateX(theta)`, `CreateRotateY(theta)`, `CreateRotateZ(theta)`, where capital X, Y, Z mark rotations around the associated axis and  $\theta$  is the angle of rotation from this

axis. For example, the following Python script shows how to rotate a pyramid by 45° around the  $z$ -axis:

```
pyramid_ff = FormFactorPyramid(10*nanometer, 5*nanometer,
    deg2rad(54.73) )
pyramid = Particle(m_particle, pyramid_ff)
angle_around_z = 45.*degree
transform = Transform3D.createRotateZ(angle_around_z)
particle_layout = ParticleLayout()
particle_layout.addParticle(pyramid, transform)
```

#### 5.4.3 Polydispersity

### 5.5 Material layers

#### 5.5.1 Roughness

#### 5.6 Polarisation

To be completed

# Chapter 6

# Fitting

In addition to the simulation of grazing incidence X-ray and neutron scattering by multi-layered samples, BornAgain also offers the option to fit the numerical model to reference data by modifying a selection of sample parameters from the numerical model. This aspect of the software is discussed in the current chapter.

Section 6.1 details the implementation of fittings in BornAgain . Python fitting examples with detailed explanations of every fitting step are given in Section 6.2. Advanced fitting techniques, including fine tuning of minimization algorithms, simultaneous fits of different data sets, parameters correlation, are covered in Section 6.3. Section 6.4 contains some practical advice, which might help the user to get right answers from BornAgain fitting.

## 6.1 Implementation in BornAgain

Fitting in BornAgain deals with estimating the optimum parameters in the numerical model by minimizing the difference between numerical and reference data. The features include

- a variety of multidimensional minimization algorithms and strategies.
- the choice over possible fitting parameters, their properties and correlations.
- the full control on objective function calculations, including applications of different normalizations and assignments of different masks and weights to different areas of reference data.
- the possibility to fit simultaneously an arbitrary number of data sets.

Figure 6.1 shows the general work flow of a typical fitting procedure.

Before running the fitting the user is required to prepare some data and to configure the fitting kernel of BornAgain . The required stages are

- Preparing the sample and the simulation description (multilayer, beam, detector parameters).

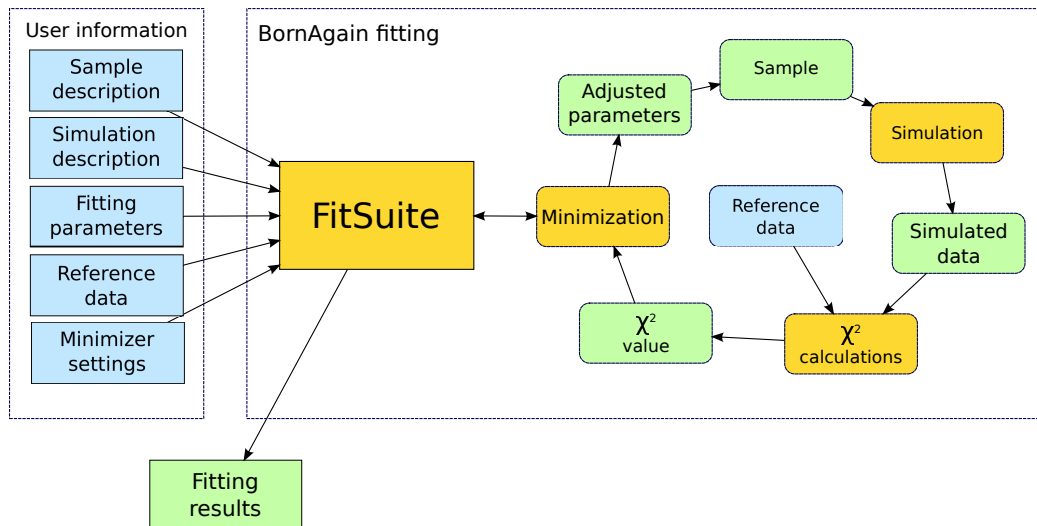


Figure 6.1: Fitting work flow.

- Choosing the fitting parameters.
- Loading the reference data.
- Defining the minimization settings.

The class `FitSuite` contains the main functionalities to be used for the fit and serves as the main interface between the user and the fitting work flow. The later involves iterations during which

- The minimizer makes an assumption about the optimal sample parameters.
- These parameters are propagated to the sample.
- The simulation is performed for the given state of the sample.
- The simulated data (intensities) are propagated to the  $\chi^2$  module.
- The later calculates  $\chi^2$  using the simulated and reference data.
- The value of  $\chi^2$  is propagated to the minimizer, which makes new assumptions about optimal sample parameters.

The iteration process is going on under the control of the selected minimization algorithm, without any intervention from the user. It stops

- when the maximum number of iteration steps has been exceeded,

- when the function's minimum has been reached within the tolerance window,
- if the minimizer could not improve the values of the parameters.

After the control is returned, fitting results can be retrieved. They consist in the best  $\chi^2$  value found, the corresponding optimal sample parameters and the intensity map simulated with this set of parameters.

Details of FitSuite class implementation and description of each interface are given in Section ???. The following parts of this section will detail each of the main stages necessary to run a fitting procedure.

### 6.1.1 Preparing the sample and the simulation description

This step is similar for any simulation using BornAgain (see Section 3). It consists in first characterizing the geometry of the system: the particles (shapes, sizes, refractive indices), the different layers (thickness, order, refractive index, a possible roughness of the interface), the interference between the particles and the way they are distributed in the layers (buried particles or particles sitting on top of a layer). Then we specify the parameters of the input beam and of the output detector.

### 6.1.2 Choice of parameters to be fitted

In principle, every parameter used in the construction of the sample can be used as a fitting parameter. For example, the particles' heights, radii or the layer's roughness or thickness could be selected using the parameter pool mechanism. This mechanism is explained in detail in Section 3.4 and it is therefore recommended to read it before proceeding any further.

The user specifies selected sample parameters as fit parameters using FitSuite and its addFitParameter method

```
fit_suite = FitSuite()
fit_suite.addFitParameter(<name>, <initial value>, <step>, <limits>)
```

where `<name>` corresponds to the parameter name in the sample's parameter pool. By using wildcards in the parameter name, a group of sample parameters, corresponding to the given pattern, can be associated with a single fitting parameter and fitted simultaneously to get a common optimal value (see Section 3.4).

The second parameter `<initial value>` correspond to the initial value of the fitting parameter, while the third one is responsible to the initial iteration steps size. The last parameter `<AttLimits>` corresponds to the boundaries imposed on parameter value. It can be

- `limitless()` by default,
- `fixed()`,
- `lowerLimited(<min_value>)`,

- `upperLimited(<max_value>),`
- `limited(<min_value>, <max_value>).`

where `<min_value>` and `<max_value>` are double values corresponding to the lower and higher boundary, respectively.

### 6.1.3 Associating reference and simulated data

The minimization procedure deals with a pair of reference data (normally associated with experimental data) and the theoretical model (presented by the sample and the simulation descriptions).

We assume that the experimental data are a two-dimensional intensity matrix as function of the output scattering angles  $\alpha_f$  and  $\phi_f$  (see Fig. 3.1). The user is required to provide the data in the form of an ASCII file containing an axes binning description and the intensity data itself.



Remark: We recognize the importance of supporting the most common data formats.  
We are going to provide this feature in the following releases and welcome users' requests on this subject.

To associate the simulation and the reference data to the fitting engine, method `addSimulationAndRealData` has to be used as shown

```
fit_suite = FitSuite()
fit_suite.addSimulationAndRealData(<simulation>, <reference>, <
chi2_module>)
```

Here `<simulation>` corresponds to a BornAgain simulation object with the sample, beam and detector fully defined, `<reference>` corresponds to the experimental data object obtained from the ASCII file and `<chi2_module>` is an optional parameter for advanced control of  $\chi^2$  calculations.

It is possible to call this given method more than once to submit more than one pair of `<simulation>`, `<reference>` to the fitting procedure. In this way, simultaneous fits of some combined data sets are performed.

By using the third parameter, `<chi2_module>`, different normalizations and weights can be applied to give user full control of the way  $\chi^2$  is calculated. This feature will be explained in Section 6.3.

### 6.1.4 Minimizer settings

BornAgain contains a variety of minimization engines from ROOT and GSL libraries. They are listed in Table 6.1. By default Minuit2 minimizer with default settings will be used and no additional configuration needs to be done. The remainder of this section explains some of the expert settings, which can be applied to get better fit results.

The default minimization algorithm can be changed using `MinimizerFactory` as shown below

```

fit_suite = FitSuite()
minimizer = MinimizerFactory.createMinimizer("<Minimizer name>", "
    <algorithm>")
fit_suite.setMinimizer(minimizer)

```

where `<Minimizer name>` and `<algorithm>` can be chosen from the first and second column of Table 6.1 respectively. The list of minimization algorithms implemented in BornAgain can also be obtained using `MinimizerFactory.printCatalogue()` command.

<b>Minimizer name</b>	<b>Algorithm</b>	<b>Description</b>
Minuit2 [11]	Migrad	According to [12] best minimizer for nearly all functions, variable-metric method with inexact line search, a stable metric updating scheme, and checks for positive-definiteness.
	Simplex	simplex method of Nelder and Mead usually slower than Migrad, rather robust with respect to gross fluctuations in the function value, gives no reliable information about parameter errors,
	Combined	minimization with Migrad but switches to Simplex if Migrad fails to converge.
	Scan	not intended to minimize, just scans the function, one parameter at a time, retains the best value after each scan
	Fumili	optimized method for least square and log likelihood minimizations
GSLMultiMin [13]	ConjugateFR	Fletcher-Reeves conjugate gradient algorithm,
	ConjugatePR	Polak-Ribiere conjugate gradient algorithm,
	BFGS	Broyden-Fletcher-Goldfarb-Shanno algorithm,
	BFGS2	improved version of BFGS,
	SteepestDescent	follows the downhill gradient of the function at each step
GSLLMA [14]		Levenberg-Marquardt Algorithm
GSLSimAn [15]		Simulated Annealing Algorithm

Table 6.1: List of minimizers implemented in BornAgain.

There are several options common to every minimization algorithm, which can be changed before starting the minimization. They are handled by `MinimizerOptions` class:

```
fit_suite.getMinimizer().getOptions().setMaxFunctionCalls(10)
```

In the above code snippet, a number of “maximum function calls”, namely the maximum number of times the minimizer is allowed to call the simulation, is limited to 10.

There are also expert-level options common for all minimizers as well as a number of options to tune individual minimization algorithms. They will be explained in Section 6.3.

### 6.1.5 Running the fitting and retrieving the results

After the initial configuration of FitSuite has been performed, the fitting can be started using the command

```
fit_suite.runFit()
```

Depending on the complexity of the sample and the number of free sample parameters the fitting process can take from tens to thousands of iterations. The results of the fit can be printed on the screen using the command

```
fit_suite.printResults()
```

Section 6.2 gives more details about how to access the fitting results.

## 6.2 Basic Python fitting example

In this section we are going to go through a complete example of fitting using BornAgain. Each step will be associated with a detailed piece of code written in Python. The complete listing of the script is given in Appendix (see Listing A.2). The script can also be found at

```
./Examples/python/fitting/ex002_FitCylindersAndPrisms/
FitCylindersAndPrisms.py
```

This example uses the same sample geometry as in Section 3.3. Cylindrical and prismatic particles in equal proportion are deposited on a substrate layer, with no interference between the particles. We consider the following parameters to be unknown

- the radius of cylinders,
- the height of cylinders,
- the length of the prisms’ triangular basis,
- the height of prisms.

Our reference data are a “noisy” two-dimensional intensity map obtained from the simulation of the same geometry with a fixed value of 5 nm for the height and radius of cylinders and for the height of prisms which have a 10-nanometer-long side length. Then we run our

fitting using default minimizer settings starting with a cylinder's height of 4 nm, a cylinder's radius of 6 nm, a prism's half side of 6 nm and a height equal to 4 nm. As a result, the fitting procedure is able to find the correct value of 5 nm for all four parameters.

### Importing Python libraries

```
1 from libBornAgainCore import *
2 from libBornAgainFit import *
```

We start from importing two BornAgain libraries required to create the sample description and to run the fitting.

### Building the sample

```
5 def get_sample():
6     """
7         Build the sample representing cylinders and pyramids on top
8             of substrate without interference.
9     """
10    # defining materials
11    m_air = HomogeneousMaterial("Air", 0.0, 0.0)
12    m_substrate = HomogeneousMaterial("Substrate", 6e-6, 2e-8)
13    m_particle = HomogeneousMaterial("Particle", 6e-4, 2e-8)
14
15    # collection of particles
16    cylinder_ff = FormFactorCylinder(1.0*nanometer, 1.0*nanometer
17        )
18    cylinder = Particle(m_particle, cylinder_ff)
19    prism_ff = FormFactorPrism3(2.0*nanometer, 1.0*nanometer)
20    prism = Particle(m_particle, prism_ff)
21    particle_layout = ParticleLayout()
22    particle_layout.addParticle(cylinder, 0.0, 0.5)
23    particle_layout.addParticle(prism, 0.0, 0.5)
24    interference = InterferenceFunctionNone()
25    particle_layout.addInterferenceFunction(interference)
26
27    # air layer with particles and substrate form multi layer
28    air_layer = Layer(m_air)
29    air_layer.addLayout(particle_layout)
30    substrate_layer = Layer(m_substrate)
31    multi_layer = MultiLayer()
32    multi_layer.addLayer(air_layer)
33    multi_layer.addLayer(substrate_layer)
34
35    return multi_layer
```

The function starting at line 5 creates a multilayered sample with cylinders and prisms using arbitrary 1 nm value for all size's of particles. The details about the generation of this multilayered sample are given in Section 3.3.

### Creating the simulation

```

35 def get_simulation():
36     """
37     Create GISAXS simulation with beam and detector defined
38     """
39     simulation = Simulation()
40     simulation.setDetectorParameters(100, -1.0*degree, 1.0*degree
41                                     , 100, 0.0*degree, 2.0*degree)
42     simulation.setBeamParameters(1.0*angstrom, 0.2*degree, 0.0*
43                                  degree)
44     return simulation

```

The function starting at line 35 creates the simulation object with the definition of the beam and detector parameters.

### Preparing the fitting pair

```

45 def run_fitting():
46     """
47     run fitting
48     """
49     sample = get_sample()
50     simulation = get_simulation()
51     simulation.setSample(sample)
52
53     real_data = IntensityDataIOFactory.readIntensityData(
54         'refdata_fitcylinderprisms.txt')

```

Lines 49- 51 generate the sample and simulation description and assign the sample to the simulation. Our reference data are contained in the file 'refdata\_fitcylinderprisms.txt'. This reference had been generated by adding noise on the scattered intensity from a numerical sample with a fixed length of 5 nm for the four fitting parameters (*i.e.* the dimensions of the cylinders and prisms). Line 53 creates the real data object by loading the ASCII data from the input file.

### Setting up FitSuite

```

55 fit_suite = FitSuite()
56 fit_suite.addSimulationAndRealData(simulation, real_data)
57 fit_suite.initPrint(10)

```

Line 55 creates a `FitSuite` object which provides the main interface to the minimization kernel of BornAgain . Line 56 submits simulation description and real data pair to the subsequent fitting. Line 57 sets up `FitSuite` to print on the screen the information about fit progress once per 10 iterations.

```

60     fit_suite.addFitParameter("*FormFactorCylinder/height", 4.*  
61         nanometer, 0.01*nanometer, AttLimits.lowerLimited(0.01))  
62     fit_suite.addFitParameter("*FormFactorCylinder/radius", 6.*  
63         nanometer, 0.01*nanometer, AttLimits.lowerLimited(0.01))  
64     fit_suite.addFitParameter("*FormFactorPrism3/height", 4.*  
65         nanometer, 0.01*nanometer, AttLimits.lowerLimited(0.01))  
66     fit_suite.addFitParameter("*FormFactorPrism3/length", 12.*  
67         nanometer, 0.02*nanometer, AttLimits.lowerLimited(0.01))

```

Lines 60– 63 enter the list of fitting parameters. Here we use the cylinders' height and radius and the prisms' height and side length. The cylinder's length and prism half side are initially equal to 4 nm, whereas the cylinder's radius and the prism half side length are equal to 6 nm before the minimization. The iteration step is equal to 0.01 nm and only the lower boundary is imposed to be equal to 0.01 nm.

### Running the fit and accessing results

```

66     fit_suite.runFit()  
67  
68     print "Fitting completed."  
69     fit_suite.printResults()  
70     print "chi2:", fit_suite.getMinimizer().getMinValue()  
71     fitpars = fit_suite.getFitParameters()  
72     for i in range(0, fitpars.size()):  
73         print fitpars[i].getName(), fitpars[i].getValue(),  
              fitpars[i].getError()

```

Line 66 shows the command to start the fitting process. During the fitting the progress will be displayed on the screen. Lines 69– 73 shows different ways of accessing the fit results.

More details about fitting, access to its results and visualization of the fit progress using matplotlib libraries can be learned from the following detailed example

```
./Examples/python/fitting/ex002_FitCylindersAndPrisms/  
FitCylindersAndPrisms_detailed.py
```

## 6.3 Advanced fitting

- 6.3.1 Affecting  $\chi^2$  calculations
- 6.3.2 Simultaneous fits of several data sets
- 6.3.3 Using fitting strategies
- 6.3.4 Masking the real data
- 6.3.5 Tuning fitting algorithms
- 6.3.6 Fitting with correlated sample parameters

## 6.4 How to get the right answer from fitting

One of the main difficulties in fitting the data with the model is the presence of multiple local minima in the objective function. Many problems can cause the fit to fail, for example:

- an unreliable physical model,
- an unappropriate choice of objective function
- multiple local minima,
- an unphysical behavior of the objective function, unphysical regions in the parameters space,
- an unreliable parameter error calculation in the presence of limits on the parameter value,
- an exponential behavior of the objective function and the corresponding numerical inaccuracies, excessive numerical roundoff in the calculation of its value and derivatives,
- large correlations between parameters,
- very different scales of parameters involved in the calculation,
- not positive definite error matrix even at minimum.

The given list, of course, is not only related to BornAgain fitting. It remains applicable to any fitting program and any kind of theoretical model. Below we give some recommendations which might help the user to achieve reliable fit results.

### General recommendations

- initially choose a small number of free fitting parameters,
- eliminate redundant parameters,

- provide a good initial guess for the fit parameters,
- start from the default minimizer settings and perform some fine tuning after some experience has been acquired,
- repeat the fit using different starting values for the parameters or their limits,
- repeat the fit, fixing and varying different groups of parameters,  
**to be continued...**

## Chapter 7

# Software architecture

BornAgain is written in C++ and uses an object oriented approach to achieve modularity, extensibility and transparency. This leads to the task driven rather than the command driven approach in different aspects of the simulation and fitting of GISAS data. The user defines the sample structure, beam and detector characteristics and fit parameters using building blocks – classes – defined in core libraries of the framework. These buildings blocks are combined by the user according to his current task using one the following approaches:

- The user creates a Python script with a sample description and simulation settings using the BornAgain API. The user then runs the simulation by executing the script in the Python interpreter and assesses the simulation results using his preferred graphics or analysis library, e.g. Python + numpy + matplotlib.
- The user may write a standalone C++ application linked to the BornAgain libraries.
- The user interacts with the framework through a graphical user interface (forthcoming).

The object oriented approach in the software design allows users to have a much higher level of flexibility in the sample construction; it also decouples the building blocks used in the internal calculations and thereby facilitates the creation of new models, with little or no modification to the existing code.

The general structure of BornAgain and the way the user interacts with it are shown in Fig. 7.1. The framework consists of two shared libraries, `libBornAgainCore` and `libBornAgainFit`. Thanks to the Python interface they can be imported into Python as external modules. The library `libBornAgainCore` contains a number of classes, grouped into several class categories, necessary for the description of a model and running a simulation. The library `libBornAgainFit` contains a number of minimization engines and interfaces to them, allowing the user to fit real data with the model previously defined.

BornAgain depends on a few external and well established open-source libraries: boost, GNU scientific library, Eigen and Fast Fourier Transformation libraries. They are required to be installed on the system to run BornAgain on Unix Platforms. In the case of Windows

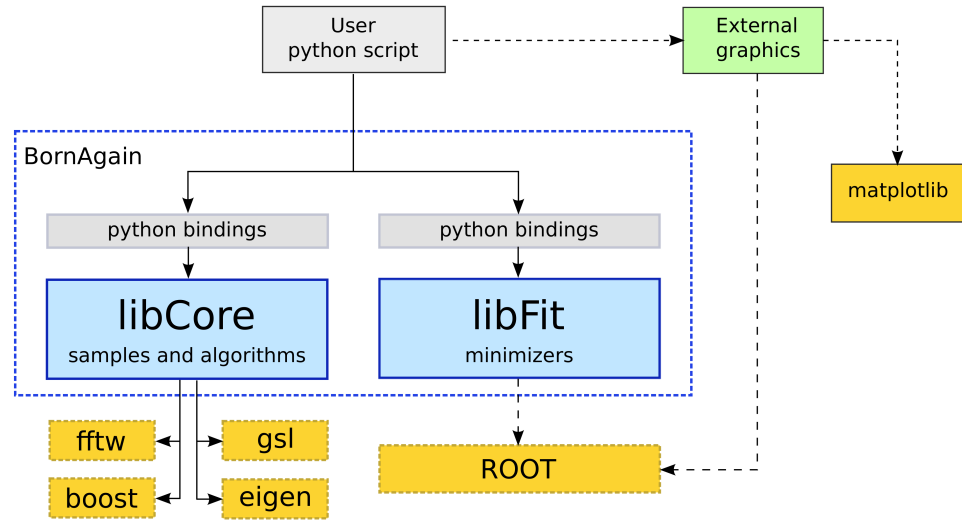


Figure 7.1: Structure of BornAgain libraries.

Platform they are added to the system automatically during BornAgain installation. Other libraries shown on the plot (ROOT, matplotlib) are optional.

## Appendix A

### Listings

#### A.1 Python simulation example

The following script can be found at

```
./Examples/python/simulation/ex001_CylindersAndPrisms/
    CylindersAndPrisms.py
```

```
1 import numpy
2 import matplotlib
3 import pylab
4 from libBornAgainCore import *
5
6
7 def get_sample():
8     """
9         Build and return the sample representing cylinders and
10            pyramids on top of
11            substrate without interference.
12 """
13     # defining materials
14     m_air = HomogeneousMaterial("Air", 0.0, 0.0)
15     m_substrate = HomogeneousMaterial("Substrate", 6e-6, 2e-8)
16     m_particle = HomogeneousMaterial("Particle", 6e-4, 2e-8)
17
18     # collection of particles
19     cylinder_ff = FormFactorCylinder(5*nanometer, 5*nanometer)
20     cylinder = Particle(m_particle, cylinder_ff)
21     prism_ff = FormFactorPrism3(10*nanometer, 5*nanometer)
22     prism = Particle(m_particle, prism_ff)
23     particle_layout = ParticleLayout()
24     particle_layout.addParticle(cylinder, 0.0, 0.5)
25     particle_layout.addParticle(prism, 0.0, 0.5)
26     interference = InterferenceFunctionNone()
27     particle_layout.addInterferenceFunction(interference)
```

```
27
28     # air layer with particles and substrate form multi layer
29     air_layer = Layer(m_air)
30     air_layer.addLayout(particle_layout)
31     substrate_layer = Layer(m_substrate, 0)
32     multi_layer = MultiLayer()
33     multi_layer.addLayer(air_layer)
34     multi_layer.addLayer(substrate_layer)
35     return multi_layer
36
37
38 def get_simulation():
39     """
40         Create and return GISAXS simulation with beam and detector
41             defined
42     """
43     simulation = Simulation()
44     simulation.setDetectorParameters(100, -1.0*degree, 1.0*degree
45                                     , 100, 0.0*degree, 2.0*degree)
46     simulation.setBeamParameters(1.0*angstrom, 0.2*degree, 0.0*
47                                  degree)
48     return simulation
49
50
51
52 def run_simulation():
53     """
54         Run simulation and plot results
55     """
56     sample = get_sample()
57     simulation = get_simulation()
58     simulation.setSample(sample)
59     simulation.runSimulation()
60     result = simulation.getIntensityData().getArray() + 1    # for
61     log scale
62     pylab.imshow(numpy.rot90(result, 1), norm=matplotlib.colors.
63                  LogNorm(), extent=[-1.0, 1.0, 0, 2.0])
64     pylab.show()
65
66
67 if __name__ == '__main__':
68     run_simulation()
```

## A.2 Python fitting example

The following script can be found at

```
./Examples/python/fitting/ex002_FitCylindersAndPrisms/
    FitCylindersAndPrisms.py
```

```

1 from libBornAgainCore import *
2 from libBornAgainFit import *
3
4
5 def get_sample():
6     """
7         Build the sample representing cylinders and pyramids on top
8             of substrate without interference.
9     """
10    # defining materials
11    m_air = HomogeneousMaterial("Air", 0.0, 0.0)
12    m_substrate = HomogeneousMaterial("Substrate", 6e-6, 2e-8)
13    m_particle = HomogeneousMaterial("Particle", 6e-4, 2e-8)
14
15    # collection of particles
16    cylinder_ff = FormFactorCylinder(1.0*nanometer, 1.0*nanometer
17        )
18    cylinder = Particle(m_particle, cylinder_ff)
19    prism_ff = FormFactorPrism3(2.0*nanometer, 1.0*nanometer)
20    prism = Particle(m_particle, prism_ff)
21    particle_layout = ParticleLayout()
22    particle_layout.addParticle(cylinder, 0.0, 0.5)
23    particle_layout.addParticle(prism, 0.0, 0.5)
24    interference = InterferenceFunctionNone()
25    particle_layout.addInterferenceFunction(interference)
26
27    # air layer with particles and substrate form multi layer
28    air_layer = Layer(m_air)
29    air_layer.addLayout(particle_layout)
30    substrate_layer = Layer(m_substrate, 0)
31    multi_layer = MultiLayer()
32    multi_layer.addLayer(air_layer)
33    multi_layer.addLayer(substrate_layer)
34    return multi_layer
35
36
37 def get_simulation():
38     """
39         Create GISAXS simulation with beam and detector defined
40     """
41     simulation = Simulation()
42     simulation.setDetectorParameters(100, -1.0*degree, 1.0*degree
43         , 100, 0.0*degree, 2.0*degree)
```

```
41     simulation.setBeamParameters(1.0*angstrom, 0.2*degree, 0.0*
42         degree)
43     return simulation
44
45 def run_fitting():
46     """
47     run fitting
48     """
49     sample = get_sample()
50     simulation = get_simulation()
51     simulation.setSample(sample)
52
53     real_data = IntensityDataIOFactory.readIntensityData(
54         'refdata_fitcylinderprisms.txt')
55
56     fit_suite = FitSuite()
57     fit_suite.addSimulationAndRealData(simulation, real_data)
58     fit_suite.initPrint(10)
59
60     # setting fitting parameters with starting values
61     fit_suite.addFitParameter("*FormFactorCylinder/height", 4. *
62         nanometer, 0.01*nanometer, AttLimits.lowerLimited(0.01))
63     fit_suite.addFitParameter("*FormFactorCylinder/radius", 6. *
64         nanometer, 0.01*nanometer, AttLimits.lowerLimited(0.01))
65     fit_suite.addFitParameter("*FormFactorPrism3/height", 4. *
66         nanometer, 0.01*nanometer, AttLimits.lowerLimited(0.01))
67     fit_suite.addFitParameter("*FormFactorPrism3/length", 12. *
68         nanometer, 0.02*nanometer, AttLimits.lowerLimited(0.01))
69
70     # running fit
71     fit_suite.runFit()
72
73     print "Fitting completed."
74     fit_suite.printResults()
75     print "chi2:", fit_suite.getMinimizer().getMinValue()
76     fitpars = fit_suite.getFitParameters()
77     for i in range(0, fitpars.size()):
78         print fitpars[i].getName(), fitpars[i].getValue(),
79             fitpars[i].getError()
80
81 if __name__ == '__main__':
82     run_fitting()
```

## Appendix B

# Theory

### B.1 Scattering on nanoparticles - Formal treatment

#### B.1.1 Green operators and the $T$ -matrix

For a particle, governed by the Schrödinger equation with Hamiltonian  $H = H_0 + V$ , the time-independent scattering theory formally consists of solving the eigenvalue equations:

$$H\Psi_\alpha = E_\alpha \Psi_\alpha ,$$

with  $E$  the scalar energy eigenvalue of the eigenstate  $\Psi(E)$ .

If the solutions of the free (or unperturbed) Hamiltonian  $H_0$  are known:

$$H_0\Psi_{0\alpha} = E_\alpha \Psi_{0\alpha} ,$$

one can write the solutions of the full Hamiltonian in terms of these asymptotic states and Green operators:

$$\begin{aligned}\Psi_\alpha^\pm &= \Psi_{0\alpha} + G_0^\pm V \Psi_\alpha^\pm \\ &= \Psi_{0\alpha} + G^\pm V \Psi_{0\alpha} ,\end{aligned}$$

where the Green operators are defined as:

$$\begin{aligned}G_0^\pm(E) &= (E - H_0 \pm ie)^{-1} \\ G^\pm(E) &= (E - H \pm i\epsilon)^{-1} .\end{aligned}$$

In these equations, the upper index or sign refers to the state corresponding with the free state  $\Psi_{0\alpha}$  at time  $t \rightarrow -\infty$  (and vice-versa for the lower sign). Since the solutions of the eigenvalue equations, both for the unperturbed as for the full Hamiltonian, are dependent on the energy eigenvalue  $E$ , the index  $\alpha$  is assumed to include this value (and possibly other quantum numbers).

The transition amplitude between two asymptotic states is given by the  $S$ -matrix elements, defined as:

$$\begin{aligned} S_{\alpha\beta} &\equiv \langle \Psi_{0\beta} | S | \Psi_{0\alpha} \rangle \\ &\equiv \langle \Psi_{\beta}^- | \Psi_{\alpha}^+ \rangle. \end{aligned} \quad (\text{B.1})$$

The  $S$ -matrix can be decomposed into a delta function, representing the absence of scattering, and a  $T$ -matrix that encodes the scattering part, caused by the potential  $V$ :

$$S_{\alpha\beta} = \delta(E_{\alpha} - E_{\beta})\delta_{\alpha\beta} - 2\pi i\delta(E_{\alpha} - E_{\beta})T_{\alpha\beta}^{\pm},$$

with

$$\begin{aligned} T_{\alpha\beta}^+ &= \langle \Psi_{0\beta} | V | \Psi_{\alpha}^+ \rangle \\ T_{\alpha\beta}^- &= \langle \Psi_{\beta}^- | V | \Psi_{0\alpha} \rangle. \end{aligned}$$

On the energy shell  $E_{\alpha} = E_{\beta}$ , one has  $T_{\alpha\beta}^+ = T_{\alpha\beta}^-$ , so that both formulations are equivalent.

By expanding the eigenstates  $\Psi_{\alpha}^{\pm}$  in these equations, the  $T$ -matrix elements (on-shell) can be expressed as:

$$T_{\alpha\beta}^{\pm} = V + VG^{\mp}V.$$

### B.1.2 Momentum representation and the scattering cross-section

The previous general formulas can also be presented in a momentum (and positon) eigenbasis, defined by:

$$\begin{aligned} \hat{\mathbf{P}}|\mathbf{k}\rangle &= \hbar\mathbf{k}|\mathbf{k}\rangle \\ \langle \mathbf{k}'|\mathbf{k}\rangle &= \delta(\mathbf{k}' - \mathbf{k}) \\ 1 &= \int d^3\mathbf{k}|\mathbf{k}\rangle\langle\mathbf{k}| \\ 1 &= \int d^3\mathbf{r}|\mathbf{r}\rangle\langle\mathbf{r}| \\ \langle \mathbf{r}|\mathbf{k}\rangle &= (2\pi)^{-3/2} \exp(i\mathbf{k}\cdot\mathbf{r}), \end{aligned}$$

where the normalization in the last equation follows from the other definitions.

The wavefunction that evolves from a momentum eigenstate  $|\mathbf{k}_i\rangle$  can then be written as:

$$\langle \mathbf{r}|\Psi^+\rangle = \langle \mathbf{r}|\mathbf{k}_i\rangle + \langle \mathbf{r}|G_0^+T|\mathbf{k}_i\rangle,$$

which in the far-field limit becomes:

$$\begin{aligned} \langle \mathbf{r}|\Psi^+\rangle &= (2\pi)^{-3/2} \left[ e^{i\mathbf{k}_i\cdot\mathbf{r}} - \frac{4\pi^2 m}{\hbar^2} \cdot \frac{e^{ik_f r}}{r} \langle \mathbf{k}_f | T | \mathbf{k}_i \rangle \right] \\ &\equiv (2\pi)^{-3/2} \left[ e^{i\mathbf{k}_i\cdot\mathbf{r}} + f(\theta, \phi) \frac{e^{ik_f r}}{r} \right], \end{aligned}$$

where the scattering amplitude was defined as

$$f(\theta, \phi) = -\frac{4\pi^2 m}{\hbar^2} \langle \mathbf{k}_f | T | \mathbf{k}_i \rangle .$$

The amount of particles per unit time that are scattered in a small solid angle  $d\Omega$  in direction  $\mathbf{k}_f$  will then be (still in the far-field limit):

$$dI_{scat} = J_0 |f(\theta, \phi)|^2 d\Omega ,$$

where  $J_0$  denotes the incident flux density. The scattering cross-section is defined as:

$$\frac{d\sigma}{d\Omega} \equiv \frac{dI_{scat}}{J_0 d\Omega} = |f(\theta, \phi)|^2 .$$

## B.2 Small angle approximation

In the case of pure nuclear scattering, the Hamiltonian describing a neutron in a scattering experiment, is given by  $H = -\frac{\hbar^2}{2m} \Delta + V$ , where

$$V = \frac{2\pi\hbar^2}{m} \rho_s(\mathbf{r}) ,$$

with  $\rho_s(\mathbf{r})$  the scattering length density of the sample. This scattering length density typically consists of a sum of weighted delta-functions, peaked at the atomic positions of the sample. For small scattering angles, the Bragg condition will not be fulfilled and the scattering length density may be replaced by a continuous function, representing the average scattering length density. In this case, one can define a refractive index, which in general will also be a continuous function of the position in the sample:

$$n^2(\mathbf{r}) \equiv 1 - \frac{4\pi}{k_0^2} \rho_s(\mathbf{r}) ,$$

with  $k_0$  the wavevector in vacuum, or alternatively  $k_0 = 2\pi/\lambda$ , with  $\lambda$  the de Broglie wavelength of the neutron.

Substituting this refractive index in the potential then gives:

$$V(\mathbf{r}) = \frac{\hbar^2}{2m} k_0^2 (1 - n^2(\mathbf{r})) .$$

Using these definitions, one can rescale the Hamiltonian with a factor  $2m/\hbar^2$ , such that

$$\begin{aligned} \tilde{H} &\equiv -\Delta + \tilde{V} \\ \tilde{V}(\mathbf{r}) &\equiv 4\pi\rho_s(\mathbf{r}) = k_0^2 (1 - n^2(\mathbf{r})) . \end{aligned}$$

It should be noted that this Hamiltonian implicitly contains the energy eigenvalue ( $E_{k_0} = (\hbar k_0)^2 / 2m$ ), so that it can only be used in the time-independent Schrödinger equation  $H\Psi_\alpha = E_\alpha \Psi_\alpha$ .

The  $T$ -matrix then also becomes rescaled and the scattering amplitude becomes:

$$f(\theta, \phi) = -2\pi^2 \langle \mathbf{k}_f | \tilde{T} | \mathbf{k}_i \rangle .$$

### B.3 Born approximation

Consider a scattering volume  $V$ , containing  $N$  scattering centers with shape functions  $S^i(\mathbf{r})$ , positions  $\mathbf{R}^i$  and scattering length density  $\rho_s$  (relative to the ambient material).

In the Born approximation ( $\tilde{T} \approx \tilde{V}$ ), the scattering amplitude is

$$\begin{aligned} f(\theta, \phi) &= -8\pi^3 \langle \mathbf{k}_f | \rho_s(\mathbf{r}) | \mathbf{k}_i \rangle \\ &= - \int d^3 \mathbf{r} e^{i \mathbf{q} \cdot \mathbf{r}} \rho_s(\mathbf{r}), \end{aligned}$$

where  $\mathbf{q} \equiv \mathbf{k}_i - \mathbf{k}_f$  denotes the wavevector transfer and

$$\rho_s(\mathbf{r}) = \frac{k_0^2}{4\pi} (1 - n^2(\mathbf{r})).$$

The differential cross-section (per scattering center) is then given by:

$$\frac{d\sigma}{d\Omega}(\mathbf{q}) = \frac{1}{N} \left| \int_V \rho_s(\mathbf{r}) e^{i \mathbf{q} \cdot \mathbf{r}} d^3 \mathbf{r} \right|^2.$$

Following the initial assumptions, the scattering length density can be written as:

$$\rho_s(\mathbf{r}) = \sum_i \rho_{s,i} S^i(\mathbf{r}) \otimes \delta(\mathbf{r} - \mathbf{R}^i),$$

with  $\rho_{s,i}$  the scattering length density of particle  $i$ . The cross-section then becomes:

$$\begin{aligned} N \frac{d\sigma}{d\Omega}(\mathbf{q}) &= \left| \sum_i F^i(\mathbf{q}) \exp(i \mathbf{q} \cdot \mathbf{R}^i) \right|^2 \\ &= \left\{ \sum_i \left| F^i(\mathbf{q}) \right|^2 + \sum_{i \neq j} F^i(\mathbf{q}) F^{j*}(\mathbf{q}) \exp[i \mathbf{q} \cdot (\mathbf{R}^i - \mathbf{R}^j)] \right\}. \end{aligned}$$

In the last expression, the formfactors  $F^i(\mathbf{q})$  are the Fourier transforms of the shape functions, including their scattering length densities:

$$F^i(\mathbf{q}) \equiv \int_V d^3 \mathbf{r} \rho_{s,i} S^i(\mathbf{r}) \exp(i \mathbf{q} \cdot \mathbf{r}).$$

Since in most real conditions only the statistical properties of the particles are known, one can consider the expectation value of this cross-section. Assuming that the particles' shapes are determined by their class  $\alpha$ , with abundance ratio  $p_\alpha \equiv N_\alpha / N$ , and defining the particle density  $\rho_V \equiv N / V$ , the expectation value becomes:

$$\begin{aligned} \left\langle \frac{d\sigma}{d\Omega}(\mathbf{q}) \right\rangle &= \sum_\alpha p_\alpha |F_\alpha(\mathbf{q})|^2 + \frac{\rho_V}{V} \sum_{\alpha, \beta} p_\alpha p_\beta F_\alpha(\mathbf{q}) F_\beta^*(\mathbf{q}) \\ &\quad \times \iint_V d^3 \mathbf{R}_\alpha d^3 \mathbf{R}_\beta \mathcal{G}_{\alpha, \beta}(\mathbf{R}_\alpha, \mathbf{R}_\beta) \exp[i \mathbf{q} \cdot (\mathbf{R}_\alpha - \mathbf{R}_\beta)]. \end{aligned}$$

In this equation, the factor  $\mathcal{G}_{\alpha,\beta}(\mathbf{R}_\alpha, \mathbf{R}_\beta)$  is called the *partial pair correlation function* and it represents a normalized probability of finding particles of type  $\alpha$  and  $\beta$  in positions  $\mathbf{R}_\alpha$  and  $\mathbf{R}_\beta$  respectively. More precisely, the probability density for finding a particle  $\alpha$  at position  $\mathbf{R}_\alpha$  and another one of type  $\beta$  at  $\mathbf{R}_\beta$  is given by:

$$\mathcal{P}(\alpha, \mathbf{R}_\alpha; \beta, \mathbf{R}_\beta) \equiv \rho_V^2 p_\alpha p_\beta \mathcal{G}_{\alpha,\beta}(\mathbf{R}_\alpha, \mathbf{R}_\beta) .$$

### B.3.1 General formulas

Even in the most general case, the partial pair correlation function will only depend on the difference  $\mathbf{R}_{\alpha\beta} \equiv (\mathbf{R}_\alpha - \mathbf{R}_\beta)$  of the particles' positions. One of the volume integrals can then be dropped, together with the volume factor, giving:

$$\begin{aligned} \left\langle \frac{d\sigma}{d\Omega}(\mathbf{q}) \right\rangle &= \sum_{\alpha} p_{\alpha} |F_{\alpha}(\mathbf{q})|^2 + \rho_V \sum_{\alpha,\beta} p_{\alpha} p_{\beta} F_{\alpha}(\mathbf{q}) F_{\beta}^{*}(\mathbf{q}) \\ &\times \int_V d^3 \mathbf{R}_{\alpha\beta} \mathcal{G}_{\alpha\beta}(\mathbf{R}_{\alpha\beta}) \exp[i\mathbf{q} \cdot \mathbf{R}_{\alpha\beta}] . \end{aligned}$$

This expression can be split into a diffuse part, which by definition should be zero for the case of only one particle type, and a coherent part, resulting from the coherent superposition of scattering amplitudes for particles at different positions:

$$\left\langle \frac{d\sigma}{d\Omega}(\mathbf{q}) \right\rangle = I_d(\mathbf{q}) + \left\langle F_{\alpha}(\mathbf{q}) S_{\alpha\beta}(\mathbf{q}) F_{\beta}^{*}(\mathbf{q}) \right\rangle_{\alpha\beta} ,$$

where

$$\begin{aligned} I_d(\mathbf{q}) &\equiv \left\langle |F_{\alpha}(\mathbf{q})|^2 \right\rangle_{\alpha} - |\langle F_{\alpha}(\mathbf{q}) \rangle_{\alpha}|^2 , \\ S_{\alpha\beta}(\mathbf{q}) &\equiv 1 + \rho_V \int_V d^3 \mathbf{R}_{\alpha\beta} \mathcal{G}_{\alpha\beta}(\mathbf{R}_{\alpha\beta}) \exp[i\mathbf{q} \cdot \mathbf{R}_{\alpha\beta}] . \end{aligned}$$

$S_{\alpha\beta}(\mathbf{q})$  is called the *interference function* and  $\langle \dots \rangle_{\alpha}$  is the expectation value over the classes  $\{\alpha\}$ .

### B.3.2 Decoupling approximation

When the partial pair correlation function is independent of the particle class  $\alpha$  ( $\mathcal{G}_{\alpha\beta}(\mathbf{R}_{\alpha\beta}) \equiv g(\mathbf{R}_{\alpha\beta})$ ), the scattering cross-section becomes:

$$\left\langle \frac{d\sigma}{d\Omega}(\mathbf{q}) \right\rangle = I_d(\mathbf{q}) + |\langle F_{\alpha}(\mathbf{q}) \rangle_{\alpha}|^2 \times S(\mathbf{q}) ,$$

where

$$S(\mathbf{q}) = 1 + \rho_V \int_V d^3 \mathbf{R} g(\mathbf{R}) \exp[i\mathbf{q} \cdot \mathbf{R}] .$$

### B.3.3 Local Monodisperse Approximation

By assuming that inside every coherence region of the beam, the particle class (or size/shape) is fixed, the cross-section will consist of an incoherent superposition of these different coherence regions and can be written as:

$$\left\langle \frac{d\sigma}{d\Omega}(\mathbf{q}) \right\rangle \approx \left\langle |F_\alpha(\mathbf{q})|^2 S_\alpha(\mathbf{q}) \right\rangle_\alpha .$$

Contrary to the Decoupling Approximation, the Local Monodisperse Approximation can account for particle class/size/shape-dependent pair correlation functions by having distinct interference functions  $S_\alpha(\mathbf{q})$ .

### B.3.4 Size-Spacing Correlation Approximation

In the Size-Spacing Correlation Approximation, a correlation is assumed between the shape/-size of the particles and their mutual spacing. A classical example would consist of particles whose closest-neighbour spacing depends linearly on the sum of their respective sizes. The following discussion of this type of correlation is inspired by [6]

The scattered intensity can also be calculated as the Fourier transform of the Patterson function, which is the autocorrelation of the scattering length density:

$$\mathcal{P}(\mathbf{r}) \equiv \sum_{ij} S_i(-\mathbf{r}) \otimes S_j(\mathbf{r}) \otimes \delta(\mathbf{r} + \mathbf{r}_i - \mathbf{r}_j) .$$

For a sample where only the statistical properties of particle positions and shape/size are known, the scattered intensity per scattering particle becomes average over an ensemble of the Fourier transform of the Patterson function:

$$I(\mathbf{q}) = \frac{1}{N} \langle \mathcal{F}(\mathcal{P}(\mathbf{r})) \rangle ,$$

where  $\mathcal{F}$  denotes the Fourier transform.

The ensemble averaged Patterson function will be denoted as:

$$Z(r) \equiv \frac{1}{N} \langle \mathcal{P}(\mathbf{r}) \rangle .$$

In the case of systems where the particles are aligned in one dimension, this autocorrelation function can be further split into nearest neighbour probabilities. First, it is split into terms for negative, zero or positive distance:

$$Z(\mathbf{r}) \equiv z_0(\mathbf{r}) + z_+(\mathbf{r}) + z_-(\mathbf{r}) .$$

Taking  $x$  as the coordinate in the direction in which the particles are arranged and  $s$  as an

orthogonal coordinate ( $\mathbf{r} \equiv (x, s)$ ), one obtains:

$$\begin{aligned} z_0(\mathbf{r}) &= \sum_{\alpha_0} p(\alpha_0) S_{\alpha_0}(-x, -s) \otimes S_{\alpha_0}(x, s) \\ z_+(\mathbf{r}) &= \sum_{\alpha_0 \alpha_1} p(\alpha_0, \alpha_1) S_{\alpha_0}(-x, -s) \otimes S_{\alpha_1}(x, s) \otimes P_1(x|\alpha_0 \alpha_1) \\ &\quad + \sum_{\alpha_0 \alpha_1 \alpha_2} p(\alpha_0, \alpha_1, \alpha_2) S_{\alpha_0}(-x, -s) \otimes S_{\alpha_2}(x, s) \otimes P_1(x|\alpha_0 \alpha_1) \otimes P_2(x|\alpha_0 \alpha_1 \alpha_2) \\ &\quad + \dots \\ z_-(\mathbf{r}) &= z_+(-\mathbf{r}), \end{aligned}$$

where  $p(\alpha_0, \dots, \alpha_n)$  denotes the probability of having a sequence of particles of the indicated sizes/shapes and  $P_n(x|\alpha_0 \dots \alpha_n)$  is the probability density of having a particle of type  $\alpha_n$  at a (positive) distance  $x$  of its nearest neighbour of type  $\alpha_{n-1}$  in a sequence of the given order.

In the Size–Spacing Correlation Approximation, one assumes that the particle sequence probabilities are just a product of their individual fractions:

$$p(\alpha_0, \dots, \alpha_n) = \prod_i p(\alpha_i),$$

and the nearest neighbour distance distribution is dependent only on the two particles involved:

$$P_n(x|\alpha_0 \dots \alpha_n) = P_1(x|\alpha_{n-1} \alpha_n).$$

Furthermore, the distance distribution  $P_1(x|\alpha_0 \alpha_1)$  depends on the particle sizes/shapes only through its mean value  $D$ :

$$P_1(x|\alpha_0 \alpha_1) = P_0(x - D(\alpha_0, \alpha_1)),$$

where  $D(\alpha_0, \alpha_1) = D_0 + \kappa [\Delta R(\alpha_0) + \Delta R(\alpha_1)]$ , with  $\Delta R(\alpha_i)$  the deviation of a size parameter of particle  $i$  with respect to the mean over all particles sizes/shapes and  $\kappa$  the coupling parameter.

In momentum space, the sum of convolutions can be written as a geometric series, which can be exactly calculated to be:

$$I(\mathbf{q}) = \left\langle |F_\alpha(\mathbf{q})|^2 \right\rangle_\alpha + 2 \operatorname{Re} \left\{ \widetilde{\mathcal{F}}_\kappa(\mathbf{q}) \widetilde{\mathcal{F}}_\kappa^*(\mathbf{q}) \cdot \frac{\Omega_\kappa(\mathbf{q})}{\tilde{p}_{2\kappa}(\mathbf{q}) [1 - \Omega_\kappa(\mathbf{q})]} \right\}, \quad (\text{B.2})$$

with

$$\begin{aligned} \tilde{p}_\kappa(\mathbf{q}) &= \int d\alpha p(\alpha) e^{i\kappa q_x \Delta R(\alpha)} \\ \Omega_\kappa(\mathbf{q}) &= \tilde{p}_{2\kappa}(\mathbf{q}) \phi(\mathbf{q}) e^{i q_x D_0} \\ \widetilde{\mathcal{F}}_\kappa(\mathbf{q}) &= \int d\alpha p(\alpha) F_\alpha(\mathbf{q}) e^{i\kappa q_x \Delta R(\alpha)}, \end{aligned}$$

and the Fourier transform of  $P_1(x|\alpha_0 \alpha_1)$  is

$$\mathcal{P}(\mathbf{q}) = \phi(\mathbf{q}) e^{i q_x D_0} e^{i\kappa q_x [\Delta R(\alpha_0) + \Delta R(\alpha_1)]}.$$

Using the result from the one-dimensional analysis, one can apply this formula ad hoc for distributions of particles in a plane, where the coordinate  $x$  will now be replaced with  $(x, y)$ , while the  $s$  coordinate encodes a position in the remaining orthogonal direction. One must be aware however that this constitutes a further approximation, since this type of correlation does not have a general solution in more than one dimension.

The intensity in equation (B.2) will contain a Dirac delta function contribution, caused by taking an infinite sum of terms that are perfectly correlated at  $\mathbf{q} = 0$ . One can leverage this behaviour by multiplying the nearest neighbour distribution by a constant factor  $e^{-D/\Lambda}$ , which removes the division by zero in equation (B.2). Another way of dealing with this infinity at  $\mathbf{q} = 0$  consists of taking only a finite number of terms, in which case the geometric series still has an analytical solution, but becomes a bit more cumbersome:

$$\begin{aligned} I(\mathbf{q}) &= \left\langle |F_\alpha(\mathbf{q})|^2 \right\rangle_\alpha + 2 \operatorname{Re} \left\{ \frac{1}{\tilde{p}_{2\kappa}(\mathbf{q})} \widetilde{\mathcal{F}}_\kappa(\mathbf{q}) \widetilde{\mathcal{F}}_\kappa^*(\mathbf{q}) \right. \\ &\quad \times \left. \left[ \left( 1 - \frac{1}{N} \right) \frac{\Omega_\kappa(\mathbf{q})}{1 - \Omega_\kappa(\mathbf{q})} - \frac{1}{N} \frac{\Omega_\kappa^2(\mathbf{q})(1 - \Omega_\kappa^{N-1}(\mathbf{q}))}{(1 - \Omega_\kappa(\mathbf{q}))^2} \right] \right\}. \end{aligned}$$

This expression has a well-defined limit for  $\Omega_\kappa(\mathbf{q}) \rightarrow 1$  (when  $\mathbf{q} \rightarrow 0$ ), namely:

$$\lim_{\mathbf{q} \rightarrow 0} I(\mathbf{q}) = \left\langle |F_\alpha(0)|^2 \right\rangle_\alpha + (N-1) |\langle F_\alpha(0) \rangle_\alpha|^2.$$

## B.4 Distorted Wave Born Approximation

In this section, one proceeds along similar lines as in the formal treatment of section B.1. This time however, the full Hamiltonian is written as  $H_2 = H_1 + V_2 = H_0 + V_1 + V_2$ , where  $H_0$  will again refer to the free Hamiltonian. In the distorted wave Born approximation (DWBA), one performs a perturbative expansion around the solutions of the Hamiltonian  $H_1$ , which are assumed to be known:

$$\begin{aligned} H_1 \Psi_{1\alpha}^\pm &= E_\alpha \Psi_{1\alpha}^\pm \\ \Psi_{1\alpha}^\pm &= \Psi_{0\alpha} + G_1^\pm V_1 \Psi_{0\alpha}, \end{aligned}$$

where the Green operators are defined to be:

$$\begin{aligned} G_1^\pm &\equiv (E - H_1 \pm i\epsilon)^{-1} \\ G_2^\pm &\equiv (E - H_2 \pm i\epsilon)^{-1}. \end{aligned}$$

The  $T$ -matrix element for scattering between the asymptotic states  $\Psi_{0\alpha}$  and  $\Psi_{0\beta}$  (note that these asymptotic states refer to the free Hamiltonian  $H_0$ ), is:

$$\begin{aligned} T_{\alpha\beta}^+ &= \langle \Psi_{0\beta} | V_1 + V_2 | \Psi_\alpha^+ \rangle \\ &= \langle \Psi_{0\beta} | V_1 + V_2 | \Psi_{0\alpha} + G_1^+ V_1 \Psi_{0\alpha} + G_2^+ V_2 \Psi_{1\alpha}^+ \rangle \\ &= \langle \Psi_{0\beta} | V_1 | \Psi_{1\alpha}^+ \rangle + \langle \Psi_{0\beta} | (V_1 G_1^+ + 1) V_2 | \Psi_\alpha^+ \rangle \\ &= \langle \Psi_{0\beta} | V_1 | \Psi_{1\alpha}^+ \rangle + \langle \Psi_{1\beta}^- | V_2 | \Psi_\alpha^+ \rangle \\ &= \langle \Psi_{0\beta} | V_1 | \Psi_{1\alpha}^+ \rangle + \langle \Psi_{1\beta}^- | T_2 | \Psi_{1\alpha}^+ \rangle, \end{aligned}$$

with  $T_2 = V_2 + V_2 G_2^+ V_2$ . By approximating this last term using  $T_2 \simeq V_2$ , one arrives at the distorted wave Born approximation:

$$T_{\alpha\beta}^+ \simeq \langle \Psi_{0\beta} | V_1 | \Psi_{1\alpha}^+ \rangle + \langle \Psi_{1\beta}^- | V_2 | \Psi_{1\alpha}^+ \rangle.$$

#### B.4.1 Multilayer systems

In multilayer systems, the first term of equation (B.4) denotes the specular part of the reflection, while the second term is responsible for the off-specular scattering. This off-specular part is caused by deviations from the perfectly smooth layered system, as e.g. interface roughnesses or included nanoparticles. In here only the case of nanoparticles will be treated.

In the conventions where  $H = -\Delta + V$ , the potential splits into two parts  $V_1$  and  $V_2$ , where only the second part is treated as a perturbation:

$$\begin{aligned} V_1 &= k_0^2 (1 - n_0^2(\mathbf{r})) \\ V_2 &= \sum_i k_0^2 (n_0^2(\mathbf{R}^i) - n_i^2) S^i(\mathbf{r}) \otimes \delta(\mathbf{r} - \mathbf{R}^i), \end{aligned}$$

where  $n_0(\mathbf{r})$  denotes the refractive index of the unperturbed system (which, in case of a multilayer system, will only depend on its  $z$ -coordinate) and  $n_i$  is the refractive index of the nanoparticle with shape function  $S^i$  and position  $\mathbf{R}^i$ .

For nanoparticles in a specific layer  $j$ , i.e.  $V_2 \neq 0$  only in layer  $j$ , one only needs the unperturbed solutions in layer  $j$ :

$$\begin{aligned} \langle \mathbf{r} | \Psi_{1k_i}^+ \rangle &= (2\pi)^{-3/2} [R_j(\mathbf{k}_i) e^{i\mathbf{k}_{j,R}(\mathbf{k}_i) \cdot \mathbf{r}} + T_j(\mathbf{k}_i) e^{i\mathbf{k}_{j,T}(\mathbf{k}_i) \cdot \mathbf{r}}] \\ \langle \Psi_{1k_f}^- | \mathbf{r} \rangle &= (2\pi)^{-3/2} [R_j(-\mathbf{k}_f) e^{i\mathbf{k}_{j,R}(-\mathbf{k}_f) \cdot \mathbf{r}} + T_j(-\mathbf{k}_f) e^{i\mathbf{k}_{j,T}(-\mathbf{k}_f) \cdot \mathbf{r}}]. \end{aligned}$$

The off-specular contribution to the scattering amplitude then becomes:

$$\begin{aligned} f(\theta, \phi) &= - \int d^3 \mathbf{r} \frac{V_2(\mathbf{r})}{4\pi} \left[ T_i T_f e^{i(\mathbf{k}_{j,i} - \mathbf{k}_{j,f}) \cdot \mathbf{r}} + R_i T_f e^{i(\tilde{\mathbf{k}}_{j,i} - \mathbf{k}_{j,f}) \cdot \mathbf{r}} \right. \\ &\quad \left. + T_i R_f e^{i(\mathbf{k}_{j,i} - \tilde{\mathbf{k}}_{j,f}) \cdot \mathbf{r}} + R_i R_f e^{i(\tilde{\mathbf{k}}_{j,i} - \tilde{\mathbf{k}}_{j,f}) \cdot \mathbf{r}} \right], \end{aligned}$$

where the following shorthand notations were used:

$$\begin{aligned} T_i &\equiv T_j(\mathbf{k}_i) & R_i &\equiv R_j(\mathbf{k}_i) \\ T_f &\equiv T_j(-\mathbf{k}_f) & R_f &\equiv R_j(-\mathbf{k}_f) \\ \mathbf{k}_{j,i} &\equiv \mathbf{k}_{j,T}(\mathbf{k}_i) & \tilde{\mathbf{k}}_{j,i} &\equiv \mathbf{k}_{j,R}(\mathbf{k}_i) \\ \mathbf{k}_{j,f} &\equiv -\mathbf{k}_{j,T}(-\mathbf{k}_f) & \tilde{\mathbf{k}}_{j,f} &\equiv -\mathbf{k}_{j,R}(-\mathbf{k}_f). \end{aligned}$$

From this expression, one sees that the scattering amplitude consists of a weighted sum of Fourier transforms of the potential  $V_2$ . Using

$$V_2(\mathbf{r}) = \sum_i 4\pi \rho_{s,rel,i} S^i(\mathbf{r}) \otimes \delta(\mathbf{r} - \mathbf{R}^i),$$

with  $\rho_{s,rel,i} \equiv k_0^2 (n_0^2(\mathbf{R}^i) - n_i^2) / 4\pi$ , the scattering amplitude becomes

$$f(\theta, \phi) = - \sum_i \rho_{s,rel,i} \mathcal{F}_{\text{DWBA}}^i(\mathbf{k}_{j,i}, \mathbf{k}_{j,f}, \mathbf{R}_z^i) e^{i(\mathbf{k}_{j,i\parallel} - \mathbf{k}_{j,f\parallel}) \cdot \mathbf{R}^i\parallel},$$

with

$$\begin{aligned} \mathcal{F}_{\text{DWBA}}^i(\mathbf{k}_i, \mathbf{k}_f, R_z) &\equiv T_i T_f F^i(\mathbf{k}_i - \mathbf{k}_f) e^{i(k_{iz} - k_{ fz})R_z} + R_i T_f F^i(\tilde{\mathbf{k}}_i - \mathbf{k}_f) e^{i(-k_{iz} - k_{ fz})R_z} \\ &+ T_i R_f F^i(\mathbf{k}_i - \tilde{\mathbf{k}}_f) e^{i(k_{iz} + k_{ fz})R_z} + R_i R_f F^i(\tilde{\mathbf{k}}_i - \tilde{\mathbf{k}}_f) e^{i(-k_{iz} + k_{ fz})R_z}, \end{aligned}$$

With this last expression, the same techniques as demonstrated in section B.3 can be applied, leading to the following expression for the expectation value of the scattering cross-section:

$$\begin{aligned} &\left\langle \frac{d\sigma}{d\Omega}(\mathbf{k}_i, \mathbf{k}_f) \right\rangle_{\text{Off-specular}} \\ &= \sum_{\alpha} p_{\alpha} |\mathcal{F}_{\alpha}(\mathbf{k}_{j,i}, \mathbf{k}_{j,f}, R_{\alpha,z})|^2 + \frac{\rho_S}{S} \sum_{\alpha, \beta} p_{\alpha} p_{\beta} \mathcal{F}_{\alpha}(\mathbf{k}_{j,i}, \mathbf{k}_{j,f}, R_{\alpha,z}) \mathcal{F}_{\beta}^*(\mathbf{k}_{j,i}, \mathbf{k}_{j,f}, R_{\beta,z}) \\ &\times \iint_S d^2 \mathbf{R}_{\alpha\parallel} d^2 \mathbf{R}_{\beta\parallel} \mathcal{G}_{\alpha, \beta}(\mathbf{R}_{\alpha\parallel}, \mathbf{R}_{\beta\parallel}) \exp[i\mathbf{q}_{j\parallel} \cdot (\mathbf{R}_{\alpha\parallel} - \mathbf{R}_{\beta\parallel})]. \end{aligned}$$

The main differences with respect to the cross-section in the Born approximation are:

1. The particle form factor now consists of a more complex expression and now depends on both incoming and outgoing wavevectors and also on the  $z$ -coordinate of the particle;
2. Since the  $z$ -coordinate of the particles is implicitly included in its formfactor, the position integrals only run over  $x$ - and  $y$ -coordinates and the volume and density gets replaced with the surface area and surface density respectively.

## Appendix C

### Form factors

In BornAgain the expression of the form factor has been implemented in the Born approximation. Each of them is defined as

$$F(\mathbf{q}) = \int_V \exp(i\mathbf{q} \cdot \mathbf{r}) d^3\mathbf{r},$$

where  $V$  is the volume of the particle's shape,  $\mathbf{q} = \mathbf{k}_i - \mathbf{k}_f$  is the scattering vector with  $\mathbf{k}_f$  and  $\mathbf{k}_i$  the scattered and incident wave vector, respectively. The Distorted Wave Born Approximation can be taken into account as it has been explained in Section 5.3.2.

The particle's shape is parametrized in a cartesian frame, with its  $z$ -axis pointing upwards and its origin at the center of the bottom of the particle:  $\mathbf{r} = (x, y, z)$ . In the followings, a schematic view will depict this layout for each form factor.

All form factors have been implemented with complex scattering vectors in order to take any material absorption into account.

## C.1 Box

### Real-space geometry

This shape is a rectangular cuboid as shown in fig. C.1.

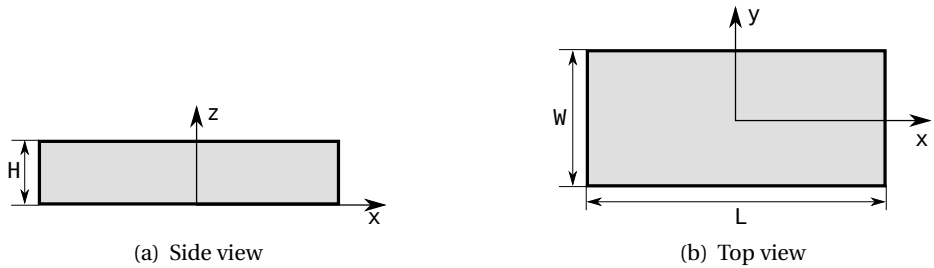


Figure C.1: Sketch of a Box.

### Parameters:

- length of the base  $L$ ,
- width of the base  $W$ ,
- height  $H$ .

### Properties:

- volume  $V = LWH$ ,
- particle surface seen from above  $S = LW$ .

### Expression of the form factor

$$F(\mathbf{q}, L, W, H) = LWH \exp\left(i q_z \frac{H}{2}\right) \text{sinc}\left(q_x \frac{L}{2}\right) \text{sinc}\left(q_y \frac{W}{2}\right) \text{sinc}\left(q_z \frac{H}{2}\right),$$

where  $\text{sinc}(x) = \sin(x)/x$  is the cardinal sine.

**Syntax:** `FormFactorBox(length, width, height)`

**Example**

Figure C.2 shows the normalized intensity  $|F|^2/V^2$ , computed with  $L = 20 \text{ nm}$ ,  $W = 16 \text{ nm}$ , and  $H = 13 \text{ nm}$ :

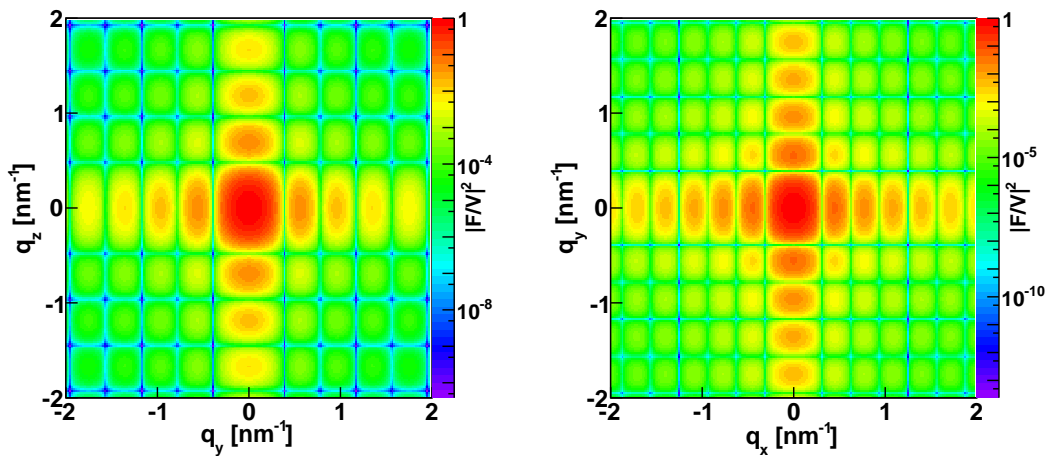


Figure C.2: Normalized intensity for the form factor of a Box plotted against  $(q_y, q_z)$  and  $(q_x, q_y)$  and computed with `FormFactorBox(20.*nanometer, 16.*nanometer, 13.*nanometer)`.

## C.2 Prism3

### Real-space geometry

This shape is a triangular prism, whose base is an equilateral triangle as shown in fig. C.3.

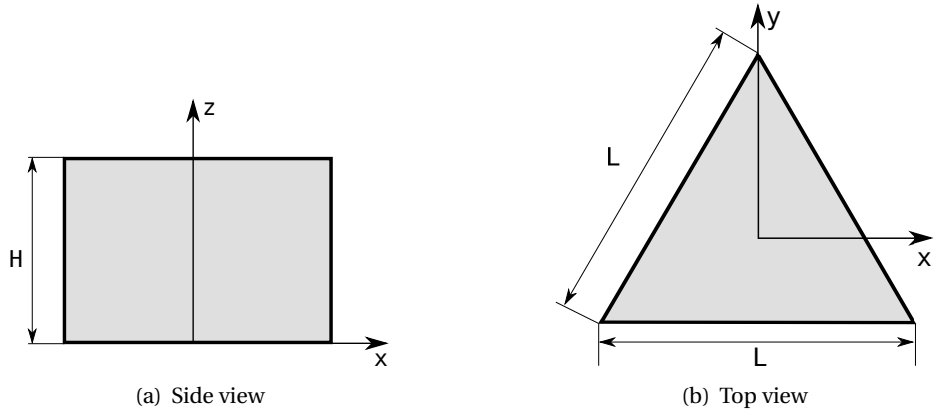


Figure C.3: Sketch of a Prism3.

### Parameters:

- length  $L$  of one side of the base,
- height  $H$ .

### Properties:

- volume  $V = \frac{\sqrt{3}}{4} HL^2$ ,
- particle surface seen from above  $S = \frac{\sqrt{3}}{4} L^2$ .

### Expression of the form factor

$$F(\mathbf{q}, L, H) = \frac{2\sqrt{3}}{q_x^2 - 3q_y^2} \exp\left(-iq_y \frac{L}{2\sqrt{3}}\right) \left[ \exp\left(i\sqrt{3}q_y \frac{L}{2}\right) - \cos\left(q_x \frac{L}{2}\right) - i\sqrt{3}q_y \frac{L}{2} \operatorname{sinc}\left(q_x \frac{L}{2}\right) \right] \\ \times H \operatorname{sinc}\left(q_z \frac{H}{2}\right) \exp\left(iq_z \frac{H}{2}\right),$$

where  $\operatorname{sinc}(x) = \sin(x)/x$  is the cardinal sine.

**Syntax:** `FormFactorPrism3(length, height)`

**Example**

Figure C.4 shows the normalized intensity  $|F|^2 / V^2$ , computed with  $L = 10 \text{ nm}$  and  $H = 13 \text{ nm}$ .

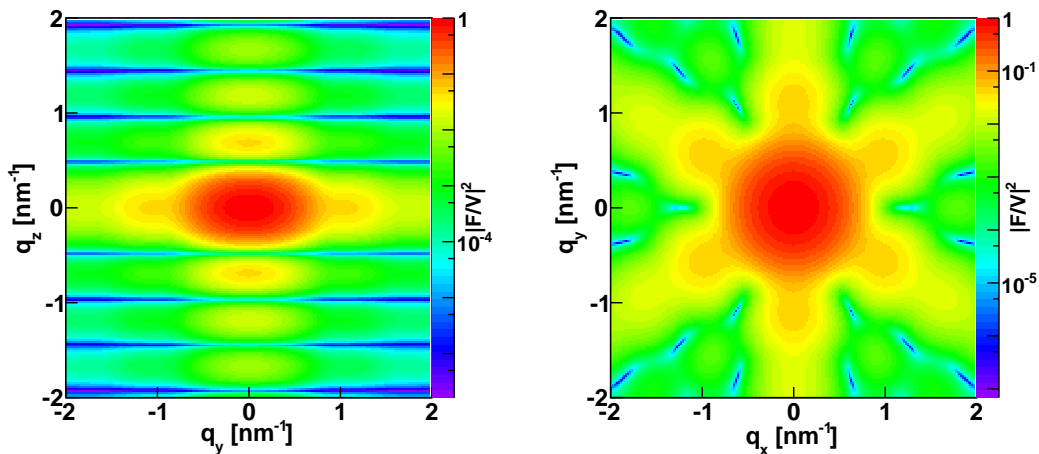


Figure C.4: Normalized intensity for the form factor of a Prism3 plotted against  $(q_y, q_z)$  and  $(q_x, q_y)$  and computed with `FormFactorPrism3(10.*nanometer, 13.*nanometer)`.

### C.3 Tetrahedron

#### Real-space geometry

This shape is a truncated tetrahedron as shown in fig. C.5.

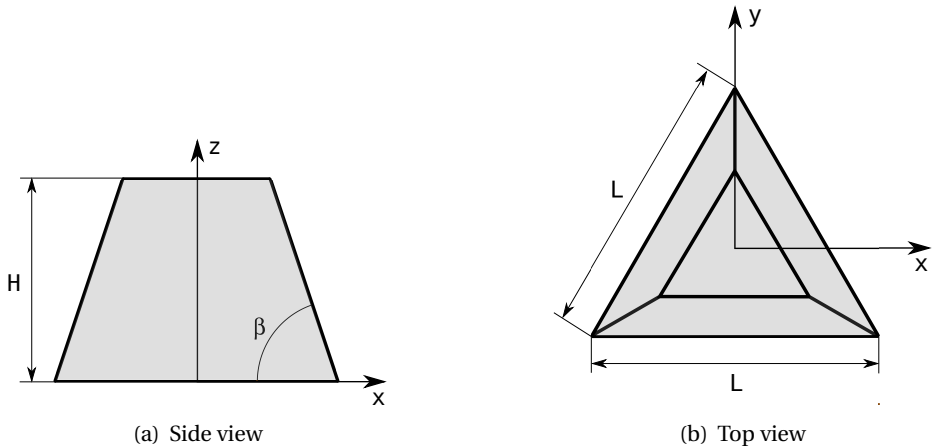


Figure C.5: Sketch of a Tetrahedron. The implementation of this shape uses angle  $\alpha$ , which is linked to  $\beta$  via  $\tan \alpha = 2 \tan \beta$ .  $\alpha$  is measured along one of the base lines and  $\beta$  at one of the base vertices.

#### Parameters:

- length of one side of the equilateral triangular base  $L$ ,
- height  $H$ ,
- angle  $\alpha$  is the angle between the base and the side faces, taken in the middle of the base lines.

**Restrictions on the parameters:**  $\frac{H}{L} < \frac{\tan \alpha}{2\sqrt{3}}$ .

#### Properties:

- volume  $V = \frac{\tan(\alpha)L^3}{24} \left[ 1 - \left( 1 - \frac{2\sqrt{3}H}{L\tan(\alpha)} \right)^3 \right]$ ,
- particle surface seen from above  $S = \frac{\sqrt{3}}{4}L^2$ .

### Expression of the form factor

$$F(\mathbf{q}, L, H, \alpha) = \frac{\sqrt{3}H}{q_x(q_x^2 - 3q_y^2)} \exp\left(i \frac{q_z L}{2 \tan(\alpha) \sqrt{3}}\right) \times \\ \left\{ 2q_x \exp(i q_3 D) \text{sinc}(q_3 H) - (q_x + \sqrt{3}q_y) \exp(i q_1 D) \text{sinc}(q_1 D) - (q_x - \sqrt{3}q_y) \exp(-i q_2 D) \text{sinc}(q_2 H) \right\},$$

with  $\text{sinc}(x) = \sin(x)/x$ ,

$$q_1 = \frac{1}{2} \left[ \frac{q_x \sqrt{3} - q_y}{\tan \alpha} - q_z \right], \quad q_2 = \frac{1}{2} \left[ \frac{q_x \sqrt{3} + q_y}{\tan \alpha} + q_z \right], \quad q_3 = \frac{q_y}{\tan \alpha} - \frac{q_z}{2}, \quad D = \frac{L \tan \alpha}{\sqrt{3}} - H.$$

**Syntax:** `FormFactorTetrahedron(length, height, alpha)`

### Example

Figure C.6 shows the normalized intensity  $|F|^2/V^2$ , computed with  $L = 15$  nm,  $H = 6$  nm and  $\alpha = 60^\circ$ .

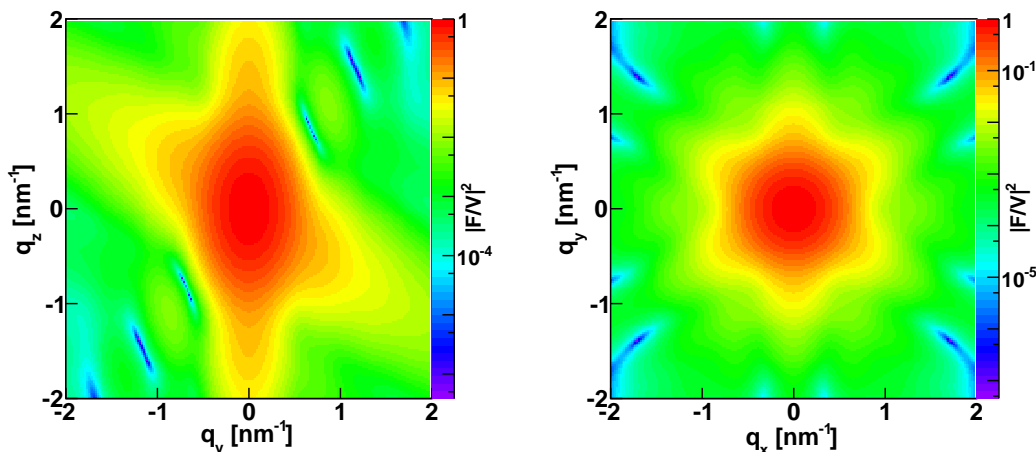


Figure C.6: Normalized intensity for the form factor of a Tetrahedron plotted against  $(q_y, q_z)$  and  $(q_x, q_y)$  and computed with `FormFactorTetrahedron(15.*nanometer, 6.*nanometer, 60.*degree)`.

## C.4 Prism6

### Real-space geometry

This shape is an hexagonal prism (see fig. C.7).

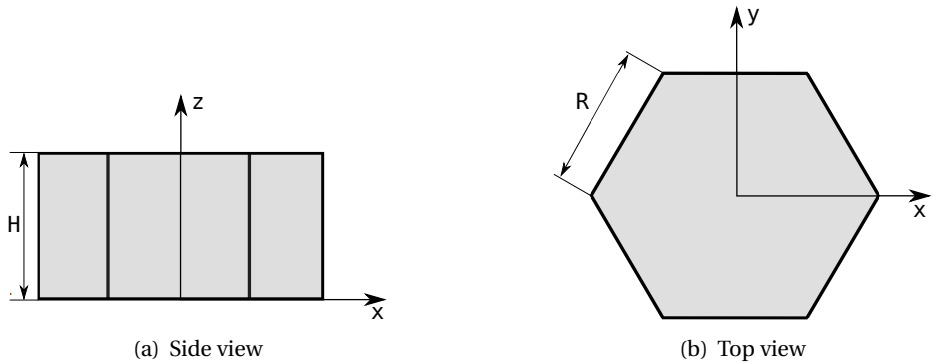


Figure C.7: Sketch of a Prism6.

### Parameters:

- radius of the hexagonal base  $R$ ,
- height  $H$ .

### Properties:

- volume  $V = \frac{3\sqrt{3}}{2}HR^2$ ,
- particle surface seen from above  $S = \frac{3\sqrt{3}R^2}{2}$ .

### Expression of the form factor

$$F(\mathbf{q}, R, H) = \frac{4H\sqrt{3}}{3q_y^2 - q_x^2} \operatorname{sinc}\left(q_z \frac{H}{2}\right) \exp\left(-iq_z \frac{H}{2}\right) \times \\ \left\{ \frac{3q_y^2 R^2}{4} \operatorname{sinc}\left(\frac{q_x R}{2}\right) \operatorname{sinc}\left(\frac{\sqrt{3}q_y R}{2}\right) + \cos(q_x R) - \cos\left(q_y \frac{\sqrt{3}R}{2}\right) \cos\left(\frac{q_x R}{2}\right) \right\},$$

with  $\operatorname{sinc}(x) = \sin(x)/x$ .

**Syntax:** `FormFactorPrism6(radius, height)`

**Example**

Figure C.8 shows the normalized intensity  $|F|^2 / V^2$ , computed with  $R = 5 \text{ nm}$  and  $H = 11 \text{ nm}$ .

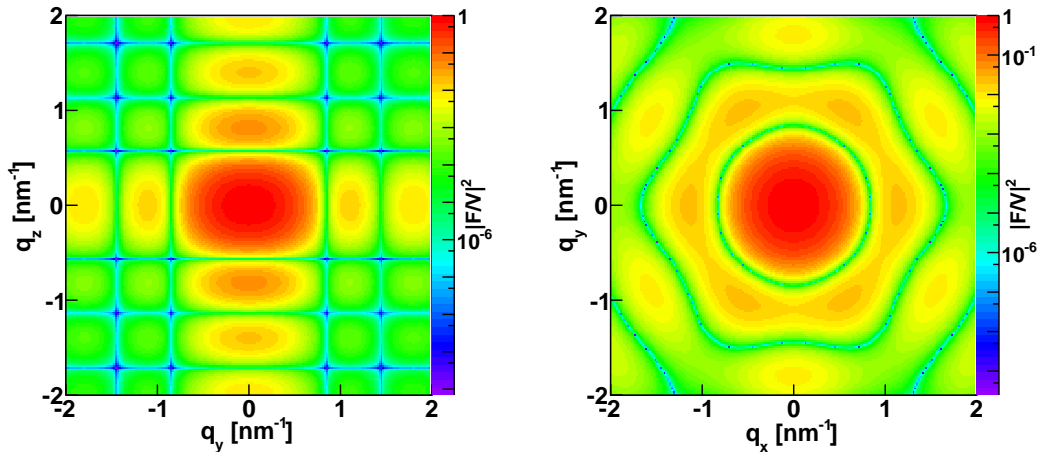


Figure C.8: Normalized intensity for the form factor of a Prism6 plotted against  $(q_y, q_z)$  and  $(q_x, q_y)$  and computed with `FormFactorPrism6(5.*nanometer, 11.*nanometer)`.

## C.5 Cone6

### Real-space geometry

It is a truncated hexagonal pyramid (see fig. C.9).

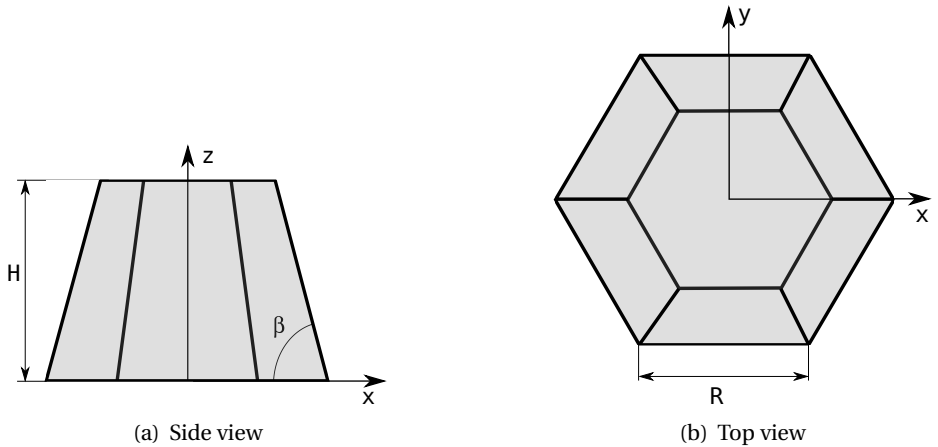


Figure C.9: Sketch of a Cone6. The implementation of this shape uses angle  $\alpha$ , which is linked to  $\beta$  via  $\tan \alpha = \frac{2}{\sqrt{3}} \tan \beta$ .  $\alpha$  is measured along one of the base lines and  $\beta$  at one of the base vertices.

### Parameters:

- radius of the regular hexagonal base  $R$ ,
- height  $H$ ,
- angle  $\alpha$  is considered between one of the side faces and the middle of a base length.

**Restrictions on the parameters:**  $\frac{2H}{\sqrt{3}R} < \tan \alpha$ .

### Properties:

- volume  $V = \frac{3}{4} \tan(\alpha) R^3 \left[ 1 - \left( 1 - \frac{2H}{\tan(\alpha) R \sqrt{3}} \right)^3 \right]$ ,
- particle surface seen from above  $S = \frac{3\sqrt{3}R^2}{2}$ .

### Expression of the form factor

The calculation can be derived from “Prism6” (Section C.4) by considering a side length varying with the vertical position:

$$F(\mathbf{q}, R, H, \alpha) = \frac{4\sqrt{3}}{3q_y^2 - q_x^2} \int_0^H \exp(iq_z z) \left[ \frac{3}{4} R_z^2 q_y^2 \operatorname{sinc}\left(\frac{q_x R_z}{2}\right) \operatorname{sinc}\left(\frac{\sqrt{3}q_y R_z}{2}\right) \right. \\ \left. + \cos(q_x R_z) - \cos\left(\frac{\sqrt{3}q_y R_z}{2}\right) \cos\left(\frac{q_x R_z}{2}\right) \right] dz$$

with  $R_z = R - \frac{2z}{\sqrt{3}\tan(\alpha)}$  and  $\operatorname{sinc}(x) = \sin(x)/x$ .

**Syntax:** FormFactorCone6(radius, height, alpha)

### Example

Figure C.10 shows the normalized intensity  $|F|^2/V^2$ , computed with  $R = 10$  nm,  $H = 13$  nm, and  $\alpha = 60^\circ$ .

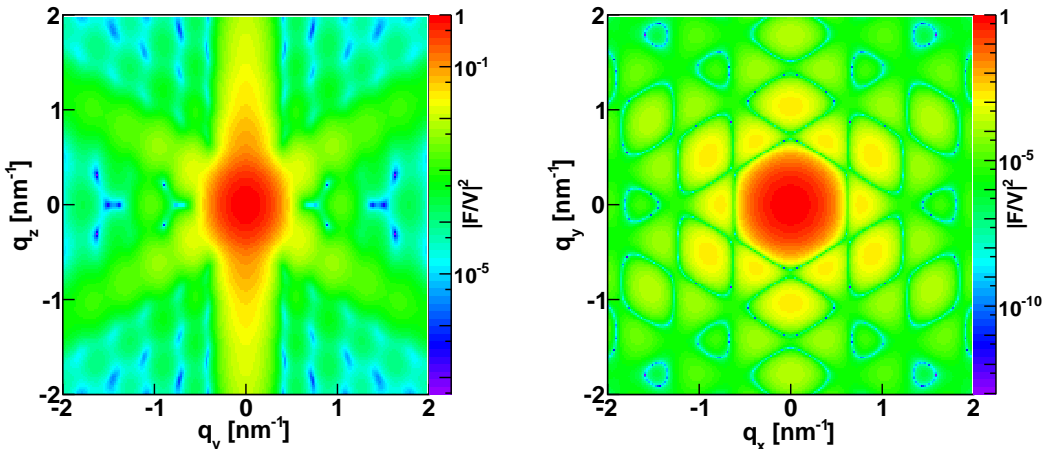


Figure C.10: Normalized intensity for the form factor of a Cone6 plotted against  $(q_y, q_z)$  and  $(q_x, q_y)$  and computed with FormFactorCone6(10.\*nanometer, 13.\*nanometer, 60.\*degree).

## C.6 Pyramid

### Real-space geometry

This shape is a truncated pyramid with a square base as shown in fig. C.11.

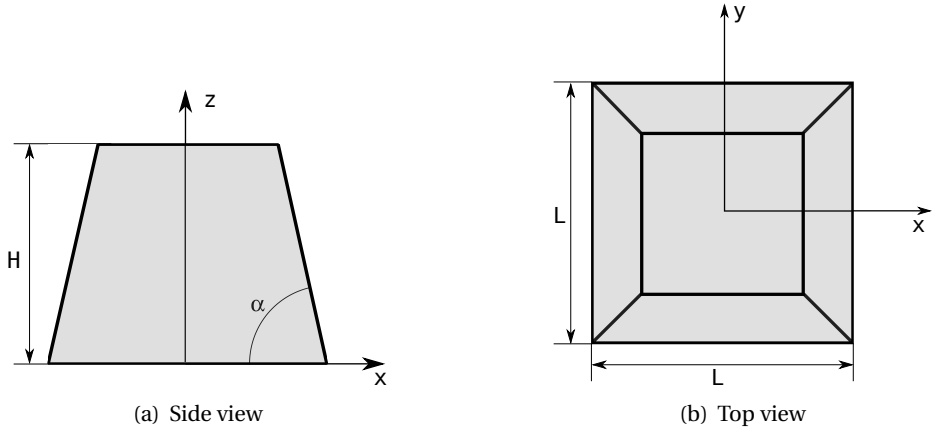


Figure C.11: Sketch of a Pyramid

### Parameters:

- length of one side of the square base  $L$ ,
- height  $H$ ,
- $\alpha$  is the angle between the base and the side faces, taken in the middle of the base lines.

**Restrictions on the parameters:**  $\frac{2H}{L} < \tan(\alpha)$ .

### Properties:

- volume  $V = \frac{1}{6} \tan(\alpha) L^3 \left[ 1 - \left( 1 - \frac{2H}{\tan(\alpha)L} \right)^3 \right]$ ,
- particle surface seen from above  $S = L^2$ .

### Expression of the form factor

$$F(\mathbf{q}, L, H, \alpha) = \frac{H}{q_x q_y} \times \left\{ K_1 \cos \left[ (q_x - q_y) \frac{L}{2} \right] + K_2 \sin \left[ (q_x - q_y) \frac{L}{2} \right] - K_3 \cos \left[ (q_x + q_y) \frac{L}{2} \right] - K_4 \sin \left[ (q_x + q_y) \frac{L}{2} \right] \right\},$$

with  $\text{sinc}(x) = \sin(x)/x$ ,

$$q_1 = \frac{1}{2} \left[ \frac{q_x - q_y}{\tan(\alpha)} + q_z \right], \quad q_2 = \frac{1}{2} \left[ \frac{q_x - q_y}{\tan(\alpha)} - q_z \right]$$

$$q_3 = \frac{1}{2} \left[ \frac{q_x + q_y}{\tan(\alpha)} + q_z \right], \quad q_4 = \frac{1}{2} \left[ \frac{q_x + q_y}{\tan(\alpha)} - q_z \right]$$

$$K_1 = \text{sinc}(q_1 H) \exp(i q_1 H) + \text{sinc}(q_2 H) \exp(-i q_2 H)$$

$$K_2 = -i \text{sinc}(q_1 H) \exp(i q_1 H) + i \text{sinc}(q_2 H) \exp(-i q_2 H)$$

$$K_3 = \text{sinc}(q_3 H) \exp(i q_3 H) + \text{sinc}(q_4 H) \exp(-i q_4 H)$$

$$K_4 = -i \text{sinc}(q_3 H) \exp(i q_3 H) + i \text{sinc}(q_4 H) \exp(-i q_4 H)$$

**Syntax:** `FormFactorPyramid(length, height, alpha)`

**Examples** Figure C.12 shows the normalized intensity  $|F|^2/V^2$ , computed with  $L = 18 \text{ nm}$ ,  $H = 13 \text{ nm}$  and  $\alpha = 60^\circ$ .

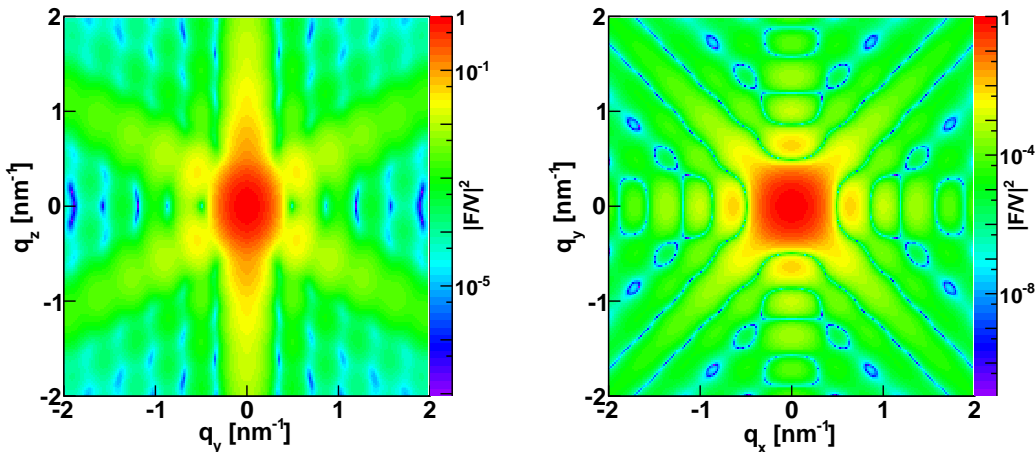


Figure C.12: Normalized intensity for the form factor of a pyramid plotted against  $(q_y, q_z)$  and  $(q_x, q_y)$  and computed with `FormFactorPyramid(18.*nanometer, 13.*nanometer, 60.*degree)`.

## C.7 Anisotropic pyramid

### Real-space geometry

This shape is a truncated right pyramid with a rectangular base as shown in fig. C.13.

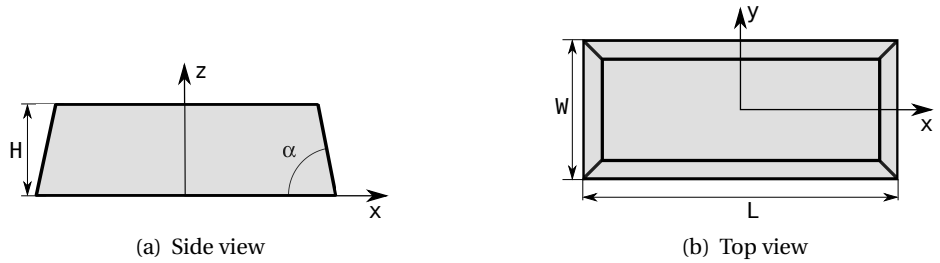


Figure C.13: Sketch of an Anisotropic Pyramid.

### Parameters:

- full length of the base  $L$ ,
- full width of the base  $W$ ,
- height  $H$ ,
- $\alpha$  is the angle between the base and the side faces, taken in the middle of the base lines.

**Restrictions on the parameters:**  $\frac{2H}{L} < \tan(\alpha)$  and  $\frac{2H}{W} < \tan(\alpha)$ .

### Properties:

- volume  $V = H \left[ LW - \frac{(L+W)H}{\tan(\alpha)} + \frac{4}{3} \frac{H^2}{\tan^2(\alpha)} \right]$ ,
- particle surface seen from above  $S = LW$ .

### Expression of the form factor

$$F(\mathbf{q}, L, W, H, \alpha) = \frac{H}{q_x q_y} \times \left\{ K_1 \cos \left( q_x \frac{L}{2} - q_y \frac{W}{2} \right) + K_2 \sin \left( q_x \frac{L}{2} - q_y \frac{W}{2} \right) - K_3 \cos \left( q_x \frac{L}{2} + q_y \frac{W}{2} \right) - K_4 \sin \left( q_x \frac{L}{2} + q_y \frac{W}{2} \right) \right\},$$

with  $\text{sinc}(x) = \sin(x)/x$ ,

$$\begin{aligned} K_1 &= \exp(-iq_2 H) \text{sinc}(q_2 H) + \exp(iq_1 H) \text{sinc}(q_1 H) \\ K_2 &= i \exp(-iq_2 H) \text{sinc}(q_2 H) - i \exp(iq_1 H) \text{sinc}(q_1 H) \\ K_3 &= \exp(-iq_4 H) \text{sinc}(q_4 H) + \exp(iq_3 H) \text{sinc}(q_3 H) \\ K_4 &= i \exp(iq_4 H) \text{sinc}(q_4 H) - i \exp(iq_3 H) \text{sinc}(q_3 H) \\ q_1 &= \frac{1}{2} \left[ \frac{q_x - q_y}{\tan \alpha} + q_z \right], \quad q_2 = \frac{1}{2} \left[ \frac{q_x - q_y}{\tan \alpha} - q_z \right] \\ q_3 &= \frac{1}{2} \left[ \frac{q_x + q_y}{\tan \alpha} + q_z \right], \quad q_4 = \frac{1}{2} \left[ \frac{q_x + q_y}{\tan \alpha} - q_z \right] \end{aligned}$$

**Syntax:** `FormFactorAnisoPyramid(length, width, height, alpha)`

### Example

Figure C.14 shows the normalized intensity  $|F|^2/V^2$ , computed with  $L = 20 \text{ nm}$ ,  $W = 16 \text{ nm}$ ,  $H = 13 \text{ nm}$ , and  $\alpha = 60^\circ$ .

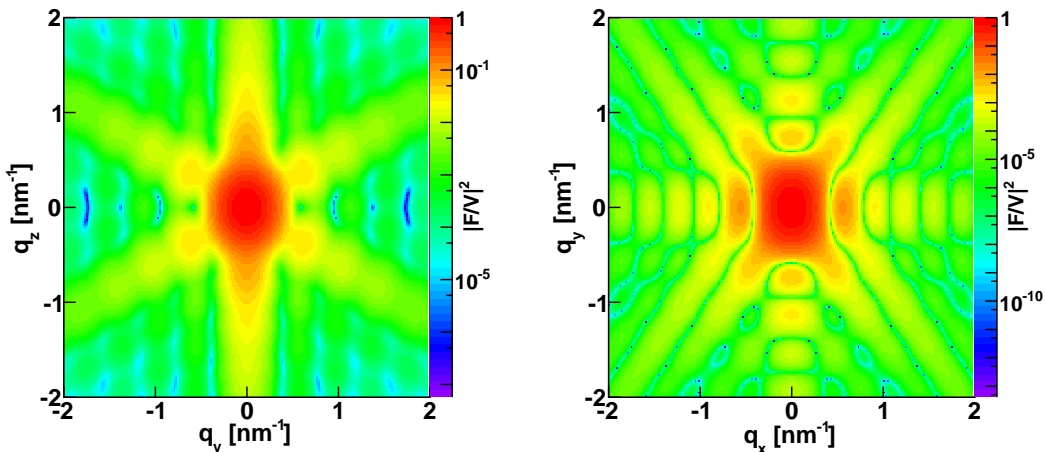


Figure C.14: Normalized intensity for the form factor of an anisotropic pyramid  $|F|^2/V^2$ , plotted against  $(q_y, q_z)$  and  $(q_x, q_y)$  and computed with `FormFactorAnisoPyramid(20.*nanometer, 16.*nanometer, 60.*degree)`.

## C.8 Cuboctahedron

### Real-space geometry

It is a combination of two pyramids with square bases, as shown in fig. C.15: the bottom one is upside down with an height  $H$  and the top one has the opposite orientation (the standard one) and an height  $r_H \times H$ .

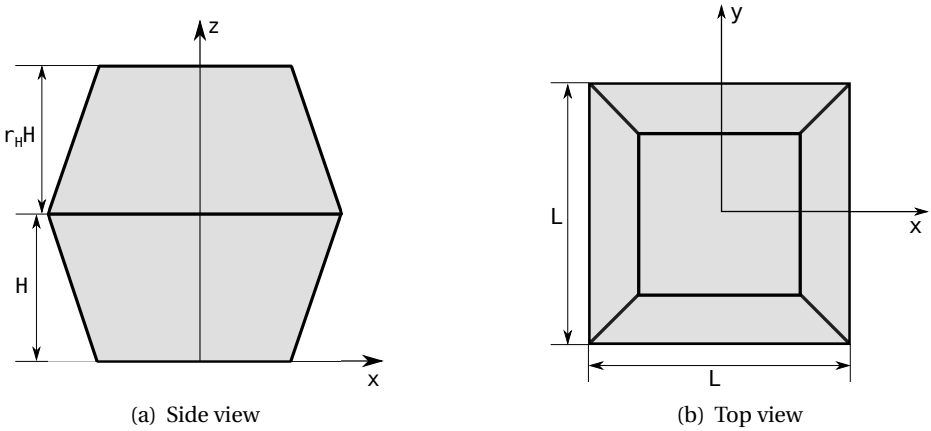


Figure C.15: Sketch of a Cuboctahedron.

### Parameters:

- length of the shared square base  $L$ ,
- height  $H$ ,
- height\_ratio  $r_H$ ,
- $\alpha$  is the angle between the base and the side faces, taken in the middle of the base lines (see fig. C.11 in Section C.6).

**Restrictions on the parameters:**  $\frac{2H}{L} < \tan(\alpha)$  and  $\frac{2r_H H}{L} < \tan(\alpha)$ .

### Properties:

- volume  $V = \frac{1}{6} \tan(\alpha) L^3 \left[ 2 - \left(1 - \frac{2H}{L \tan(\alpha)}\right)^3 - \left(1 - \frac{2r_H H}{L \tan(\alpha)}\right)^3 \right]$ ,
- particle surface seen from above  $S = L^2$ .

### Expression of the form factor

$$F(\mathbf{q}, L, H, r_H, \alpha) = \exp(i q_z H) \left[ F_{\text{Pyramid}}(q_x, q_y, q_z, L, r_H H, \alpha) + F_{\text{Pyramid}}(q_x, q_y, -q_z, L, H, \alpha) \right]$$

**Syntax:** FormFactorCuboctahedron(length, height, height\_ratio, alpha)

**Example**

Figure C.16 shows the normalized intensity  $|F|^2/V^2$ , computed with  $L = 20 \text{ nm}$ ,  $H = 13 \text{ nm}$ ,  $r_H = 0.7$ , and  $\alpha = 60^\circ$ .

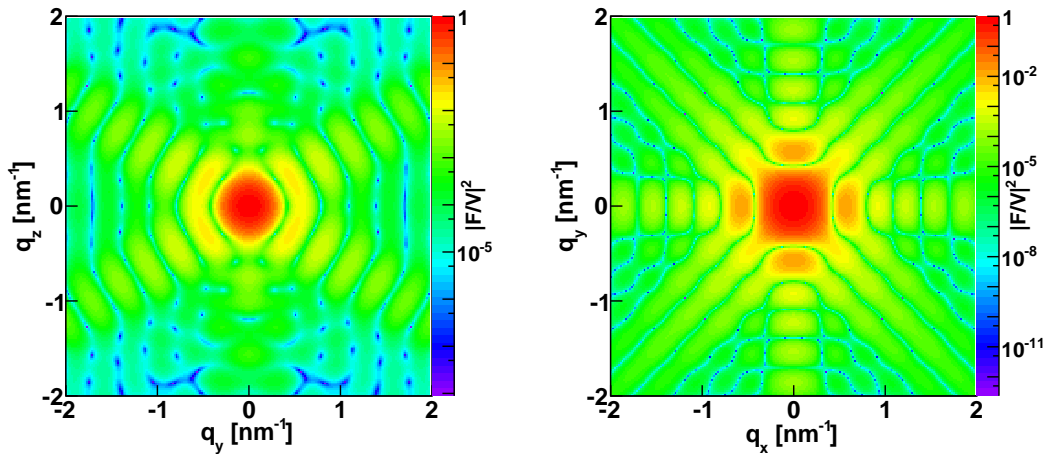


Figure C.16: Normalized intensity for the form factor of a cuboctahedron plotted against  $(q_y, q_z)$  and  $(q_x, q_y)$  and computed with FormFactorCuboctahedron(20.\*nanometer, 13.\*nanometer, 0.7, 60.\*degree).

## C.9 Cylinder

### Real-space geometry

This shape is a right circular cylinder (see fig. C.17).

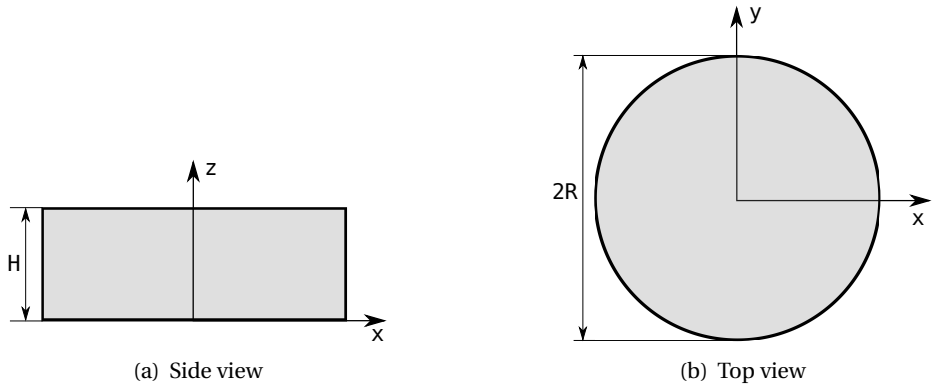


Figure C.17: Sketch of a Cylinder.

### Parameters:

- radius of the circular base  $R$ ,
- height  $H$ .

### Properties:

- volume  $V = \pi R^2 H$ ,
- particle surface seen from above  $S = \pi R^2$ .

### Expression of the form factor

$$F(\mathbf{q}, R, H) = 2\pi R^2 H \operatorname{sinc}\left(q_z \frac{H}{2}\right) \exp\left(i q_z \frac{H}{2}\right) \frac{J_1(q_{\parallel} R)}{q_{\parallel} R},$$

with  $q_{\parallel} = \sqrt{q_x^2 + q_y^2}$  and  $J_1(x)$  is the first order Bessel function of the first kind [16].

**Syntax:** `FormFactorCylinder(radius, height)`

**Example**

Figure C.18 shows the normalized intensity  $|F|^2 / V^2$ , computed with  $R = 8 \text{ nm}$  and  $H = 16 \text{ nm}$ .

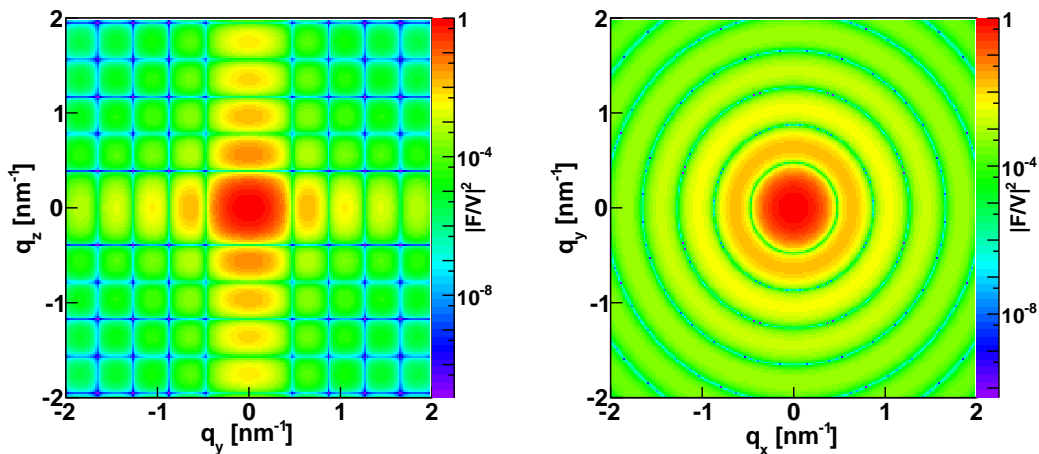


Figure C.18: Normalized intensity for the form factor of a cylinder plotted against  $(q_y, q_z)$  and  $(q_x, q_y)$ . It has been computed with `FormFactorCylinder(8.*nanometer, 16.*nanometer)`.

## C.10 Ellipsoidal cylinder

### Real-space geometry

This is a cylinder whose cross section is an ellipse.

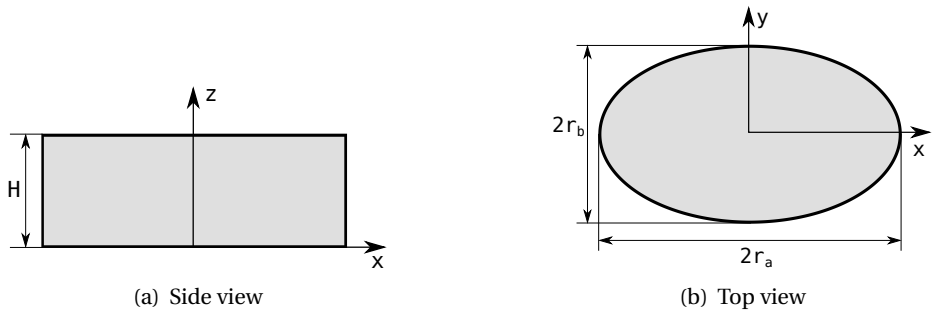


Figure C.19: Sketch of an Ellipsoidal Cylinder.

### Parameters:

- $r_a$  = half length of the ellipse main axis parallel to  $x$ ,
- $r_b$  = half length of the ellipse main axis parallel to  $y$ ,
- height  $H$ .

### Properties:

- volume  $V = \pi r_a r_b H$ ,
- particle surface seen from above  $S = r_a r_b$ .

**Expression of the form factor** The total form factor is given by

$$F(\mathbf{q}, R, W, H) = 2\pi r_a r_b H \exp\left(i \frac{q_z H}{2}\right) \text{sinc}\left(\frac{q_z H}{2}\right) \frac{J_1(\gamma)}{\gamma},$$

with  $\gamma = \sqrt{(q_x r_a)^2 + (q_y r_b)^2}$  and  $J_1(x)$  is the first order Bessel function of the first kind [16].

**Syntax:** `FormFactorEllipsoidalCylinder(ra, rb, height)`

**Example**

Figure C.20 shows the normalized intensity  $|F|^2/V^2$ , computed with  $r_a = 13 \text{ nm}$ ,  $r_b = 8 \text{ nm}$ , and  $H = 16 \text{ nm}$ .

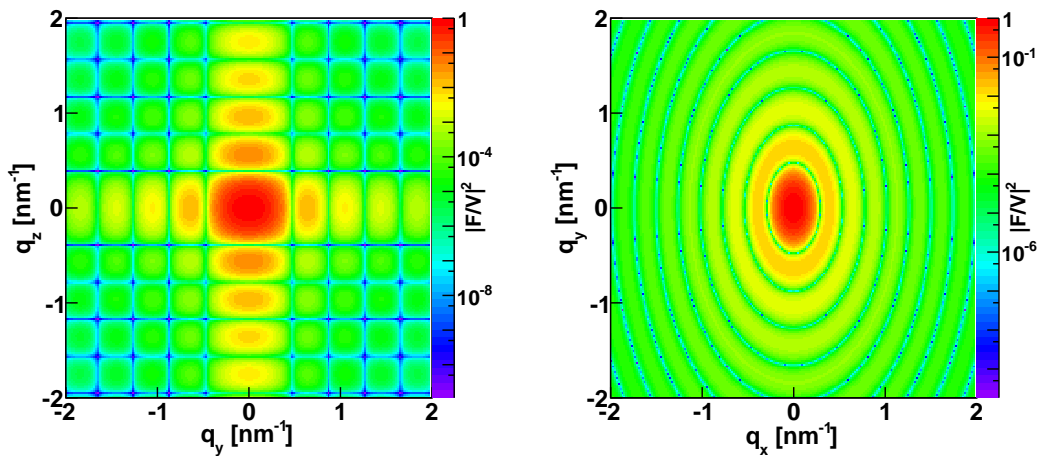


Figure C.20: Normalized intensity for the form factor of an ellipsoidal cylinder plotted against  $(q_y, q_z)$  and  $(q_x, q_y)$  and computed with `FormFactorEllipsoidalCylinder(8.*nanometer, 13.*nanometer, 16*nanometer)`.

## C.11 Cone

**Real-space geometry** This shape is a truncated cone as shown in fig. C.21.

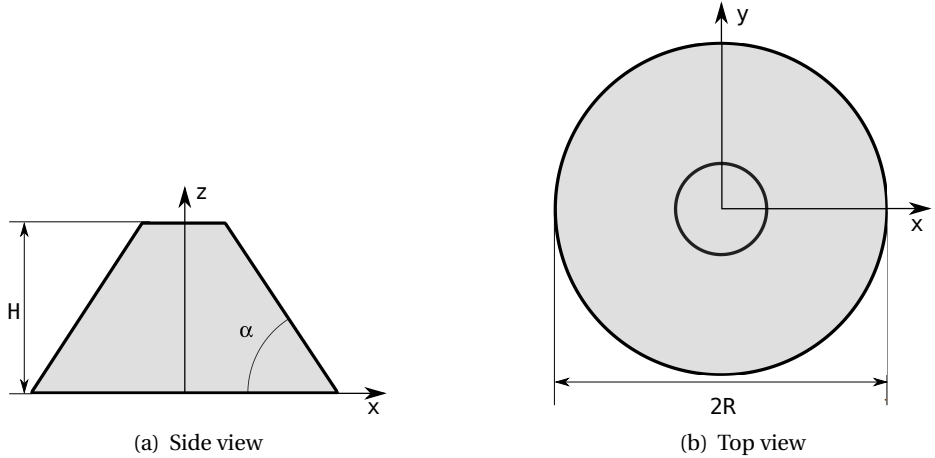


Figure C.21: Sketch of a Cone.

### Parameters:

- radius  $R$ ,
- height  $H$ ,
- $\alpha$  is the angle between the side and the circular base.

**Restrictions on the parameters:**  $\frac{H}{R} < \tan(\alpha)$ .

### Properties:

- volume  $V = \frac{\pi}{3} \tan(\alpha) R^3 \left[ 1 - \left( 1 - \frac{H}{\tan(\alpha) R} \right)^3 \right]$ ,
- particle surface seen from above  $S = \pi R^2$ .

### Expression of the form factor

$$F(\mathbf{q}, R, H, \alpha) = \int_0^H 2\pi R_z^2 \frac{J_1(q_{\parallel} R_z)}{q_{\parallel} R_z} \exp(i q_z z) dz,$$

with  $R_z = R - \frac{z}{\tan \alpha}$ ,  $\mathbf{q}_{\parallel} = \sqrt{q_x^2 + q_y^2}$  and  $J_1(x)$  is the first order Bessel function of the first kind [16].

**Syntax:** FormFactorCone(radius, height, alpha).

**Example**

Figure C.22 shows the normalized intensity  $|F|^2/V^2$ , computed with  $R = 10 \text{ nm}$ ,  $H = 13 \text{ nm}$ , and  $\alpha = 60^\circ$ .

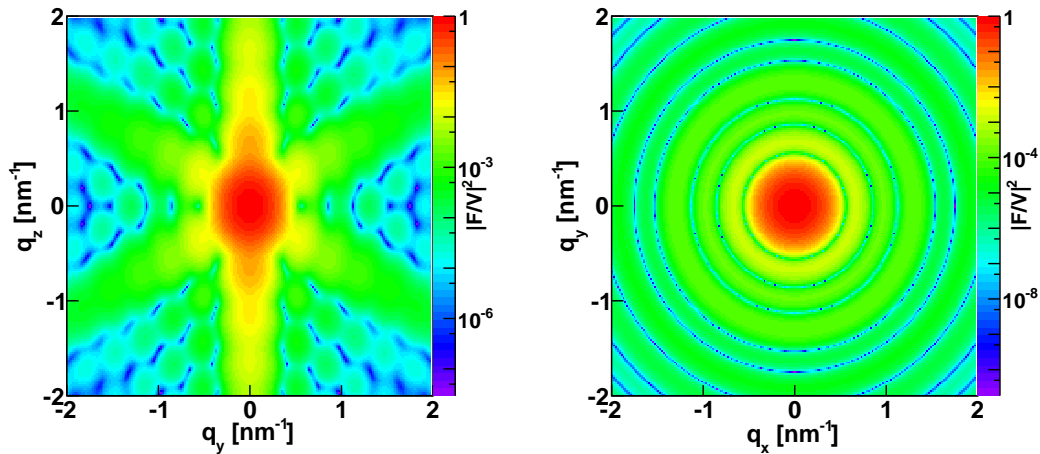


Figure C.22: Normalized intensity for the form factor of a Cone plotted against  $(q_y, q_z)$  and  $(q_x, q_y)$ . It has been computed with FormFactorCone(10.\*nanometer, 13.\*nanometer, 60.\*degree).

## C.12 Full Sphere

### Real-space geometry

The full sphere is parametrized by its radius  $R$ .

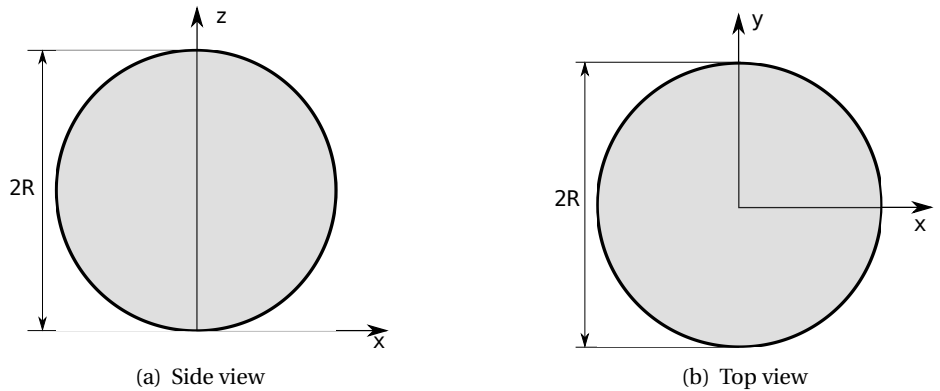


Figure C.23: Sketch of a Full Sphere.

**Parameters:** radius  $R$ .

**Properties:**

- volume  $V = \frac{4\pi}{3}R^3$ ,
- particle surface seen from above  $S = \pi R^2$ .

**Expression of the form factor**

$$F(\mathbf{q}, R) = 4\pi R^3 \exp(i q_z R) \frac{\sin(qR) - qR \cos(qR)}{(qR)^3},$$

where  $q = \sqrt{q_x^2 + q_y^2 + q_z^2}$ .

**Syntax:** `FormFactorFullSphere(radius)`

**Example**

Figure C.24 shows the normalized intensity  $|F|^2/V^2$ , computed with  $R = 8 \text{ nm}$ .

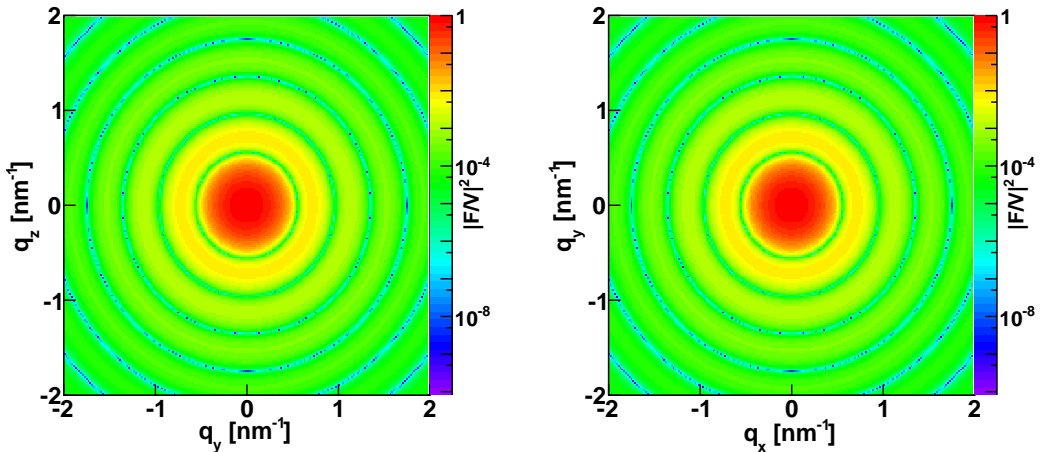


Figure C.24: Normalized intensity for the form factor of a Full Sphere plotted against  $(q_y, q_z)$  and  $(q_x, q_y)$  and computed with `FormFactorFullSphere(8.*nanometer)`.

### C.13 Truncated Sphere

#### Real-space geometry

This shape is a spherical dome, *i.e.* a portion of a sphere cut off by a plane (perpendicular to  $z$ -axis) as shown in fig. C.25.

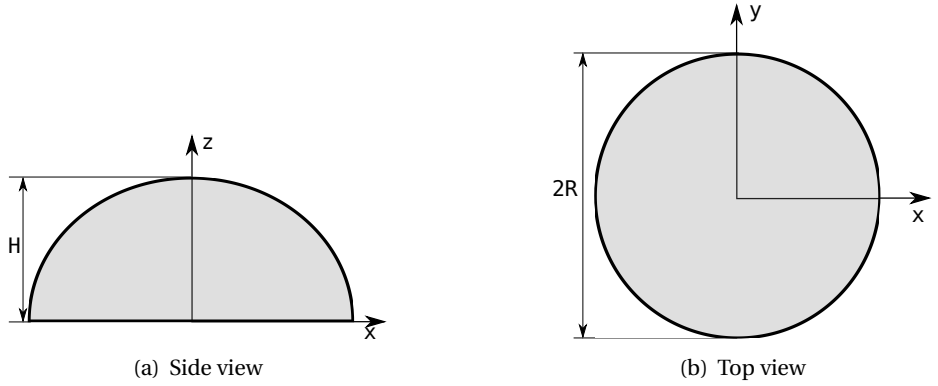


Figure C.25: Sketch of a Truncated Sphere.

#### Parameters:

- radius  $R$ ,
- height  $H$ .

**Restrictions on the parameters:**  $0 \leq H \leq 2R$ .

#### Properties:

- volume  $V = \pi R^3 \left[ \frac{2}{3} + \frac{H-R}{R} - \frac{1}{3} \left( \frac{H-R}{R} \right)^3 \right]$ ,
- particle surface seen from above  $S = \begin{cases} \pi R^2, & H \geq R \\ \pi (2RH - H^2), & H < R \end{cases}$ .

#### Expression of the form factor

$$F(\mathbf{q}, R, H) = 2\pi \exp[iq_z(H-R)] \int_{R-H}^R R_z^2 \frac{J_1(q_{\parallel} R_z)}{q_{\parallel} R_z} \exp(iq_z z) dz,$$

with  $J_1(x)$  the first order Bessel function of the first kind [16],  $q_{\parallel} = \sqrt{q_x^2 + q_y^2}$ , and  $R_z = \sqrt{R^2 - z^2}$

**Syntax:** FormFactorTruncatedSphere(radius, height)

**Example**

Figure C.26 shows the normalized intensity  $|F|^2/V^2$ , computed with  $R = 5$  nm and  $H = 7$  nm:

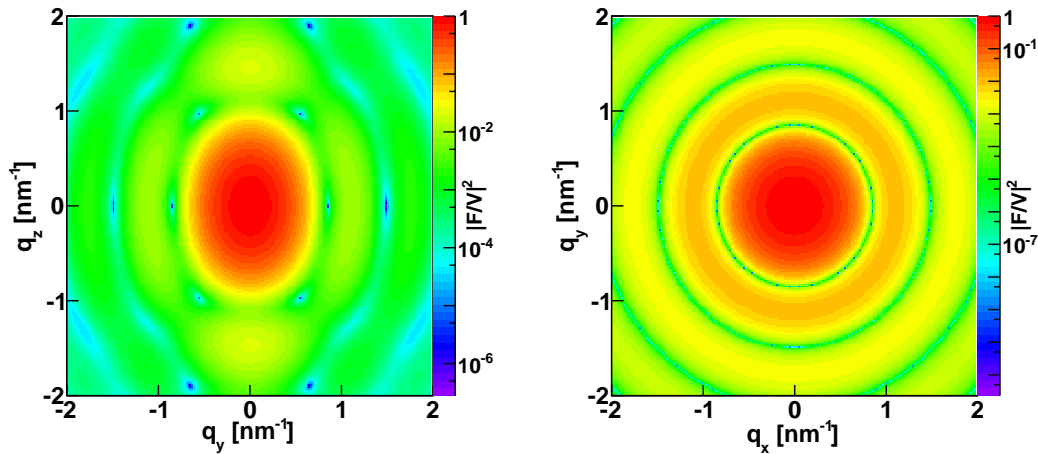


Figure C.26: Normalized intensity for the form factor of a Truncated Sphere plotted against  $(q_y, q_z)$  and  $(q_x, q_y)$  and computed with `FormFactorTruncatedSphere(5.*nanometer, 7.*nanometer)`.

## C.14 Full Spheroid

### Real-space geometry

A full spheroid is generated by rotating an ellipse around the vertical axis (see fig. C.27).

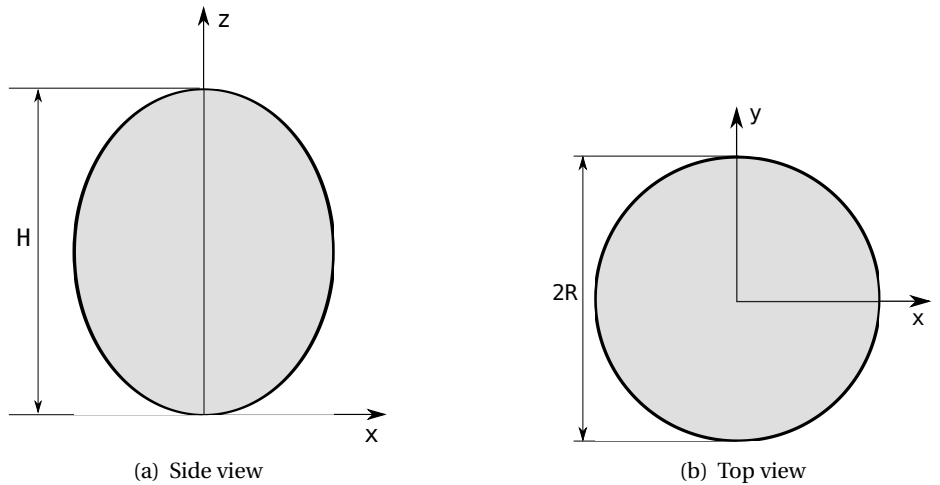


Figure C.27: Sketch of a Full Spheroid.

### Parameters:

- radius  $R$ ,
- height  $H$ .

### Properties:

- volume  $V = \frac{2}{3}R^2H$ ,
- particle surface seen from above  $S = \pi R^2$ .

### Expression of the form factor

$$F(\mathbf{q}, R, H) = 4\pi \exp(i q_z H/2) \int_0^{H/2} R_z^2 \frac{J_1(q_{\parallel} R_z)}{q_{\parallel} R_z} \cos(q_z z) dz,$$

with  $J_1(x)$  the first order Bessel function of the first kind [16],  $R_z = R \sqrt{1 - \frac{4z^2}{H^2}}$ ,  $\gamma_z = \sqrt{(q_x R_z)^2 + (q_y R_z)^2}$

**Syntax:** `FormFactorFullSpheroid(radius, height)`

**Example**

Figure C.28 shows the normalized intensity  $|F|^2/V^2$ , computed with  $R = 10 \text{ nm}$ , and  $H = 13 \text{ nm}$ .

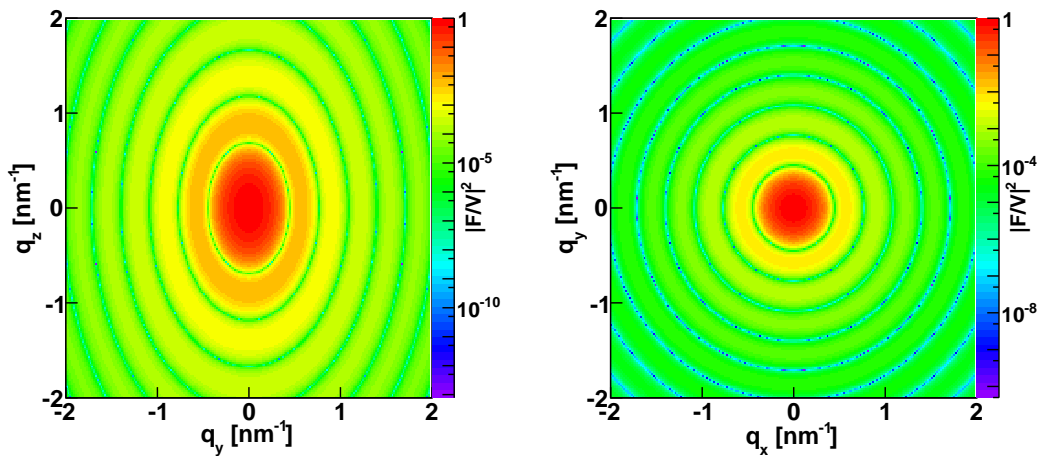


Figure C.28: Normalized intensity for the form factor of a full spheroid plotted against  $(q_y, q_z)$  and  $(q_x, q_y)$  and computed with `FormFactorFullSpheroid(10.*nanometer, 13.*nanometer)`.

## C.15 Truncated Spheroid

### Real-space geometry

This shape is a spheroidal dome: a portion of a full spheroid cut off by a plane perpendicular to the  $z$ -axis.

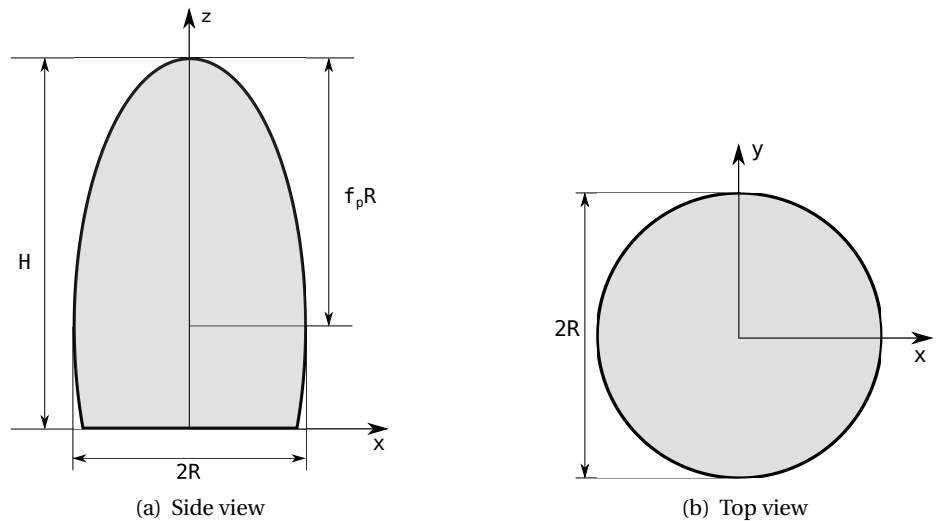


Figure C.29: Sketch of a Truncated Spheroid.

### Parameters:

- radius  $R$ ,
- height  $H$ ,
- height\_flattening coefficient in the perpendicular direction  $f_p$ .

**Restrictions on the parameters:**  $0 < \frac{H}{R} < 2f_p$ .

### Properties:

- volume  $V = \frac{\pi R H^2}{f_p} \left(1 - \frac{H}{3f_p R}\right)$ ,
- particle surface seen from above  $S = \begin{cases} \pi R^2, & H \geq f_p R \\ \pi \left(\frac{2RH}{f_p} - \frac{H^2}{f_p^2}\right), & H < R \end{cases}$ .

### Expression of the form factor

$$F(\mathbf{q}, R, H, f_p) = 2\pi \exp[i q_z(H - f_p R)] \int_{f_p R - H}^{f_p R} R_z^2 \frac{J_1(q_{\parallel} R_z)}{q_{\parallel} R_z} \exp(i q_z z) dz$$

with  $J_1(x)$  the first order Bessel function of the first kind [16],  $q_{\parallel} = \sqrt{q_x^2 + q_y^2}$  and  $R_z = \sqrt{R^2 - z^2/f_p^2}$ .

**Syntax:** FormFactorTruncatedSpheroid(radius, height, height\_flattening)

### Example

Figure C.30 shows the normalized intensity  $|F|^2/V^2$ , computed with  $R = 7.5$  nm,  $H = 9$  nm and  $f_p = 1.2$ .

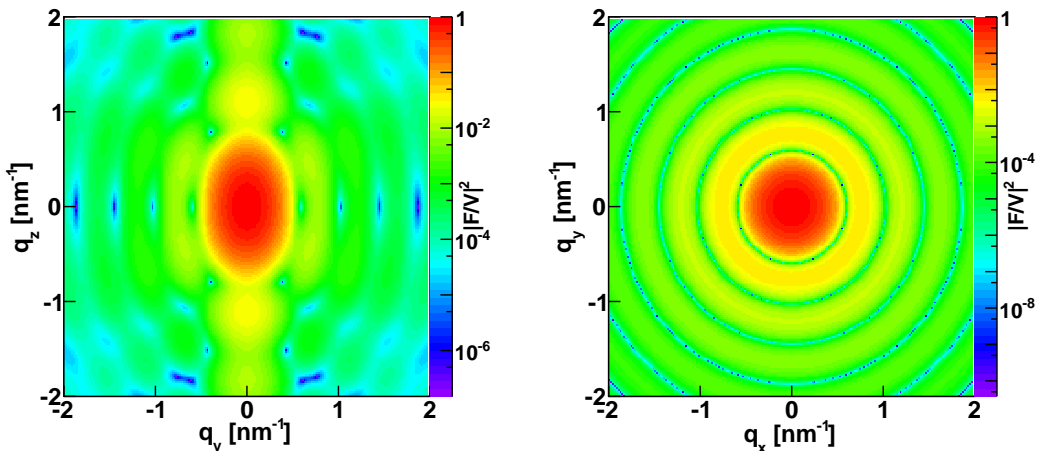


Figure C.30: Normalized intensity for the form factor of a Truncated Spheroid plotted against  $(q_z, q_y)$  and  $(q_x, q_y)$  and computed with FormFactorTruncatedSpheroid(7.5\*nanometer, 9.\*nanometer, 1.2).

## C.16 Hemi ellipsoid

### Real-space geometry

This shape is a truncated ellipsoid as shown in fig. C.31.

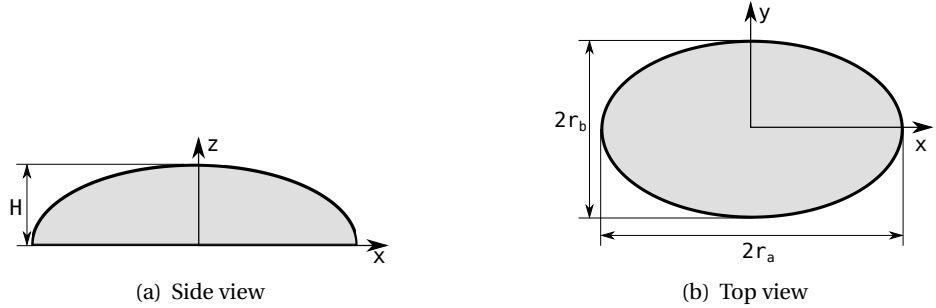


Figure C.31: Sketch of an Hemi-ellipsoid.

### Parameters:

- $r_a$  = half length of the ellipse main axis parallel to  $x$ ,
- $r_b$  = half length of the ellipse main axis parallel to  $y$ ,
- $H$  = height (half length of the vertical main axis of a full ellipsoid).

### Properties:

- volume  $V = \frac{2}{3}\pi r_a r_b H$ ,
- particle surface seen from above  $S = \pi r_a r_b$ .

### Expression of the form factor

$$F(\mathbf{q}, r_a, r_b, H) = 2\pi \int_0^H r_{a,z} r_{b,z} \frac{J_1(\gamma_z)}{\gamma_z} \exp(i q_z z) dz,$$

with  $J_1(x)$  the first order Bessel function of the first kind [16],  $r_{a,z} = r_a \sqrt{1 - \left(\frac{z}{H}\right)^2}$ ,  $r_{b,z} = r_b \sqrt{1 - \left(\frac{z}{H}\right)^2}$  and  $\gamma_z = \sqrt{(q_x r_{a,z})^2 + (q_y r_{b,z})^2}$ .

**Syntax:** FormFactorHemiEllipsoid( $r_a$ ,  $r_b$ , height)

**Example**

Figure C.32 shows the normalized intensity  $|F|^2/V^2$ , computed with  $r_a = 10 \text{ nm}$ ,  $r_b = 6 \text{ nm}$  and  $H = 8 \text{ nm}$ .

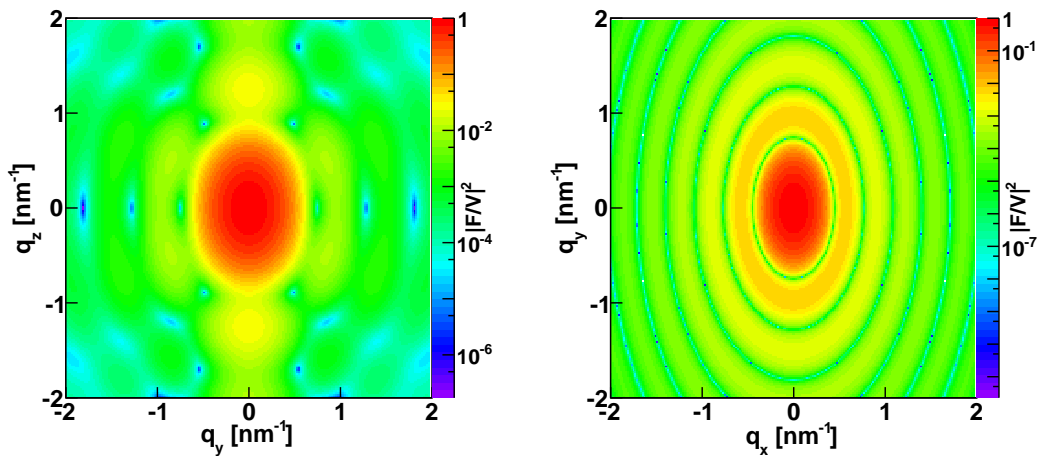


Figure C.32: Normalized intensity for the form factor of an Hemi-Ellipsoid plotted against  $(q_y, q_z)$  and  $(q_x, q_y)$  computed with `FormFactorHemiEllipsoid(10.*nanometer, 6.*nanometer, 8.*nanometer)`.

## C.17 Ripple1

### Real-space geometry

This shape has a sinusoidal profile (see fig. C.33).

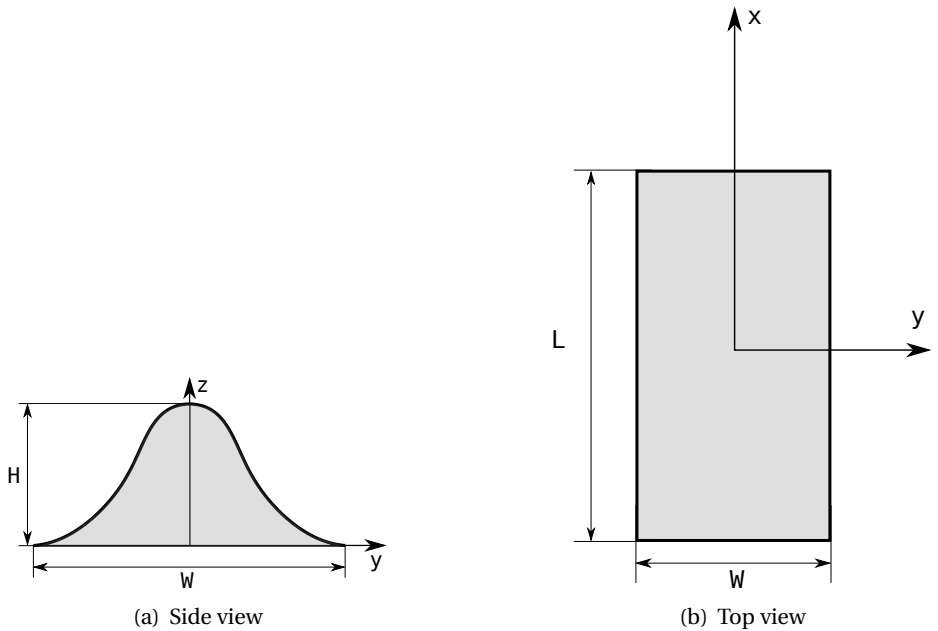


Figure C.33: Sketch of a Ripple1.

### Parameters:

- length  $L$ ,
- width  $W$ ,
- height  $H$ .

### Properties:

- volume  $V = \frac{LWH}{2}$ ,
- particle surface seen from above  $S = LW$ .

### Expression of the form factor

$$F(\mathbf{q}, L, W, H) = L \cdot \frac{W}{\pi} \cdot \text{sinc}\left(\frac{q_x L}{2}\right) \times \\ \int_0^H dz \arccos\left(\frac{2z}{H} - 1\right) \text{sinc}\left[\frac{q_y W}{2\pi} \arccos\left(\frac{2z}{H} - 1\right)\right] \exp(i q_z z),$$

where  $\arccos$  is the arc cosine (*i.e.* the inverse operation of cosine).

**Syntax:** `FormFactorRipple1(length, width, height)`

### Example

Figure C.34 shows the normalized intensity  $|F|^2/V^2$ , computed with  $L = 27 \text{ nm}$ ,  $W = 20 \text{ nm}$  and  $H = 14 \text{ nm}$ .

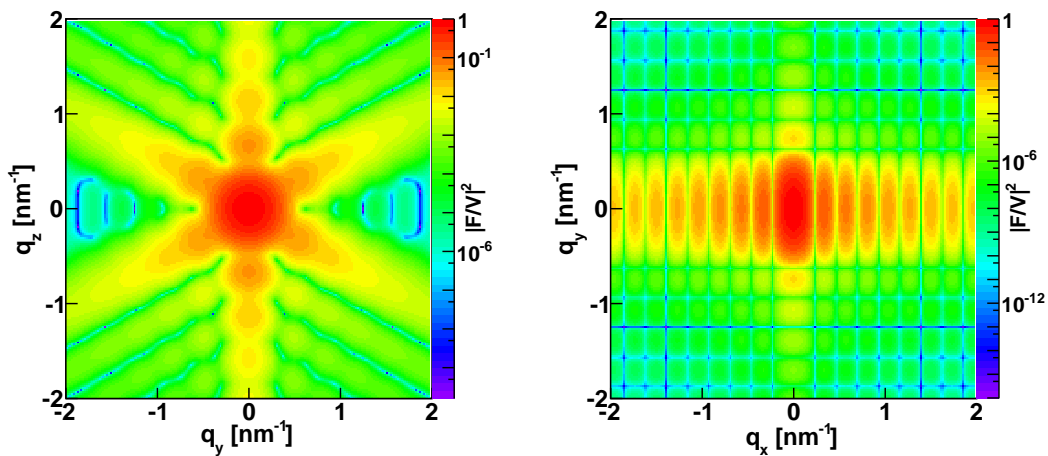


Figure C.34: Normalized intensity for the form factor of a ripple1  $|F|^2/V^2$ , plotted against  $(q_y, q_z)$  and  $(q_x, q_y)$  computed with `FormFactorRipple1(27.*nanometer, 20.*nanometer, 14.*nanometer)`.

## C.18 Ripple2

### Real-space geometry

This shape has an asymmetric sawtooth profile.

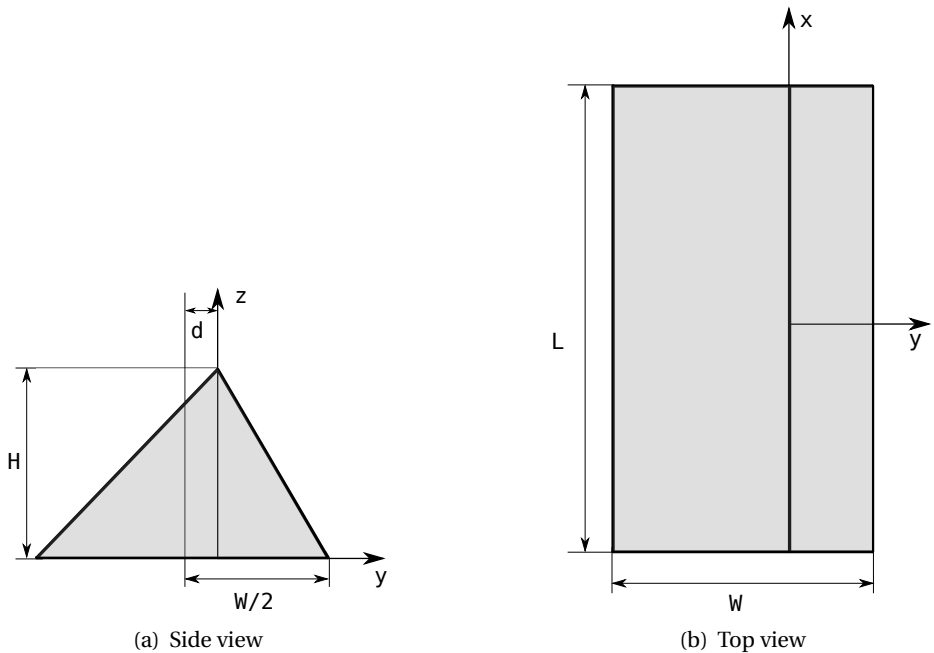


Figure C.35: Sketch of a Ripple2.

### Parameters:

- length  $L$ ,
- width  $W$ ,
- height  $H$ ,
- asymmetry  $d$ .

**Restriction on the parameters:**  $|d| < \frac{W}{2}$ .

### Properties:

- volume  $V = \frac{LWH}{2}$ ,
- particle surface seen from above  $S = LW$ .

### Expression of the form factor

$$F(\mathbf{q}, L, W, H, d) = LW \operatorname{sinc}\left(\frac{q_x L}{2}\right) \times \\ \int_0^H \left(1 - \frac{z}{H}\right) \operatorname{sinc}\left[\frac{q_y W}{2} \left(1 - \frac{z}{H}\right)\right] \exp\left\{i \left[q_z z - q_y d \left(1 - \frac{z}{H}\right)\right]\right\} dz$$

**Syntax:** FormFactorRipple2(length, width, height, asymmetry)

**Examples** Figure C.36 shows the normalized intensity  $|F|^2 / V^2$ , computed with  $L = 36$  nm,  $W = 25$  nm,  $H = 14$  nm, and  $d = 3$  nm.

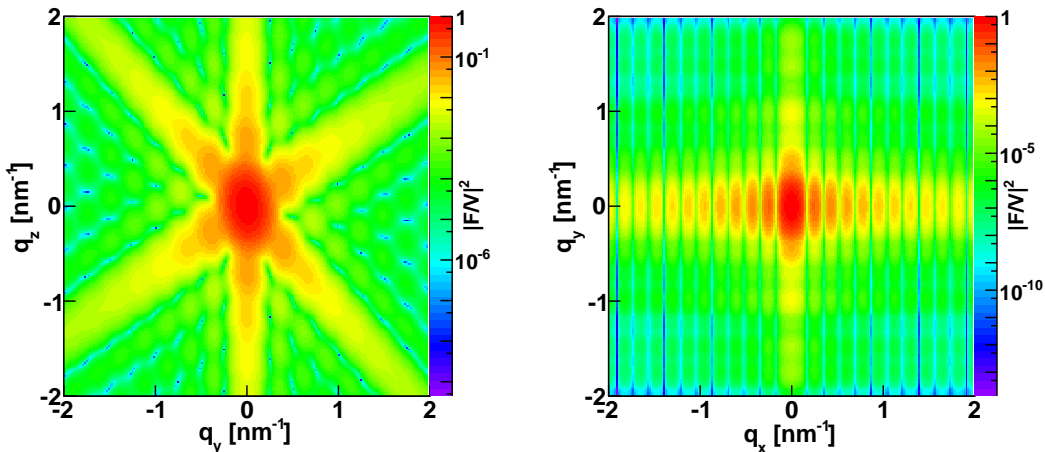


Figure C.36: Normalized intensity for the form factor of a ripple2 plotted against  $(q_y, q_z)$  and  $(q_x, q_y)$  computed with FormFactorRipple2(36.\*nanometer, 25.\*nanometer, 14.\*nanometer, 3.\*nanometer).

# Appendix D

# User API

## D.1 IntensityData

The `IntensityData` object stores the simulated or real intensity data together with the axes definition of the detector in BornAgain's internal format. During the simulation setup it is created automatically when the user specifies the detector characteristics and is filled with the simulated intensities after the simulation is completed.

```

1 simulation = Simulation()
2 simulation.setDetectorParameters(10, -5.0*degree, 5.0*degree, 5,
3                                0.0*degree, 1.0*degree)
4 ...
5 simulation.runSimulation()
6 intensity = simulation.getIntensityData()
```

The `IntensityData` object retrieved in line 5 corresponds to the two dimensional detector pixel array as shown in Fig. D.1.

The x-axis and y-axis of the figure correspond to the  $\phi_f$  and  $\alpha_f$  axes of the detector. The x-axis is divided into 10 bins, with low edge of the first bin set to  $-5.0\text{ deg}$  and upper edge of the last bin set to  $+5.0\text{ deg}$ . The y-axis is divided into 5 bins, with low edge of the first bin set to  $0.0\text{ deg}$  and upper edge of the last bin set to  $1.0\text{ deg}$ . There are 50 bins in total (they are marked on the plot with indexes from 0 to 49), each bin will contain one intensity value.

During a standard simulation (i.e. no Monte-Carlo integration involved) intensities are calculated for  $\phi_f, \alpha_f$  values corresponding to the bin centers, e.g. the intensity stored in bin#42 will correspond to  $\phi_f = 3.5\text{ deg}, \alpha_f = 0.5\text{ deg}$ .

 The `IntensityData` object is not intended for direct usage from Python API. The idea is that the API provides the user with the possibility to export the data from BornAgain internal format to the format of his choice as well as import user's data into BornAgain. For the moment this functionality is limited to a few options explained below. We encourage users feedback to implement the support of most requested formats.

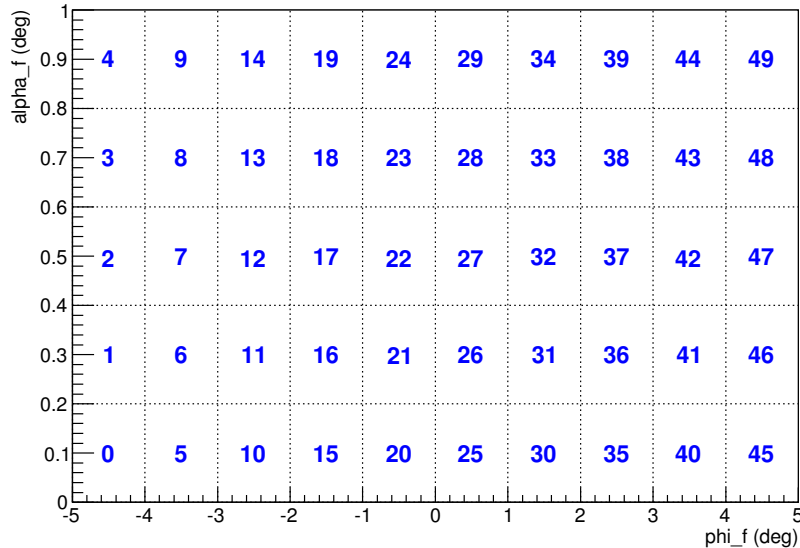


Figure D.1: The axes layout of IntensityData object.

### D.1.1 Import/export of intensity data

For the moment we provide following options:

- Import/export of IntensityData object from/to numpy array.
- Import/export of IntensityData object from/to text file.

#### Export to numpy array

To export intensity data into numpy array the method `getArray()` should be used on IntensityData object as shown in line 2 of following code snippet.

```

1 intensity = simulation.getIntensityData()
2 array = intensity.getArray()
3 ...
4 pylab.imshow(numpy.rot90(array, 1))
5 pylab.show()

```

For the detector settings defined in the previous paragraph the dimensions of the resulting array will be (10,5). By using numpy indexes the user can get access to the intensity values, e.g. `array[0][0]` corresponds to the intensity in bin#0 of Fig. D.1, `array[0][4]` to bin#4, `array[1][0]` to bin#5, `array[8][2]` to bin#42, `array[9][4]` to bin#49.

To plot this resulting numpy array with `matplotlib` it has to be rotated counter-clockwise to match `matplotlib` conventions as shown in line 4.

### D.1.2 Importing from numpy array

To use fitting the user has to load experimental data into BornAgain fitting kernel. To read experimental data the user has to create IntensityData object, fill it with the experimental intensity values and pass this object to the fitting kernel.

First, the user creates empty IntensityData as shown in line 1 of the following code snippet.

```

1 data = IntensityData()
2 data.addAxis(FixedBinAxis("phi_f", 10, -5.0*degree, 5.0*degree))
3 data.addAxis(FixedBinAxis("alpha_f", 5, 0.0*degree, 1.0*degree))
4 ...
5 array = numpy.zeros((10, 5)) # fill array with experimental
     intensities
6 ...
7 data.setRawDataVector(array.flatten().tolist())
8
9 fitSuite = FitSuite()
10 fitSuite.addSimulationAndRealData(simulation, data)

```

In lines 2, 3 two axes with fixed bin sizes are defined to represent the detector layout as shown in Fig. D.1. The constructor of FixedBinAxis object has the following signature

```
FixedBinAxis(title, nbins, min_angle, max_angle)
```

The created IntensityData object has to be filled with experimental intensities using numpy array prepared by the user (lines 5- 7). In lines 9,10 the fitting kernel is created and initialized with Simulation object and IntensityData object representing the experimental data.

### D.1.3 Saving intensity data to text file.

The special class IntensityDataIOFactory is intended for saving the intensity data in different datafile formats. For the moment, it only supports saving the data in specific BornAgain's text files (the file extention \*.int).

```

1 intensity = simulation.getIntensityData()
2 IntensityDataIOFactory.writeIntensityData(intensity, 'file_name.
     int')

```

### D.1.4 Reading intensity data from a text file.

The same class is also intended for reading intensity data from files with different formats. For the moment, it only supports reading the data from text files of special BornAgain's format (the file extention \*.int).

```

1 intensity = IntensityDataIOFactory.readIntensityData('file_name.
     int')

```

## Appendix E

# Python examples

This appendix describes the samples and the simulated output intensity maps of the examples, whose Python scripts are contained in the folder /Examples/python/simulation.

### E.1 General conventions

#### E.1.1 Geometry

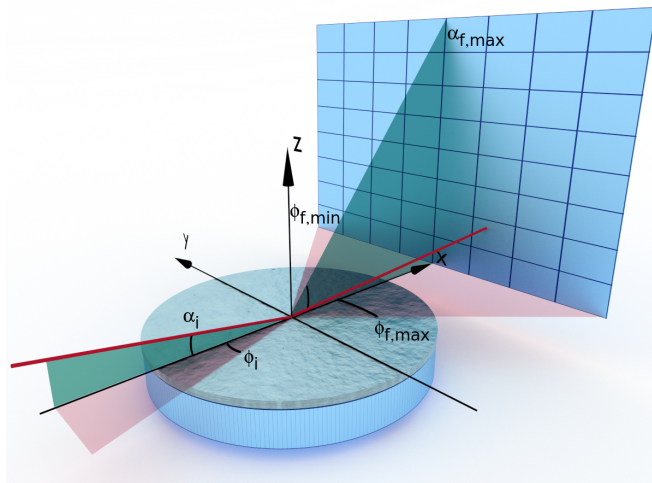


Figure E.1: The GISAS setup and the coordinate system used in BornAgain. The incoming beam propagates with incidence angles  $\alpha_i$  and  $\phi_i$  with respect to the sample axes as shown. A scattered (outgoing) beam, characterized by  $\alpha_f$  and  $\phi_f$  propagates toward the area detector.

- The axis are defined on the interface of the sample with the air. The incoming beam points towards the positive  $x$ -axis direction. The  $z$ -axis points in the vertical upwards

direction (see fig. E.1).

- The planes are assumed to be infinite in the planar direction ( $x, y$ ).
- The substrate and the air layers are considered infinitely thick.
- The scattered wave vector is defined as  $\mathbf{q} = \mathbf{k}_i - \mathbf{k}_f$
- The angles  $\alpha_i$  and  $\alpha_f$  are defined in such a way that those shown in fig. E.1 are positive.
- The refractive index of any material is defined as  $n = 1 - \delta + i\beta$ , where the values  $\delta, \beta \in \mathbb{R}$  are the inputs used in BornAgain.

Please refer to Section 3 for further details.

### E.1.2 Default settings

By default the simulations with BornAgain are performed using the Distorted Wave Born Approximation and the Decoupling Approximation regarding the spatial distribution of particles.

### E.1.3 Requirements

- The sample is built starting from the top layer.
- The particles are always associated with only one layer; they can be deposited on the top surface or buried in the layer. But they cannot cross interfaces.

The following sections describe some examples illustrating the main functionalities of BornAgain.

## E.2 Example 1: Cylinders and prisms

The sample used in this example comprises a substrate on which are deposited, in equal proportion, cylinders and prisms (see fig. E.2(a)). All particles are made of the same material. Each type of particle has the same orientation.

The cylinders are 5 nm high and 5 nm in radius. The prisms are 5 nm high with a triangular base whose side length is equal to 10 nm (see Section C.2 and Section C.9 for a description of these form factors).

There is no interference between the waves scattered by these particles. The distribution is therefore diluted.

The incident neutron beam is characterized by a wavelength of 1 Å, and incident angles  $\alpha_i = 0.2^\circ$  and  $\phi_i = 0^\circ$ .

The simulation is performed using the Distorted Wave Born Approximation by omitting by using only the air layer (no substrate). The output intensity generated by this simulation is shown in fig. E.2(b).

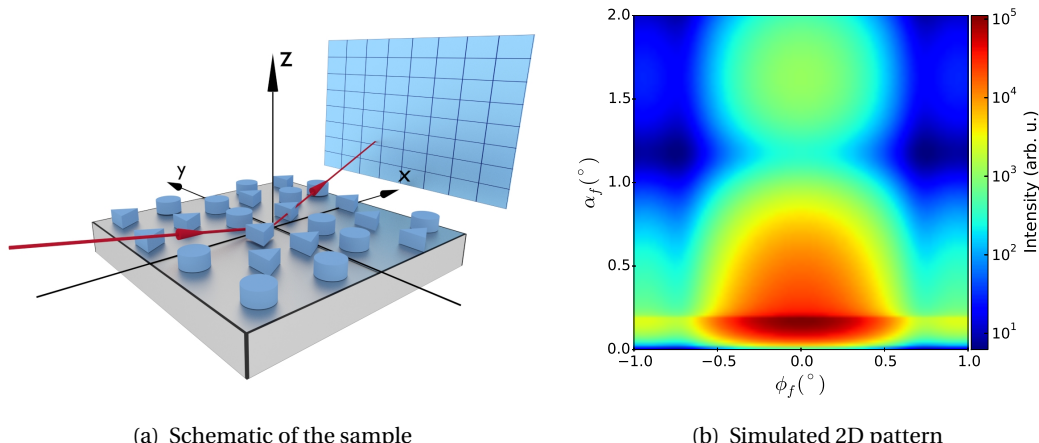


Figure E.2: Example 1: equal proportion of cylinders and prisms deposited on a substrate without interference.

### E.3 Example 2: Cylinders with size distribution

Here the sample is made of polydisperse cylinders of two different sizes (see fig. E.3(a)).

$R_1 = H_1$ ,  $R_2 = H_2$ , where  $R_i$  and  $H_i$  are the radius and width of cylinder of type  $i$ .

There are 95% of cylinders of type 1 and 5% of cylinders of type 2.

The polydispersity affects the radii of the cylinders, following a normal distribution. For the small cylinder, their characteristic size varies about  $R_1 = 5 \text{ nm}$  with a standard deviation  $\sigma_1 = 0.2 R_1$ . For type 2, the average value  $R_2$  is 10 nm and  $\sigma_2 = 0.02 R_2$ .

There is no substrate and no interference between the scattered beams.

The simulation is performed using the Born approximation, *i.e.* the sample contains only "air" as a layer without any substrate.

The incident beam is characterized by a wavelength of 1 Å and incident angles  $\alpha_i = 0.2^\circ$  and  $\phi_i = 0^\circ$ .

The result of the simulation is shown in fig. E.3(b).

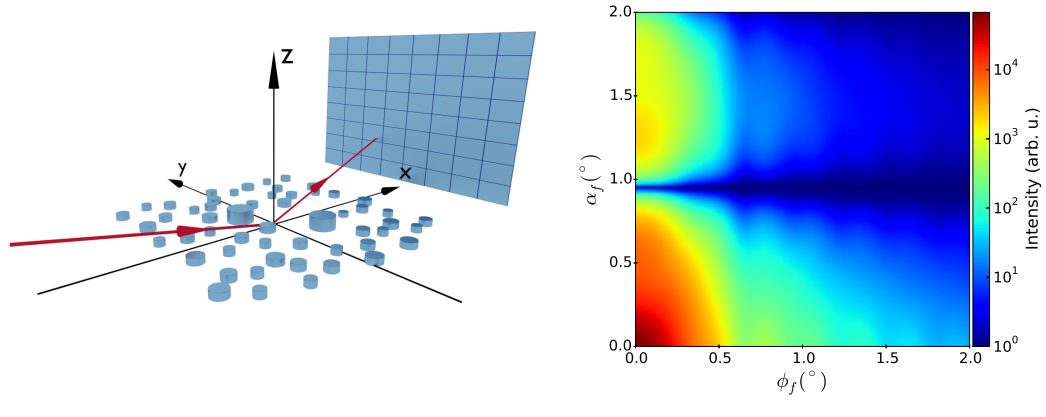


Figure E.3: Example 2: Polydisperse distribution of two types of cylinders.

## E.4 Example 3: "Cylinder" form factor

This example simulates cylindrical particles in three different configurations. In each case the wavelength is equal to 1 Å and the incident angles to  $\alpha_i = 0.2^\circ$ ,  $\phi_i = 0^\circ$ . There is no interference between the scattered waves.

### E.4.1 Cylindrical form factor in Born approximation

The sample considered for this example and the output intensity generated using BornAgain are shown in fig. E.4(a) and (b), respectively. The cylinders are all identical with a radius and height equal to 5 nm. There is no substrate. The simulation is performed in the Born approximation.

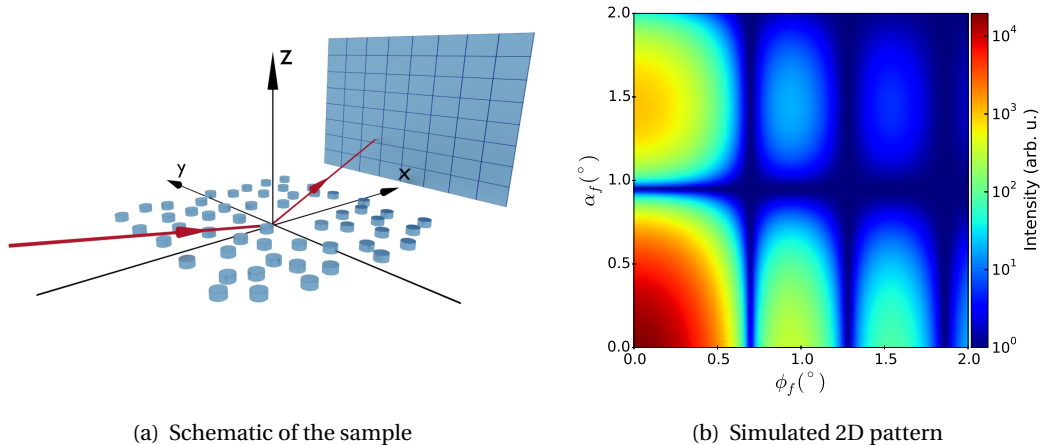


Figure E.4: Example 3: Scattering from a monodisperse distribution of cylinders using the Born approximation.

### E.4.2 Cylindrical form factor in the Born approximation with size distribution

This example considers a polydisperse distribution of cylinders (see fig. E.5(a)). Their average radii and heights are equal to 5 nm. The radii of the cylinders vary according to a normal distribution with a standard deviation  $\sigma$  equal to 0.2 times the average radius. The simulated output pattern is shown in fig. E.5(b).

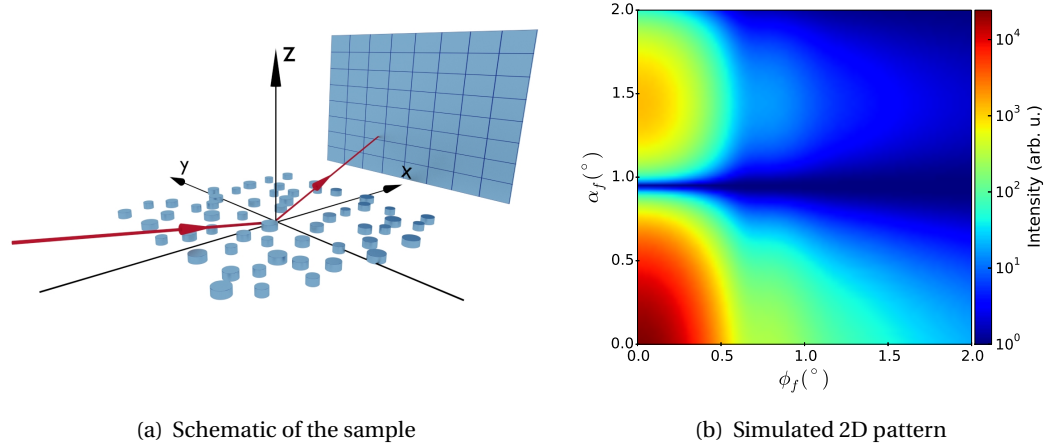


Figure E.5: Example 3: Scattering from a polydisperse distribution of cylinders using the Born approximation.



#### Remark:

This example differs from the one described in Section E.3 by the presence of a single distribution of cylinders.

### E.4.3 Cylindrical form factor in DWBA

This example is similar to the case with the Born Approximation (Section E.4.1) with the addition of a substrate (see fig. E.6)(a)). Therefore the Distorted Wave Born Approximation is implemented in order to take additional reflections and transmission at the substrate interface into account. The distribution of cylinders is monodisperse with a height and a radius of 5 nm.

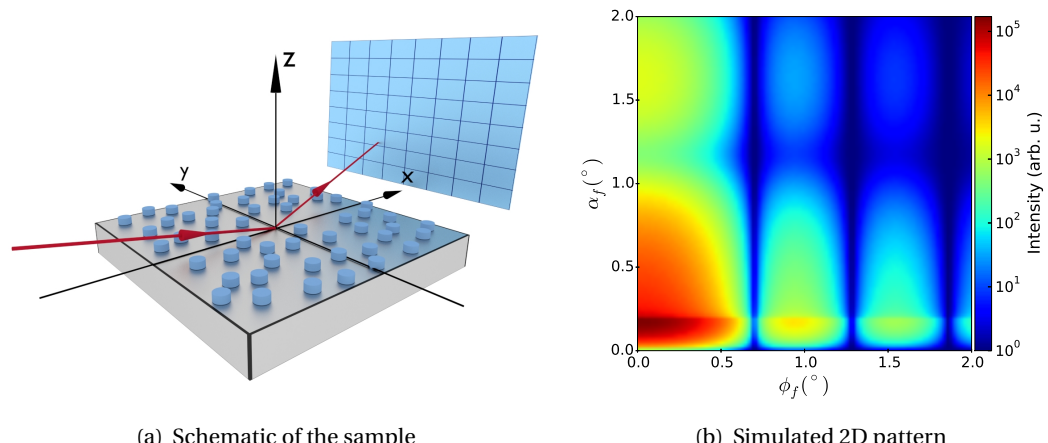


Figure E.6: Example 3: Scattering from a monodisperse distribution of cylinders deposited on a substrate using the Distorted Wave Born approximation.

## E.5 Example 4: Cylinders - Paracrystal

The example focuses on the planar distribution of particles. Two cases are considered: a one- and a two-dimensional paracrystal. The two examples of this section share the following settings:

- The incident beam is characterized by a wavelength of 1 Å and angles  $\alpha_i = 0.2^\circ$  and  $\phi_i = 0^\circ$ .
- The particles are cylinders with constant radii and heights equal to 5 nm. They are deposited on a substrate.

### E.5.1 "One dimension"

The disorder is radially propagated. It is characterized by a Gaussian distribution  $\exp(-\omega^2 q^2/2)$  with  $\omega = 7$  nm.

The average distance between the particles  $D$  is equal to 20 nm.

Finite size effects are modelled by introducing a damping length  $\Gamma$  equal to 1e3 nm.

In this case, the structure factor is given by

$$S(q_{\parallel}) = \frac{1 - \phi^2}{1 - 2\phi \cos(q_{\parallel} D) + \phi^2} \text{ with } \phi = \exp(-\omega^2 q_{\parallel}^2/2) \exp(-D/\Gamma).$$

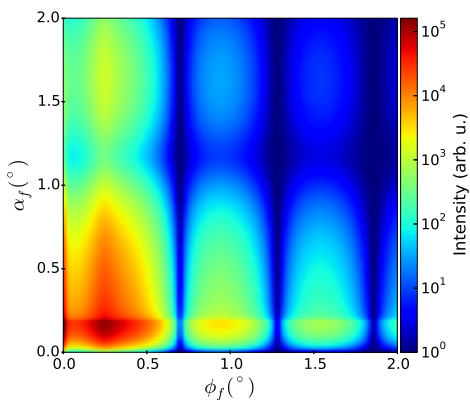
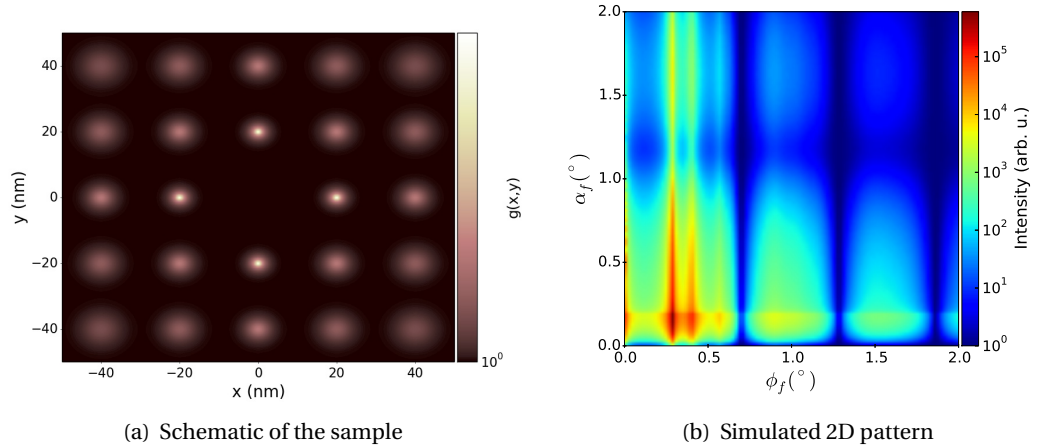


Figure E.7: Example 4 - One dimension : Scattering from a distribution of cylinders deposited on a substrate using the Distorted Wave Born approximation, distribution according to a 1D paracrystal.

### E.5.2 Two dimensions

The cylindrical particles are distributed along a square lattice whose order is gradually distorted. The average distance between the particles is 20 nm. The size of the domains is 20 μm in both directions.

The distribution function is a two-dimensional Cauchy function with correlation lengths equal to 1 nm in both directions.



(a) Schematic of the sample

(b) Simulated 2D pattern

Figure E.8: Output ex004 2DDL.

## E.6 Example 5: Lattice with disorder

The examples of this section focus on the available options to characterize the pattern according to which the particles are deposited.

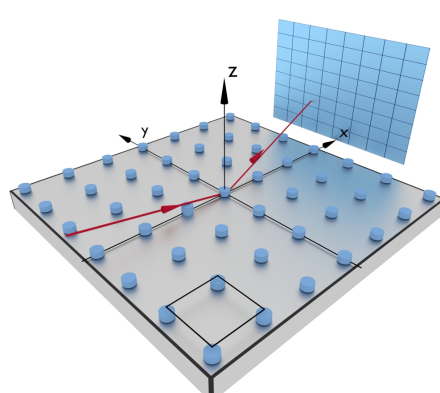
### E.6.1 Disorder 1

Cylinders with radii and heights of 3 nm are deposited on a substrate (fig. E.9(a)). They are distributed along a square lattice with a lattice length of 25 nm, whose one of the main axes is parallel to the  $x$ -axis. The lattice is initialized by placing a cylinder at the origin.

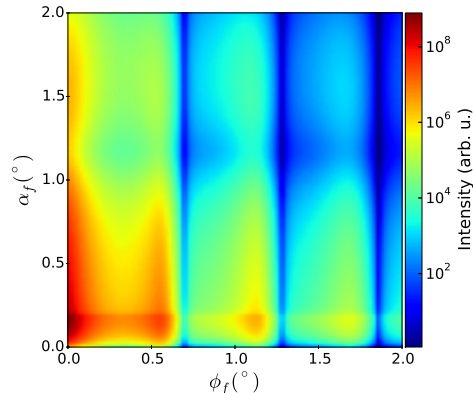
The rod shape distribution is a two-dimensional Cauchy function in reciprocal space with anisotropic correlation lengths equal to  $cl_x = 300/(2\pi)$  nm and  $cl_y = 100/(2\pi)$  nm.

The incident beam is characterized by a wavelength of 1 Å and angles  $\alpha_i = 0.2^\circ$  and  $\phi_i = 0^\circ$ .

The simulation is run using the DWBA.



(a) Schematic of the sample

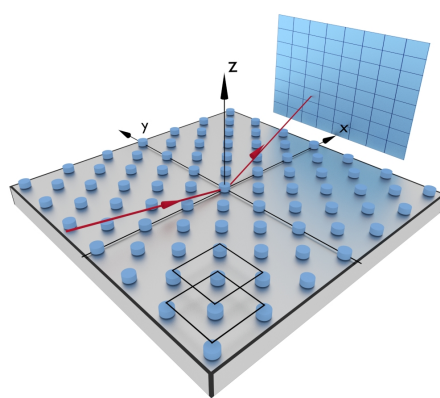


(b) Simulated 2D pattern

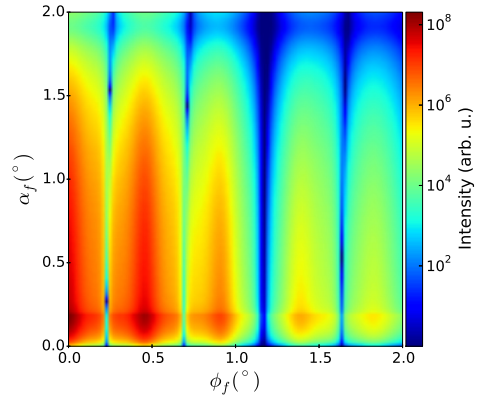
Figure E.9: Example 005 - Disorder1: Scattering from a monodisperse distribution of cylinders deposited on a substrate along a squared lattice using the Distorted Wave Born approximation.

### E.6.2 Disorder 2

This sample differs from the previous one by an overlap of two spatial distributions of cylinders. The first square lattice is centered at the origin. The second one, with the same lattice spacing and the same cylinders at the nodes is initialized at  $x = y = 12.5$  nm.



(a) Schematic of the sample

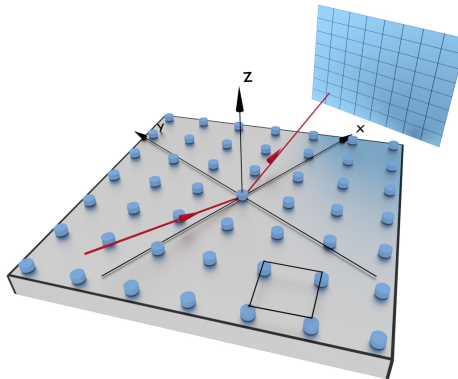


(b) Simulated 2D pattern

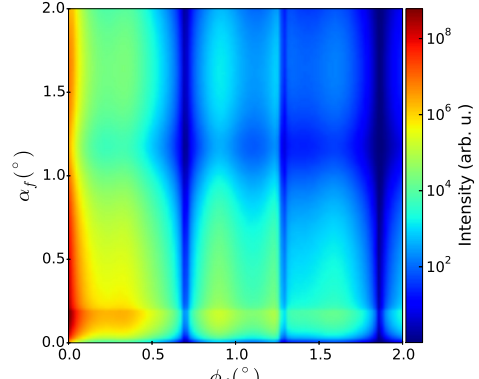
Figure E.10: Example 005 - Disorder2: Scattering from two monodisperse distributions of cylinders deposited on a substrate along a squared lattice using the Distorted Wave Born approximation. One of the lattices is laterally offset with respect to the other by 12.5 nm along the  $x$ - and  $y$ - axes.

### E.6.3 Disorder 3

Compared to Section E.6.1, the square lattice used in this example is now rotated with respect to the main referential by  $30^\circ$ . Note that the axes of the rod shape's distribution are also rotated using `setGamma`.



(a) Schematic of the sample

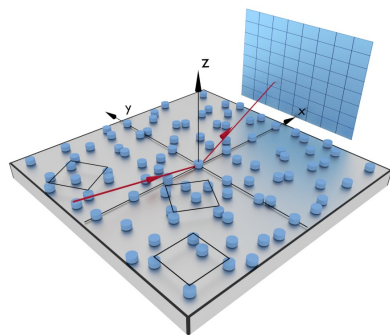


(b) Simulated 2D pattern

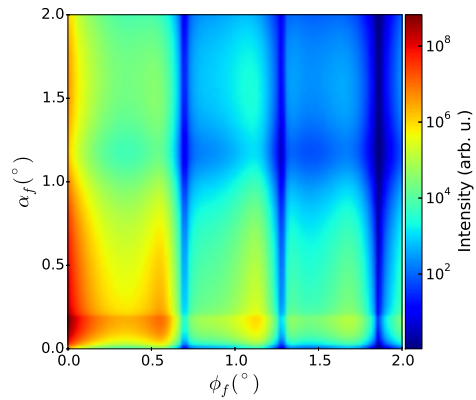
Figure E.11: Example 005 - Disorder3: Scattering from a monodisperse distribution of cylinders deposited on a substrate along a squared lattice using the Distorted Wave Born approximation. The main axes of the square lattice are rotated by  $30^\circ$  with respect to the main referential.

#### E.6.4 Disorder 4

This sample is composed of identical cylinders. Their distribution is generated as a random subset of three square lattices, whose main axes are rotated with respect to the  $x$ -axis by  $0^\circ$ ,  $120^\circ$ ,  $240^\circ$ , respectively.



(a) Schematic of the sample



(b) Simulated 2D pattern

Figure E.12: Example 005 - Disorder4: Scattering from a monodisperse distribution of cylinders deposited on a substrate.

## E.7 Example 6: Rotated pyramids

This example illustrates how the in-plane rotation of non-radially symmetric particles influences the scattering pattern.

The sample is made of pyramids (squared-base side length = 10 nm, height = 5 nm,  $\alpha = 54.73^\circ$ , see Section C.6) deposited on a substrate. There is no interference.

The wavelength is 1 Å. The incident angles are  $\alpha_i = 0.2^\circ$  and  $\phi_i = 0^\circ$ .

For the second example, shown in fig. E.14, the pyramids are rotated in the  $(x, y)$  plane by  $45^\circ$ .

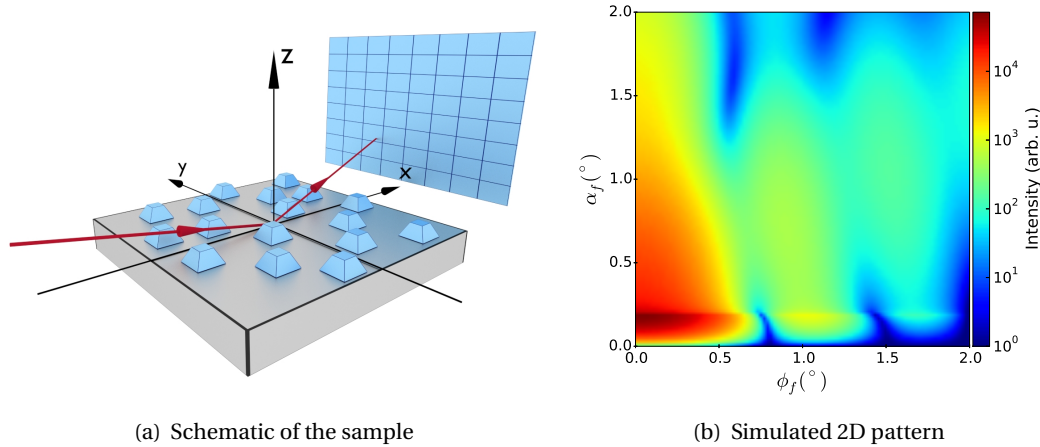


Figure E.13: Example 6: Pyramids deposited on a substrate.

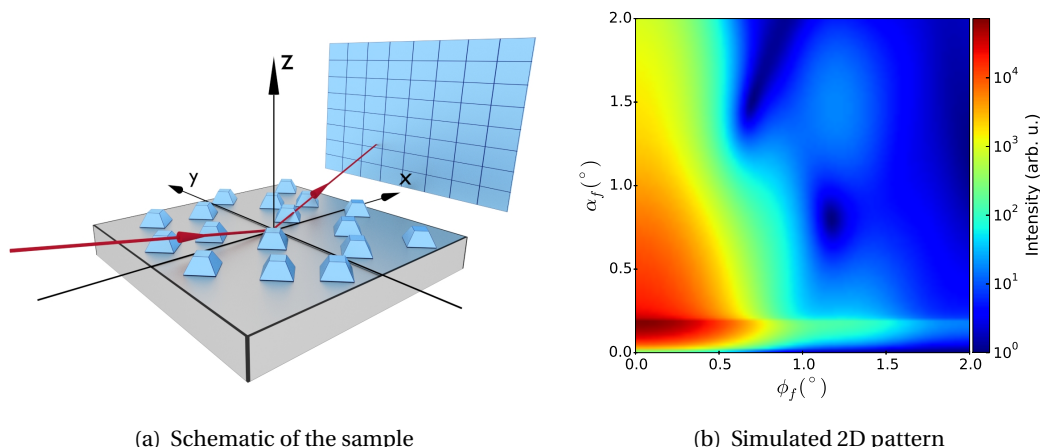


Figure E.14: Example 6: Rotated pyramids deposited on a substrate.

## E.8 Example 7: Core-shell nanoparticles

The sample is made of core-shell particles whose inner and outer shells are parallelepipeds with dimensions  $L_1 = W_1 = 16 \text{ nm}$ ,  $H_1 = 8 \text{ nm}$  and  $L_2 = W_2 = 12 \text{ nm}$ ,  $H_2 = 7 \text{ nm}$ , respectively, where  $L_i$ ,  $W_i$ , and  $H_i$  are the length, width and height of box  $i$  (see fig. E.15). The smaller box is positioned so that the centres of the bottom faces of both particles coincide (see 5.4.1 for details about this form factor).

The simulation is run using the Born approximation. There is no substrate and no interference between the different scattered beams.

The incident beam is characterized by a wavelength of  $1 \text{ \AA}$ , incident angles  $\alpha_i = 0.2^\circ$  and  $\phi_i = 0^\circ$ .

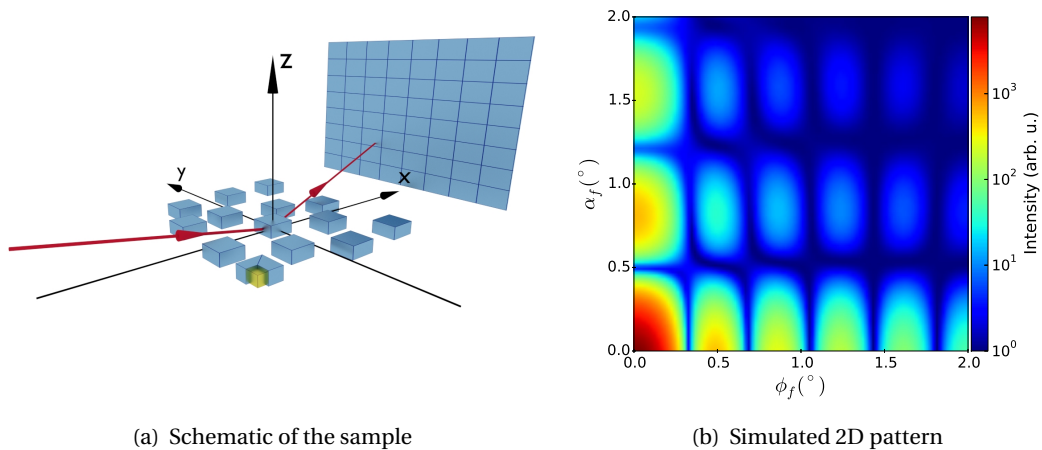


Figure E.15: Example 7: Core-shell particles simulated using the Born approximation. The particle at the forefront had been truncated in order to illustrate the core-shell structure.

## E.9 Example 8: Correlated roughness

The sample is made in the following way from top to bottom:

- layer A: A: 2.5 nm-thick,  $n = 1 - 5e - 6.$
  - layer B: 5 nm-thick,  $n = 1 - 1e - 5.$
  - substrate: infinitely thick,  $n = 1 - 15e - 6$
- $\left. \right\} \times 5.$

There is no added particle. All layers present the same type of roughness on the top surface, which is characterized by

- $\sigma = 1 \text{ nm},$
- a Hurst parameter  $H$  equal to 0.3,
- a lateral correlation length  $\xi$  of 5 nm,
- a cross correlation length  $\xi_{\perp}$  equal to 1e-4 nm.

**Roughness in BornAgain** The implementation is based on Reference [17, 18].

The roughness profile is described by a normally-distributed random function. The roughness correlation function at  $j^{\text{th}}$  interface is expressed as  $\langle U_j(x, y)U_j(x', y') \rangle = \sigma^2 \exp(-(\tau/\xi)^{2H})$ ,  $\tau = \sqrt{(x - x')^2 + (y - y')^2}$ , where  $U_j(x, y)$  is the height deviation of the  $j^{\text{th}}$  interface at position  $(x, y)$ .

$\sigma$  gives the rms roughness of the interface.

The Hurst parameter  $H$ , comprised between 0 and 1 is connected to the fractal dimension  $D = 3 - H$  of the interface. The smaller  $H$  is, the more serrate the surface profile looks. If  $H = 1$ , the interface has a non fractal nature.

The lateral correlation length  $\xi$  acts as a cut-off for the lateral length scale on which an interface begins to look smooth. If  $\xi \gg \tau$  the surface looks smooth.

The cross correlation length  $\xi_{\perp}$  is the vertical distance over which the correlation between layers is damped by a factor  $1/e$ . It is assumed to be the same for all interfaces. If  $\xi_{\perp} = 0$  there is no correlations between layers. If  $\xi_{\perp}$  is much larger than the layer thickness, the layers are perfectly correlated.

The incident beam is characterized by a wavelength of 1 Å and incident angles  $\alpha_i = 0.2^\circ$  and  $\phi_i = 0^\circ$ .

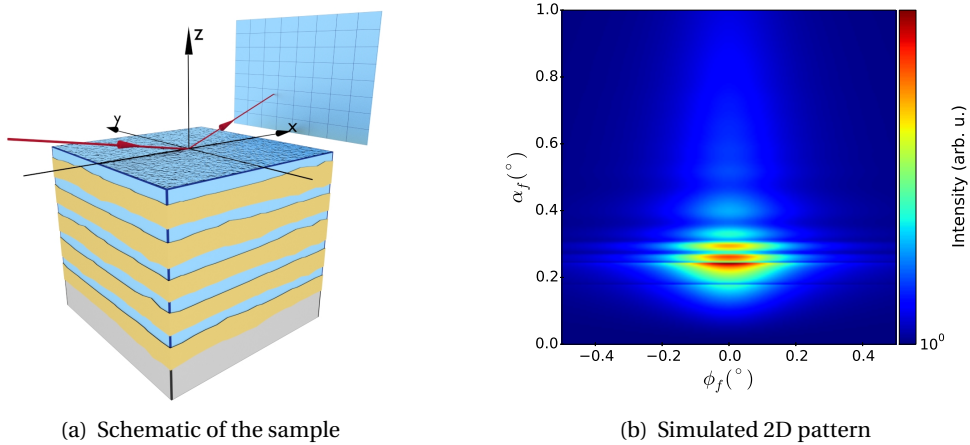


Figure E.16: Example 8: Correlated roughness between layers.

## E.10 Example 9: Ripple

These particles have one of their dimensions much larger than the others. Two different transverse profiles are simulated: one cosine and one asymmetric triangular. These particles are deposited on a substrate. The input beam is characterized by a wavelength of  $1.6 \text{ \AA}$  and angles  $\alpha_i = 0.3^\circ$ ,  $\phi_i = 0^\circ$ .

### E.10.1 Cosine ripple

The particles have a cosine cross section (see Section C.17 for an illustration) with  $L = 100 \text{ nm}$ ,  $W = 20 \text{ nm}$ ,  $H = 4 \text{ nm}$ . The interference considered is a two-dimensional orthogonal lattice with  $L_1 = 200 \text{ nm}$ ,  $L_2 = 50 \text{ nm}$ . The rod shape distribution is an anisotropic 2D Gaussian with  $cl_x = 1000/(2\pi) \text{ nm}$  and  $cl_y = 100/(2\pi) \text{ nm}$ .

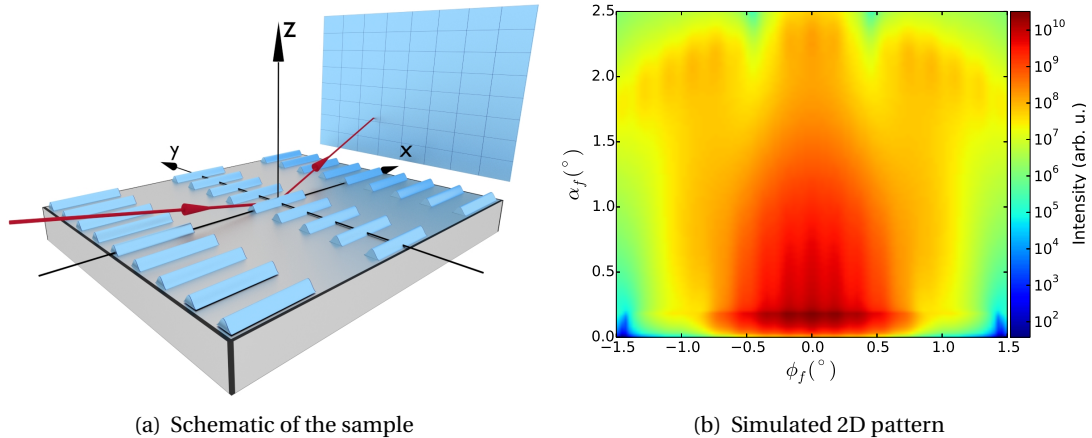


Figure E.17: Example 9: Scattering from a distribution of cosine ripples deposited on a substrate along a rectangular lattice.

The influence of the interference function on the output pattern can be seen by comparing figures E.17(b) and E.18. The latter has been generated without any interference (*i.e.* with a diluted distribution of particles).

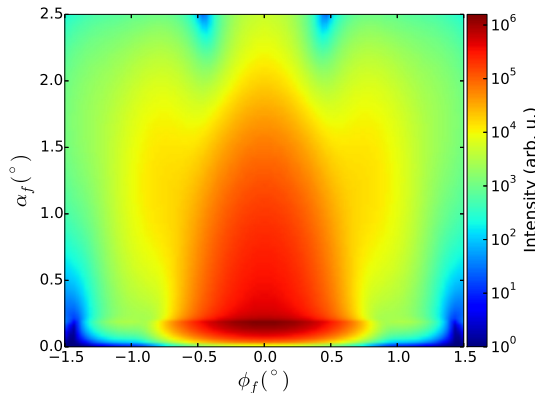


Figure E.18: Example 9: Scattering from a distribution of cosine ripples deposited on a substrate with no interference.

### E.10.2 Triangular ripple

The particles are long particles with an asymmetric triangular cross section (see Section C.18) with  $L = 100$  nm,  $W = 20$  nm,  $H = 4$  nm, an asymmetry coefficient of  $-3$  nm. The interference function has the same characteristics as in the previous example.

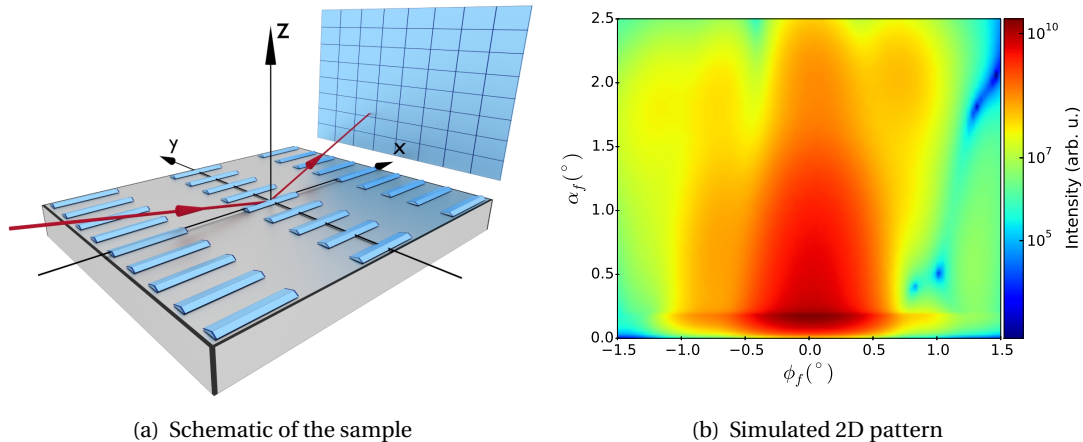


Figure E.19: Example 9: Scattering from a distribution of triangular ripples deposited on a substrate with no interference.

Figure E.20 was generated with asymmetrical triangular ripples but with no interference. It therefore illustrates the influence of the particle's shape on the scattering pattern.

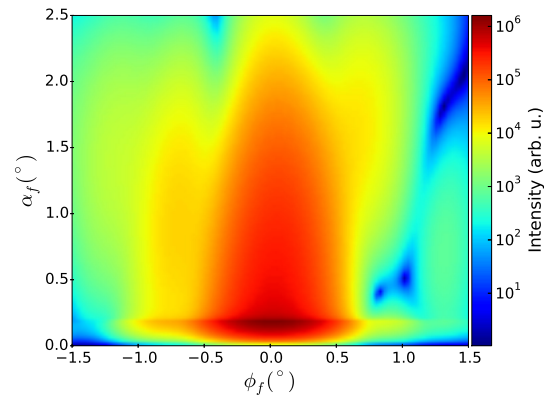


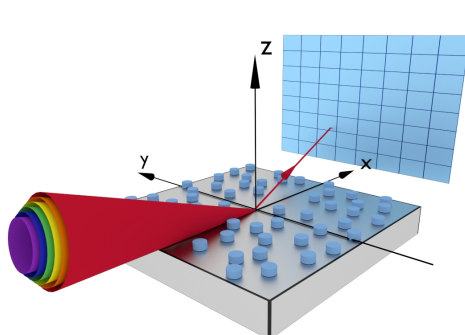
Figure E.20: Example 9: Scattering from a distribution of triangular ripples deposited on a substrate with no interference.

## E.11 Example 10: Beam divergence

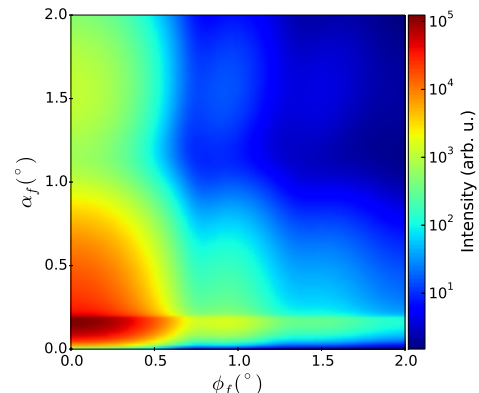
The main point of this example is the input beam, which presents a divergence for:

- the wavelength, following a log-normal distribution around the mean value of  $1 \text{ \AA}$  with a scale parameter equal to 0.1 (see the remark at the end of this section for a definition of these parameters).
- both incident angles following a Gaussian distribution with  $\bar{\alpha}_i = 0.2^\circ$ ,  $\bar{\phi}_i = 0^\circ$  and  $\sigma_{\alpha_i} = \sigma_{\phi_i} = 0.1^\circ$ .

The sample is made of cylinders (5 nm in radius and height) deposited on a substrate, whose scattered beams do not interfere (fig. E.21(a)). The simulation is run using the Distorted Wave Born Approximation.



(a) Schematic of the sample



(b) Simulated 2D pattern

Figure E.21: Example 10: An input beam presented a divergence for the wavelength and the incident angles impinges on a sample made of monodisperse cylinders deposited on a substrate.

This example and the one presented in Section E.4.3 differ only by the divergence of the input beam. Comparing the output patterns shows that the largest impact of input beam divergence is a reduction of the sharpness in the intensity pattern for larger values of  $\phi_f$  and  $\alpha_f$ .

Remark: The Gaussian distribution is characterised by

$$p(\bar{x}, \sigma) = \frac{1}{2\sigma^2} \exp \left[ -\frac{(x - \bar{x})^2}{2\sigma^2} \right],$$



and the log-normal by

$$p(\text{median}, \text{scale}) = \frac{1}{x \text{ scale} \sqrt{2\pi}} \exp \left[ -\frac{1}{2} \left( \frac{\log(x/\text{median})}{\text{scale}} \right)^2 \right].$$

# Bibliography

- [1] R. Lazzari, J. Appl. Cryst. **35**, 406–421 (2002).
- [2] M. Lutz, *Python pocket reference*, O'Reilly media (4<sup>th</sup> 2009).
- [3] <http://www.numpy.org>.
- [4] G. Renaud, R. Lazzari and F. Leroy, Surface Science Reports **64**, 255 (2009).
- [5] J. K. Pedersen, J. Appl. Cryst. **27**, 595 (1994).
- [6] R. Lazzari, F. Leroy and G. Renaud, Phys. Rev. B **76**, 125411 (2007).
- [7] R. Hosemann, Acta Cryst. **4**, 520 (1951).
- [8] M. Rauscher, T. Salditt and H. Sphon, Phys. Rev. B **52**, 16855 (1995).
- [9] L. G. Parratt, Phys. Rev. E **95**, 359 (1954).
- [10] M. Born and E. Wolf, *Principles of Optics*, Cambridge University Press (1999).
- [11] Minuit user's guide, <http://seal.web.cern.ch/seal/documents/minuit/mnusersguide.pdf>.
- [12] <http://seal.web.cern.ch/seal/documents/minuit/mntutorial.pdf>.
- [13] [http://www.gnu.org/software/gsl/manual/html\\_node/Multidimensional-Minimization.html](http://www.gnu.org/software/gsl/manual/html_node/Multidimensional-Minimization.html).
- [14] [http://www.gnu.org/software/gsl/manual/html\\_node/Nonlinear-Least\\_002dSquares-Fitting.html#Nonlinear-Least\\_002dSquares-Fitting](http://www.gnu.org/software/gsl/manual/html_node/Nonlinear-Least_002dSquares-Fitting.html#Nonlinear-Least_002dSquares-Fitting).
- [15] [http://www.gnu.org/software/gsl/manual/html\\_node/Simulated-Annealing.html](http://www.gnu.org/software/gsl/manual/html_node/Simulated-Annealing.html).
- [16] M. Abramowitz and I. Stegun, *Handbook of Mathematical Functions*, National Bureau of Standards (1964).
- [17] D. K. G. de Boer, Phys. Rev. B **51**, 5297 (1995).
- [18] J.-P. Schlomka, M. Tolan, L. Schwalowsky, O. H. Seeck, J. Stettner and W. Press, Phys. Rev. B **51**, 2312 (1995).